A THERMODYNAMIC STUDY OF SELF-ASSOCIATION IN β-CASEIN AND BRIJ 35 SOLUTIONS

A thesis presented in partial fulfilment

of the requirements for the degree of

Doctor of Philosophy

in Chemistry

at

Massey University

New Zealand

John Leslie Woodhead

1978

ABSTRACT

The self-association of both β-casein A^1 and Brij 35 in aqueous solution has been studied at several temperatures using the techniques of microcalorimetry, sedimentation equilibrium, sedimentation velocity, pycnometry and surface tension measurements. Attempts to obtain the equilibrium concentration of the various β-casein species in solution by ultracentrifugation have been unsuccessful owing to both degradation and the rate of equilibration. The equilibrium concentrations for β-casein were estimated from published fluorescence data.

The results have been analysed by treating each self-association process as being one of micelle formation. For both systems the standard free energy of micelle formation was negative whereas the corresponding standard enthalpy and entropy changes were positive. The temperature trends in the various thermodynamic parameters were inconclusive owing to experimental uncertainty.

The significance of the values of the thermodynamic parameters is discussed qualitatively. The driving force behind the self-association process for both systems appears to be the positive entropy change associated with the hydrophobic effect. A comparison is made between the two systems and it is concluded that β-casein self-association is similar in several respects to micelle formation in solutions of synthetic detergents.

ACKNOWLEDGEMENTS

I would like to express my gratitude to Professor G.N. Malcolm, Dr I.D. Watson and Dr J.A. Lewis for the help and encouragement they provided during their supervision of this thesis.

I would also like to thank Dr G.R. Hedwig for his helpful comments and suggestions.

The advice and assistance of Dr L.K. Creamer, Dr K.N. Pearce and the Technical Staff of the Protein Section of the New Zealand Dairy Research Institute was greatly appreciated.

I acknowledge the financial assistance provided by a Postgraduate Scholarship from the University Grants Committee, a Departmental Demonstratorship from Massey University and a Bursary from the Dairy Research Institute.

TABLE OF CONTENTS

LIST OF FIGURES

LIST OF TABLES

CHAPTER 1

INTRODUCTION

1. INTRODUCTION

1.1 Self-Associating Systems

Self-associating systems are defined as those systems in which a molecule in solution becomes associated with other molecules of the same kind to form a cluster of like molecules. This phenomenon has also been termed aggregation, polymerization, multimerization and complex formation. Self-association only includes those processes in which the physical bonds which hold the molecules together are non-covalent. In this thesis the free molecules in solution will be called monomers, although they are also known as unimers or monomolecules. The number of monomers in each associated species will be called the degree of association (N) and the associated species will be designated as an N-mer. The terms multimer, polymer, complex and aggregate have also been used in the literature to refer to the N-mer species. When N is small the N-mer can also be referred to as a dimer (N = 2), trimer (N = 3), tetramer (N = 4), hexamer (N = 6) or octamer (N = 8).

Self-association can be divided into reversible and irreversible processes. In the case of reversible self-association there is thermodynamic equilibrium between the monomers and the N-mers. Only reversible processes will be considered in this thesis. Reversible self-association can be divided into two basic types (Elias, 1976); open association, which is also known as random polymerization (Van Holde and Rossetti, 1967) or indefinite self-association (Adams, 1967), and closed association. Open association is a consecutive process which proceeds indefinitely and can be represented by the following equilibria,

$$A_1 + A_{N-1} \rightleftharpoons A_N \qquad (N = 2, 3, 4 \ldots\ldots) \qquad (1\text{-}1)$$

All N-mer species from dimers upwards are present in solution. Closed association involves processes in which there are only two species present in solution; monomers and N-mers. This process can be represented

by,

$$NA_1 \rightleftharpoons A_N \qquad (1\text{-}2)$$

An intermediate self-association process can occur in which there is a limited number of different sized N-mer species formed (e.g. monomer-dimer-trimer equilibrium). This type of self-association, along with the monomer-N-mer process, is also known as discrete self-association (Adams, 1967) as there is a discrete number of different species formed, as opposed to the indefinite number of species present in open association.

Both synthetic and biological systems have been observed to undergo self-association. Of particular interest is self-association in protein systems as this is very important in many of the life processes. An understanding of many biochemical processes requires some insight into the nature of the forces which cause some proteins to self-associate. The kinds of bonds which may hold the associated species together can be determined by consideration of the thermodynamics of the association process. One of the proteins which have been observed to undergo reversible self-association is the bovine milk protein, β-casein. The object of this thesis is to determine the reasons for β-casein association by analysing the thermodynamics of the process, and comparing its behaviour with that of the synthetic detergent, Brij 35.

1.2 Bovine β-Casein

The total protein content in bovine milk consists of about 76-86% casein (Swaisgood, 1973). β-casein makes up about 25% of this casein content, with α_s-, γ-and κ-caseins providing the remaining portion. There are several genetic variants of β-casein and these are classified as A^1, A^2, A^3, B, C and D on the basis of their electrophoretic mobility (Aschaffenburg, 1961; Peterson and Kopfler, 1966; Rose *et al.*, 1970; Aschaffenburg, *et al.*, 1968). The most common variants are A^1, A^2 and B. The variant used in this study was β-casein A^1. β-casein is a phosphoprotein

containing 209 amino acid residues in a single polypeptide chain. The A^1 amino acid sequence has been well established by Grosclaude *et al.* (1972) and is shown in Figure (1-1). The amino acid content for the A^1 variant can be written as follows,

$$Asp_4\ Asn_5\ Thr_9\ Ser_{11}\ SerP_5\ Glu_{17}\ Gln_{22}\ Pro_{34}\ Gly_5\ Ala_5\ Val_{19}\cdots$$
$$Met_6\ Ile_{10}\ Leu_{22}\ Tyr_4\ Phe_9\ Trp\ Lys_{11}\ His_6\ Arg_4$$

The molar mass of β-casein A^1 is 24,020 g mol^{-1} calculated from the amino acid content. It can be seen that there are five phosphate groups and these are attached to serine residues. The positions of these serine phosphate residues in the polypeptide chain, numbering from the N-terminal end, is as follows,

$$SerP_{15},\ SerP_{17},\ SerP_{18},\ SerP_{19},\ SerP_{35}$$

There is a total of 49 ionizable sidechains and of these 22 are cationic and 27 are anionic. The first 21 N-terminal amino acid residues contain 13 of the ionizable groups including 4 of the 5 phosphate groups. At pH 6.6 there is a net charge of -13 in this section of the chain (Waugh *et al.*, 1970) with the remainder of the chain having essentially zero net charge. At this pH the 21 residue N-terminal sequence carries approximately 30% of the total charge of the molecule although it accounts for only 10% of the residues (Swaisgood, 1973). The first 50 N-terminal residues contain 23 of the ionizable groups including all of the phosphate sidechains. The 159 amino acids which make up the remaining three-quarters of the molecule are predominately nonpolar and therefore hydrophobic. In fact, β-casein is one of the most hydrophobic proteins yet isolated.

Another unusual feature of the structure of β-casein is the high proline content. Proline residues make up 17% of the total amino acid content of the molecule and are uniformly distributed along the chain. The secondary and tertiary structure of β-casein in solution is not known

Figure (1-1) Amino Acid Sequence of β-Casein A[1]

H_2N-Arg-Glu-Leu-Glu-Glu-Leu-Asn-Val-Pro-
Gly-Glu-Ile-Val-Glu-SerP-Leu-SerP-SerP-SerP-
Glu-Glu-Ser-Ile-Thr-Arg-Ile-Asn-Lys-Lys-
Ile-Glu-Lys-Phe-Gln-SerP-Glu-Glu-Gln-Gln-
Gln-Thr-Glu-Asp-Glu-Leu-Gln-Asp-Lys-Ile-
His-Pro-Phe-Ala-Gln-Thr-Gln-Ser-Leu-Val-
Tyr-Pro-Phe-Pro-Gly-Pro-Ile-His-Asn-Ser-
Leu-Pro-Gln-Asn-Ile-Pro-Pro-Leu-Thr-Gln-
Thr-Pro-Val-Val-Val-Pro-Pro-Phe-Leu-Gln-
Pro-Glu-Val-Met-Gly-Val-Ser-Lys-Val-Lys-
Glu-Ala-Met-Ala-Pro-Lys-His-Lys-Glu-Met-
Pro-Phe-Pro-Lys-Tyr-Pro-Val-Gln-Pro-Phe-
Thr-Glu-Ser-Gln-Ser-Leu-Thr-Leu-Thr-Asp-
Val-Glu-Asn-Leu-His-Leu-Pro-Pro-Leu-Leu-
Leu-Gln-Ser-Trp-Met-His-Gln-Pro-His-Gln-
Pro-Leu-Pro-Pro-Thr-Val-Met-Phe-Pro-Pro-
Gln-Ser-Val-Leu-Ser-Leu-Ser-Gln-Ser-Lys-
Val-Leu-Pro-Val-Pro-Glu-Lys-Ala-Val-Pro-
Tyr-Pro-Gln-Arg-Asp-Met-Pro-Ile-Gln-Ala-
Phe-Leu-Leu-Tyr-Gln-Gln-Pro-Val-Leu-Gly-
Pro-Val-Arg-Gly-Pro-Phe-Pro-Ile-Ile-Val-COOH

to a high degree of certainty. The high proline content would be expected to prevent appreciable α-helix structure. Garnier (1966) suggested that some poly-L-proline II structure could be present based on evidence provided by optical rotatory dispersion studies. This view was also supported by Evans et al. (1971) and Herskovits (1966). Waugh et al. (1970) have suggested that the hydrophobic portion of the β-casein monomer is folded into a compact body and that the highly polar N-terminal portion of the chain is extended out into solution. However, the large number of hydrophobic residues in the C-terminal sequence would probably prevent all of them being packed internally. It is therefore likely that a portion of these residues would be in contact with the solvent at the surface of the molecule. The viscosity studies of Noelken and Reibstein (1968), the nuclear magnetic resonance experiments of Leslie et al. (1969) and Evans et al. (1971) and also the titration studies of Creamer (1971) indicate that the solvent has access to most of the hydrophobic and all of the ionizable residues. Kresheck (1965) and Herskovits (1966) concluded from the results of optical rotation studies that the β-casein monomer is loosely folded in solution. Noelken and Reibstein (1968) have suggested that the molecule has a random coil configuration.

The tendency for β-casein to undergo self-association in solution was first reported by Halwer (1954). He observed that the association process was dependent on ionic strength by studying the light scattering of β-casein solutions. The sedimentation experiments of Sullivan et al. (1955) revealed that the self-association at pH 7 was reversible and strongly temperature dependent, with only the monomer being present at low temperatures but both the monomer and an associated species being observed at room temperature. This phenomenon was also observed by von Hippel and Waugh (1955). The self-association was shown to be dependent on pH and the presence of urea by the sedimentation studies of McKenzie and Wake

(1959). The first comprehensive study of β-casein self-association was carried out by Payens and van Markwijk (1963) using the Archibald and sedimentation velocity ultracentrifuge techniques and also viscosity experiments at temperatures between 4° and 13.5°C. These workers showed that the association process was concentration dependent in addition to being temperature dependent. The results appeared to be best interpreted by a closed monomer-N-mer model with a narrow size distribution for the N-mers. At 8.5°C, pH 7.5 and an ionic strength (I) of 0.20 the molar mass of the N-mer was determined to be in the range of 5 to 6 x 10^5 g mol^{-1} which corresponds to a degree of association of about 20 to 24 monomer units. The sedimentation velocity patterns were used to determine the relative amounts of monomer and N-mer present from which values for equilibrium constants based on the monomer-N-mer model were calculated. The rate of equilibration was reported to be slow. The monomers appeared to exhibit ideal behaviour whereas the N-mers had a positive second virial coefficient similar in value to species which are thought to exist as fairly stiff rods or as interlinked flexible coils.

Kresheck et al. (1964) studied the light scattering behaviour of β-casein solutions at temperatures between 30° and 90°C at pH 6.5 and I = 0.066. The N-mer was reported to have a molar mass greater than 10^6 g mol^{-1} and to be possibly spherical in shape. Hoagland (1966) studied the self-association of both β-casein and acylated derivatives of β-casein. He concluded that the association was probably the result of a balance between hydrophobic and electrostatic forces. Difference spectrophotometry and optical rotation techniques at pH 7.0 and I = 0.10 were used by Garnier (1966) to show that β-casein underwent a reversible temperature dependent transition from one state at 5°C to another state at 40°C. The equilibrium was found to be rapid in contrast to the conclusions of Payens and van Markwijk (1963).

The combined light scattering and sedimentation velocity experi-

ments of Payens et al. (1969) at pH 7.0, 21°C and several ionic strengths over a wide concentration range provided further evidence for the monomer-N-mer nature of β-casein association. The degree of association appeared to decrease with increasing ionic strength. The change in the apparent weight average molar mass with concentration was also determined and strong positive nonideal effects were observed. Payens and Heremans (1969) studied the effect of pressure on β-casein association and observed that the N-mers tended to reversibly dissociate at high pressures. Viscosity, sedimentation velocity and Archibald techniques were used by Waugh et al. (1970) to study the association process at pH 6.6. They found that the degree of association was about 30 at the high ionic strength of 2.0 and at a temperature of 37°C. The self-association was observed to be greatly enhanced by the addition of calcium ions. A model was proposed for the N-mer which was similar to that of a spherical soap micelle with a radius of about 10nm. The resemblance of β-casein association to the formation of soap micelles was reiterated by Schmidt and Payens (1972).

Pearce (1975) used fluorescence techniques to study β-casein association under a variety of conditions, including the effect of changing the temperature, pH, ionic strength and concentration of the solution. Values for various thermodynamic parameters were determined by regarding the process as a two-state transition. It was observed that association increased with temperature, ionic strength and concentration but decreased with increasing pH. The rate of equilibration appeared to be relatively fast. Again, it was noted that many of the properties of the system were similar to those observed for the formation of soap or detergent micelles. The gel chromatography studies of Berry and Creamer (1975) indicated that there was a reversible association process between a monomer and N-mer species in solution. The N-mer appeared to have a molar mass of a least 1.34×10^6 g mol^{-1} at pH 6.5, I = 0.10 and 36°C. It was found that the

removal of some of the C-terminal residues from the monomer considerably reduced the ability of the protein to self-associate. The size distribution of the β-casein N-mers was determined by Schmidt and Buchheim (1976) using electron microscopy. They observed that the N-mers were approximately spherical with the diameters narrowly distributed around a value of about 10 to 12nm. The molar mass of the N-mers was estimated to be about 6×10^5 g mol^{-1}.

The magnitudes of the degree of association for the β-casein N-mer obtained by several workers are summarized in Table (1-1). It can be seen that the apparent value of N varies with the experimental conditions and also with the experimental technique used. Although there is no general agreement as to the size of the N-mer, in all cases the experimentally determined N values are much larger than those usually observed for self-associating proteins with the exception of myosin (Josephs and Harrington, 1966).

1.3 Amphiphiles

An amphiphile is a molecule which has a discrete polar "head" group attached to a nonpolar "tail" group. Typical amphiphiles are synthetic detergents and soaps. The polar portion of the amphiphile is readily water soluble (i.e. hydrophilic), whereas the nonpolar section is either completely insoluble or only slightly soluble in water (i.e. hydrophobic). When an amphiphile is dissolved in water the hydrophilic head group compensates for the insolubility of the hydrophobic tail and thus imparts solubility to the molecule as a whole. The nonpolar portion of an amphiphile usually consists of a hydrocarbon chain and therefore these molecules are normally classified according to the nature of the head group. The three main classes of amphiphile that can be distinguished on this basis are ionic, zwitterionic and nonionic amphiphiles. Ionic amphiphiles have charged head groups and are called cationic if they are positively charged or anionic if they are negatively charged. Zwitterionic

Table (1-1) Literature Values for the Molar Mass and Degree of Association of the β-Casein N-mer

Experimental Technique	Temp/°C	pH	I	Molar Mass of N-mer/10^5 g mol^{-1}	Degree of Association	Reference
Ultracentrifugation (combined Archibald and sedimentation velocity)	8.5	7.5	0.2	5.95	24[a]	Payens and van Markwijk (1963)
Light scattering	30	6.5	0.07	29.4	123[b]	Kresheck et al. (1964)
Combined light scattering and sedimentation velocity	21	7.0	0.2	12.5	50[a]	Payens et al. (1969) Payens and Heremans (1969)
"	21	7.0	0.05	10.2	41[a]	ibid.
Archibald	37	6.6	2.0	8.20	34[b]	Waugh et al. (1970)
"	23	6.6	0.05	6.50	27[b]	ibid.
Combined sedimentation velocity and viscosity	8.5	7.5	0.2	4.88	20[a]	Payens and van Markwijk (1963)
"	37	6.6	2.0	7.45	31[b]	Waugh et al. (1970)
"	23	6.6	0.005	7.20	30[b]	ibid.
Gel filtration	36	6.7	0.1	>13.4	>56[b]	Berry and Creamer (1975)
Electron microscopy	20	6.7	0.07	6.50	27[b]	Schmidt and Buchheim (1976)

[a] Assuming a monomer molar mass of 24,900 g mol^{-1}

[b] Assuming a monomer molar mass of 24,100 g mol^{-1}

amphiphiles carry both positive and negative charges with an overall net charge of zero. Nonionic amphiphiles have polar head groups which do not carry any charge.

The structure of bovine β-casein bears a marked similarity to a typical amphiphile. The 50 N-terminal amino acid residues are highly polar with the net negative charge of -13 at pH 6.6 being concentrated in the first 20 of these residues. This region of the polypeptide chain can be regarded as the head group of an amphiphile. The 159 residue polypeptide attached to this N-terminal sequence is remarkably nonpolar and thus approximates the tail group of an amphiphile. The β-casein molecule as a whole can therefore be considered to be approximate to an anionic amphiphile at pH values near neutrality and could be expected to exhibit some of the properties of this type of molecule. The self-association behaviour of β-casein in solution reported in the literature strongly suggests that this protein does behave in a similar way in many respects to a typical amphiphile.

At low concentration amphiphiles exist mainly as monomers in aqueous solution. The molecules tend to migrate to the solution-air interface and minimize the unfavourable contact of the hydrophobic groups with water by extending the nonpolar portion out into the air, with the hydrophilic head group remaining in the aqueous phase. At higher concentrations the hydrophobic groups can also be segregated from the solvent without migration to the surface by the self-association of a group of monomers. The monomers form a cluster in such a way that the nonpolar groups are protected from contact with water. This type of associated species is called a micelle, and has the hydrophilic groups exposed to the solvent at the surface of the cluster with the hydrophobic groups in contact with each other in the interior or "core" of the micelle.

A marked characteristic of micelle formation is the relatively narrow micelle size distribution. The association of amphiphiles to form a micelle is caused by the tendency of the tail groups to come together

in order to reduce the size of the hydrocarbon-water interface. A minimum number of amphiphiles is required to eliminate effectively the contact of the nonpolar groups with water, which determines the lower limit of the size distribution. The upper size limit is reached when the effect of the repulsive forces between the polar head groups in the micelle equals the propensity for the hydrophobic tail groups to associate. If these repulsive forces did not exist then the amphiphiles would continue to associate until the associated species came out of solution as a separate phase. Thus, micellization can be considered to be the result of two opposing tendencies; the clustering tendency associated with the tail groups and the repulsion associated with the head groups. The tendency for the tail groups to associate is usually called the "hydrophobic effect" (Tanford, 1973). The nature of the repulsion between the head groups is electrostatic for charged head groups but is thought to be related to solvation effects in the case of nonionic amphiphiles.

1.4 Thermodynamics of Micelle Formation

Measurement of the thermodynamic parameters associated with micelle formation gives some guidance as to the nature of the processes which may be involved. There have been two main approaches to the thermodynamic analysis of the process. In one of these, micelle formation is regarded as being analogous to the precipitation of a solute from a saturated solution, with the micelles being considered to form a separate phase from the solution of the remaining monomers. This approach is referred to as the phase separation model (Shinoda and Hutchinson, 1962; Matijevic and Pethica, 1958). The alternative approach has been to regard micelle formation as being analogous to a monomer-N-mer equilibrium in which the micelles are regarded as N-mers. This latter approach is known as the mass action model (Jones and Bury, 1927; Murray and Hartley, 1935; Debye, 1949; Phillips, 1955).

A characteristic of micellar systems is the experimental obser-

vation of a critical micelle concentration (cmc). The cmc is a solute concentration below which micelles cannot be experimentally detected,but as the solute concentration is increased from below the cmc micelles can be suddenly detected when the cmc is reached. Both the phase separation and the mass action models are able to account for the experimental observation of a cmc but both models suffer from a number of difficulties or limitations. A recent evaluation of these difficulties has been given by Fisher and Oakenfull (1977), and earlier by Tanford (1973) and by Hall and Pethica (1967). A comparison of the two models will not be repeated here, but (following Tanford) preference will be given to the mass action model. This will be discussed briefly in its simple form, and will be elaborated (as suggested by Hall and Pethica (1967)) in terms of the treatment of ideal associated solutions given by Prigogine and Defay (1954).

1.4.1 Simple Mass Action Model

Consider the monomer-N-mer association process defined by equation (1-2). At equilibrium the chemical potentials (μ) of the two species A_1 and A_N are related by the following equation,

$$N\mu_{A1} = \mu_{AN} \qquad (1\text{-}3)$$

(In equation (1-3) the subscript A1 will be used to denote a property of the monomer and the subscript AN to denote a property of a micelle of degree of association N. This notation will be used throughout this discussion, with the addition of the subscript s to denote a property of the solvent.)

The chemical potentials are related to the mole fractions (x) and the activity coefficients (f) of the species by the equations,

$$\mu_{A1} = \mu^{\circ}_{A1} + RT \ln x_{A1} f_{A1} \qquad (1\text{-}4)$$

$$\mu_{AN} = \mu^{\circ}_{AN} + RT \ln x_{AN} f_{AN} \qquad (1\text{-}5)$$

The superscripts o denote the standard states, which in this case are the pure substances. It follows from equations (1-3), (1-4) and (1-5)

that,

$$\mu^{\circ}_{AN} - N\mu^{\circ}_{A1} = - RT \ln x_{AN} f_{AN} + NRT \ln x_{A1} f_{A1} \quad (1\text{-}6)$$

$$= - RT \ln K_N \quad (1\text{-}7)$$

$$\text{where} \quad K_N = \frac{x_{AN} f_{AN}}{x_{A1}^N f_{A1}^N} \quad (1\text{-}8)$$

K_N is the equilibrium constant for the association process with concentrations expressed in mole fraction units. It should be noted that if the monomer is ionic any counterions which become firmly bound to the micelle must be included in the equation for the equilibrium reaction. For example, if the monomers are singly charged anions then the equilibrium can be represented by the following reaction,

$$NA_1^- + m\, C^+ \rightleftharpoons (A_N C_m)^{(N - m) -} \quad (1\text{-}9)$$

The counterions are represented in equation (1-9) as C^+ and m is the number of counterions which become firmly bound to the micelle. The expression for the equilibrium constant in this case must include the concentration of C^+, that is

$$K_E = \frac{x_{AN} f_{AN}}{x_{A1}^N f_{A1}^N x_c^m f_c^m} \quad (1\text{-}10)$$

However, if an electrolyte containing C^+ is added to the solution to give a large excess of C^+ the concentration of this species will remain virtually constant and its value can be included in a modified equilibrium constant (K_N'') where,

$$K_N'' = K_E x_c^m f_c^m \quad (1\text{-}11)$$

Thus, if the ionic strength of the solution is sufficiently high, the formation of micelles from ionic monomers can be treated as a normal monomer-N-mer system with K_N being replaced by K_N''.

1.4.2 Critical Micelle Concentration

It will be shown in this section that the simple mass action model is consistent with the experimental observation of a critical micelle concentration. Very little information is yet available about the activity coefficients of species in micelle-forming systems, and this discussion of the cmc will be confined to thermodynamically ideal solutions where the value of the activity coefficients is assumed to be unity. In this case, equation (1-8) can be written as,

$$K_N = \frac{x_{AN}}{x_{A1}^N} \tag{1-12}$$

Critical micelle concentrations are usually very low and hence are determined in dilute solutions where ideality is usually assumed. Many of the usual methods of analysis for the concentrations of the species in micelle forming systems do not lead directly to a value of the number of moles of micelles which are present, but rather to a value of the amount of monomer which has been incorporated into micelles. Another practical point is that for dilute solutions the mole fractions of the solute species are very nearly proportional to their concentrations on a weight per unit volume scale. On the basis of the above points the phenomenon of a critical micelle concentration can be demonstrated as follows.

Consider a dilute solution of a substance of molar mass M_{A1} which forms micelles of molar mass NM_{A1}. Let the total solute concentration in the solution be C_A mg cm^{-3} of which C_{A1} mg cm^{-3} are present as monomers and C_{AN} mg cm^{-3} as micelles. Then

$$C_A = C_{A1} + C_{AN} \tag{1-13}$$

Let n_{A1}, n_{AN} and n_s represent the number of moles of monomers, micelles and solvent present in the solution. If the solvent density in g cm^{-3} is denoted by ρ_s then for a dilute solution,

$$x_1 = \frac{n_{A1}}{(n_{A1} + n_{AN} + n_s)} \simeq \frac{n_{A1}}{n_s} \simeq \frac{(C_{A1}/M_{A1})}{(1000\,\rho_s/M_s)} = k\,C_{A1} \qquad (1\text{-}14)$$

$$x_N = \frac{n_{AN}}{(n_A + n_{AN} + n_s)} \simeq \frac{n_{AN}}{n_s} \simeq \frac{(C_{AN}/NM_{A1})}{(1000\,\rho_s/M_s)} = \frac{k\,C_{AN}}{N} \qquad (1\text{-}15)$$

$$\text{where} \quad k = \frac{M_s}{(1000\,\rho_s\,M_{A1})} \qquad (1\text{-}16)$$

Substitution of (1-14) and (1-15) into (1-12) gives,

$$(N\,k^{N-1})K_N \equiv K_N' = \frac{C_{AN}}{C_{A1}^N} \qquad (1\text{-}17)$$

By combining equations (1-13) and (1-17) it can be seen that,

$$C_A = C_{A1} + K_N'\,C_{A1}^N \qquad (1\text{-}18)$$

$$\text{and} \quad C_A = C_{AN} + \left(\frac{C_{AN}}{K_N'}\right)^{1/N} \qquad (1\text{-}19)$$

For specified values of K_N' and N it is now possible to use equations (1-18) and (1-19) to calculate the variation of C_{A1} and C_{AN} with C_A. Equation (1-18) can be used to plot C_{A1} versus C_A by assigning values to C_{A1}. Similarly, equation (1-19) can be used to obtain a plot of C_{AN} versus C_A. The results of such calculations for several arbitrarily chosen systems are illustrated in Figure (1-2). It is apparent from an inspection of the hypothetical plots that the phenomenon of a critical micelle concentration is predicted by the mass action model provided that the value of N is large. The sharpness of the transition at the cmc is reduced as N becomes smaller. When N = 30, for example, the cmc is represented by a narrow concentration range rather than by a specific concentration point, and there is also a small but significant increase in C_{A1} with C_A above the cmc. These effects are accentuated for the case of N = 10. In cases where the cmc is not sharply defined it is customary to define the cmc empirically as the point of intersection when the linear portions of the C_{A1} (or C_{AN}) versus C_A plots are extrapolated into the cmc region. This extrapolation is illustrated in Figure (1-3).

Figure (1-2) Hypothetical Plots of Monomer and Micelle Concentration vs Total Amphiphile Concentration

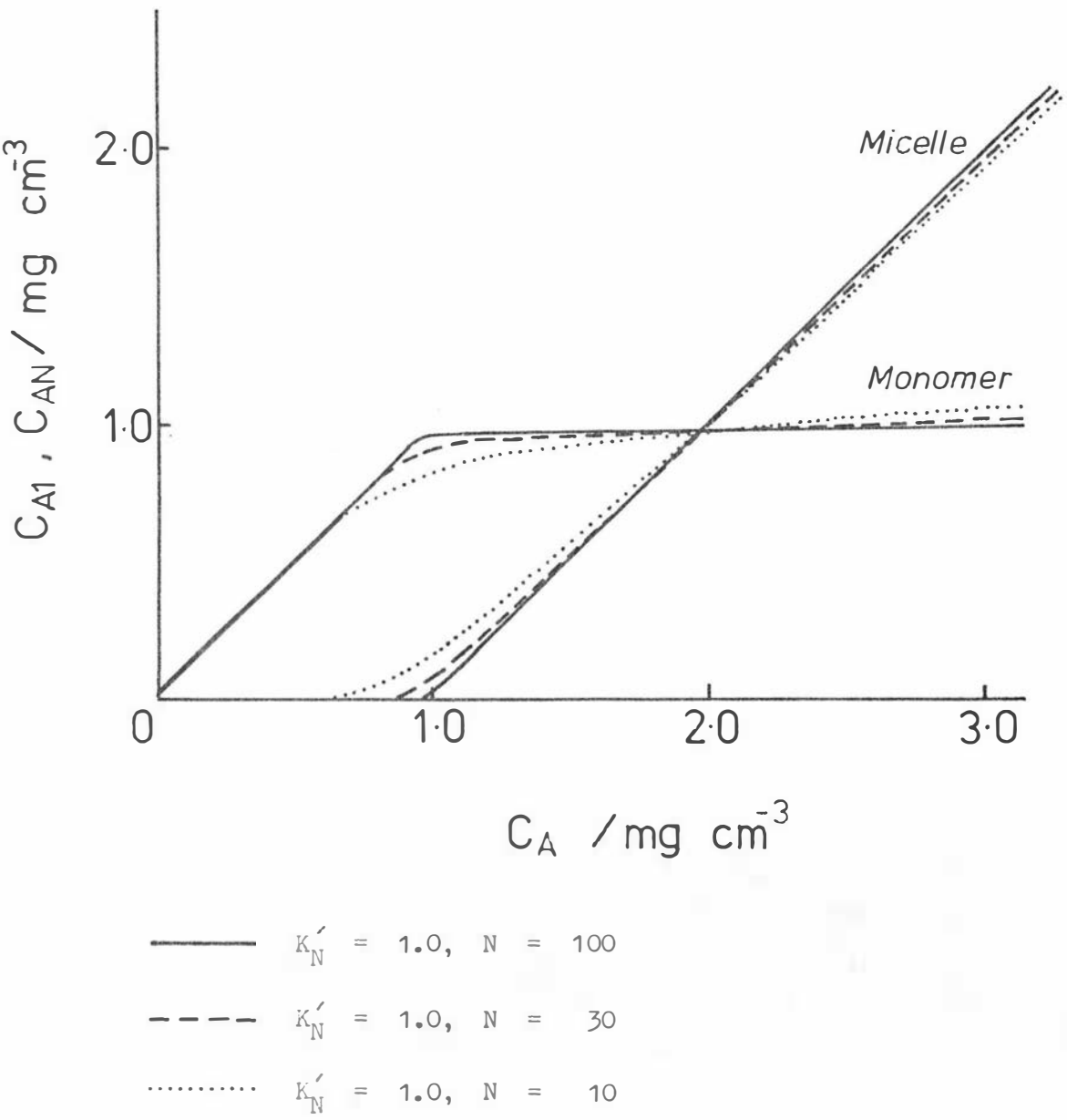

Figure (1-3) Extrapolation to Determine Critical Micelle Concentration

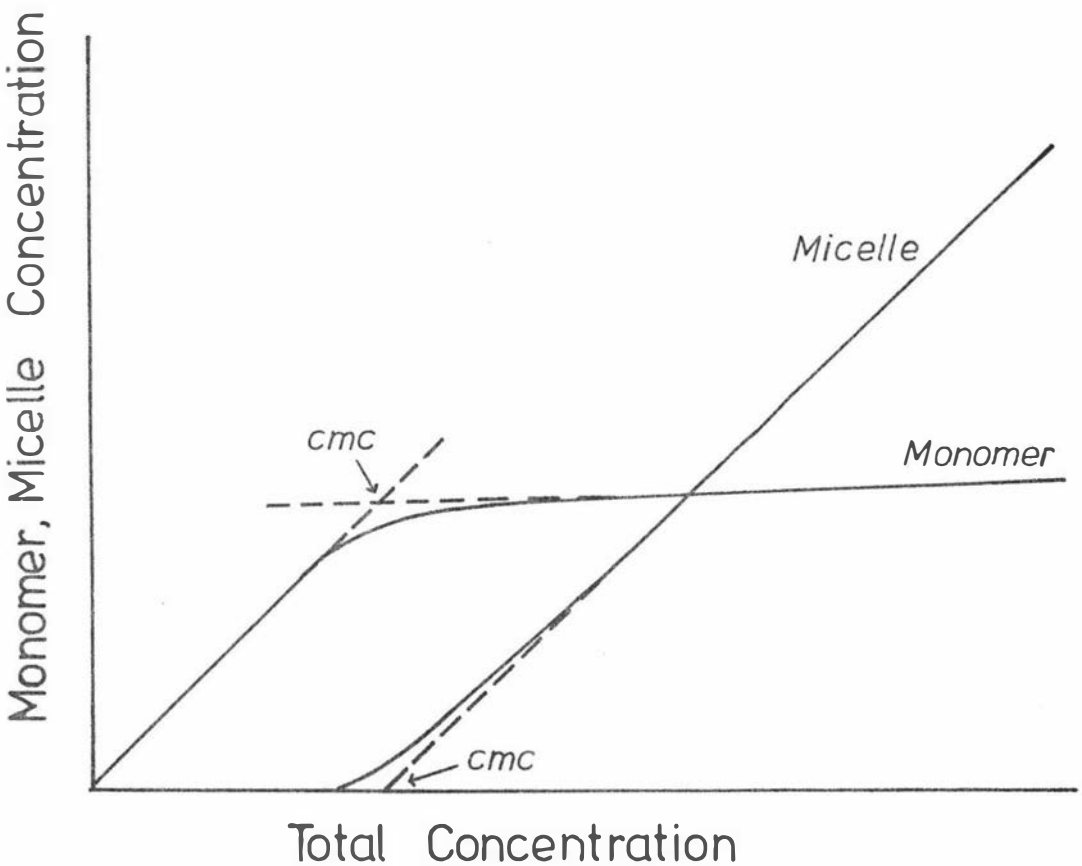

1.4.3 Free Energy of Micelle Formation

The change in standard chemical potential for the association of N moles of monomers to give one mole of micelles is given by equations (1-6) and (1-7). It has become customary in the discussion of micelle formation to write,

$$\mu^{\circ}_{AN} - N\mu^{\circ}_{A1} = N(\Delta G^{\circ}_{N}) \qquad (1\text{-}20)$$

so that ΔG°_{N} is the standard free energy change per mole of monomer for forming a micelle from the free monomers. From equations (1-6) and (1-20) ΔG°_{N} can be expressed as,

$$\Delta G^{\circ}_{N} = -\left(\frac{RT}{N}\right) \ln x_{AN} f_{AN} + RT \ln x_{A1} f_{A1} \qquad (1\text{-}21)$$

By expressing the concentrations in mole fraction units equation (1-21) gives the standard unitary free energy change for the process (Gurney, 1953; Tanford, 1973), i.e. the statistical cratic or mixing contribution to the free energy change is excluded. In principle equation (1-21) provides a means of determining the value of ΔG°_{N}. However, in practice little if any information is available concerning the activity coefficients. These will depend partly on the intermolecular forces between the various species (excluding the interactions which lead to the self-association of the monomers), and partly on the different sizes and shapes of the micelles, the monomers and the solvent molecules. All of these factors will be neglected at this stage in the discussion, and the activity coefficients in equation (1-21) will be assumed to have a value of unity. With this approximation ΔG°_{N} is given by,

$$\Delta G^{\circ}_{N} = -\left(\frac{RT}{N}\right) \ln x_{AN} + RT \ln x_{A1} \qquad (1\text{-}22)$$

Values of ΔG°_{N} can be calculated from equation (1-22) using measured values of N, x_{AN} and x_{A1}. If the concentrations are expressed in mg cm^{-3}, by combining equations (1-14) and (1-15) with equation (1-22) ΔG°_{N} is given by,

$$\Delta G_N^\circ = -\left(\frac{RT}{N}\right) \ln C_{AN} + RT \ln C_{A1} + RT\left(1 - \frac{1}{N}\right) \ln k \qquad (1\text{-}23)$$

It can be shown, for a given value of K_N', that if the values of C_{A1} and C_{AN} when C_A is close to the value of the cmc are introduced into equation (1-23), if N is large the $(RT/N) \ln C_{AN}$ term is negligible and the factor $(1 - 1/N)$ is close to unity. Also, it is found that C_{A1} closely approximates the cmc in value. Hence, equation (1-23) can be approximated as,

$$\Delta G_N^\circ \simeq RT \ln \text{cmc} + RT \ln k \qquad (1\text{-}24)$$

where cmc is expressed in units of mg cm^{-3}. The reason why equation (1-24) is useful is that the value of cmc can often be much more readily determined than pairs of corresponding values of C_{A1} and C_{AN}.

1.4.4 Enthalpy of Micelle Formation

For the simple mass action model the standard enthalpy of micelle formation is given by the equation,

$$\Delta H_N^\circ = -T^2 \left(\frac{\partial(\Delta G_N^\circ/T)}{\partial T}\right)_p \qquad (1\text{-}25)$$

If equation (1-22) is used for ΔG_N° the following expression is obtained for ΔH_N° in an ideal system,

$$\Delta H_N^\circ = \left(\frac{RT^2}{N}\right)\left(\frac{\partial \ln x_{AN}}{\partial T}\right)_p - RT^2 \left(\frac{\partial \ln x_{A1}}{\partial T}\right)_p \qquad (1\text{-}26)$$

If the approximate expression in equation (1-24) is used for ΔG_N° then,

$$\Delta H_N^\circ = -RT^2 \left(\frac{\partial \ln \text{cmc}}{\partial T}\right)_p \qquad (1\text{-}27)$$

Equation (1-27) has frequently been used for the estimation of enthalpies of micellization because of its convenience. Unfortunately for many micellar systems the degree of association is itself temperature

dependent. Under these circumstances the simple mass action model becomes invalid if it is applied at more than one temperature since the micelle species would be different at each temperature. Equations (1-26) and (1-27) therefore do not offer a valid means of determining ΔH_N°. It is also well known that micelles tend to be polydisperse rather than monodisperse, although micelle formation is usually characterized by a narrow micelle size distribution. The simple mass action model would require a different K_N, and hence ΔG_N° and ΔH_N°, for each size of micelle present at any given temperature.

It is possible to modify the simple mass action model in such a way that a valid expression for ΔH_N° in terms of the temperature coefficients of the concentrations can be obtained to take the place of equation (1-26). Allowance can also be made for the effect of polydispersity in the micelles. This modification is described in the following section.

1.4.5 Ideal Associated Solution Model

The concept of an ideal associated solution has been well described by Prigogine and Defay (1954), and Hall and Pethica (1967) have shown that this model can be applied to a micelle forming system. Only a brief outline of the treatment will be given here.

Consider a solution made up by mixing n_A moles of A (solute) and n_s moles of S (solvent) such that the respective macroscopic chemical potentials are given by,

$$\mu_A = \mu_A^\circ + RT \ln x_A f_A \qquad (1\text{-}28)$$

$$\text{and } \mu_s = \mu_s^\circ + RT \ln x_s f_s \qquad (1\text{-}29)$$

where superscript $^\circ$ denotes a property of a reference state. The mole fractions x_A and x_s are defined as,

$$x_A = \frac{n_A}{(n_A + n_s)} \; ; \qquad x_s = \frac{n_s}{(n_A + n_s)}$$

Suppose there exist in this solution associated species of various

sizes (denoted by A_N, where N is any positive integer greater than 1) formed from the solute monomers (denoted by A_1). If each of the associated species is in equilibrium with the monomers, then for each N,

$$\mu_{AN} = N\mu_{A1} \tag{1-30}$$

It can be readily shown for such a system that,

$$\mu_A = \mu_{A1} \tag{1-31}$$

Suppose now that at equilibrium there are n_{AN} associated species of size N and n_{A1} free monomers such that,

$$n_A = n_{A1} + \sum_N N n_{AN}$$

Let the symbol n_m be used for the total number of moles of associated species, where the subscript m indicates all micelles regardless of size. Thus,

$$n_m = \sum_N n_{AN}$$

The mole fractions x_{A1} and $x_{s'}$ are then defined by,

$$x_{A1} = \frac{n_{A1}}{(n_{A1} + n_m + n_s)} ; \qquad x_{s'} = \frac{n_s}{(n_{A1} + n_m + n_s)}$$

In this solution at equilibrium there can be no strong intermolecular interactions between the various independent molecules or associated species because any such interactions present in the original mixture have already led to association. If any deviations from ideality which arise from the different sizes and shapes of the associated species, monomers and solvent molecules are neglected there will be an ideal mixture of associated species, monomers and solvent. The chemical potentials of the monomer and solvent molecules in this solution are given by,

$$\mu_{A1} = \mu_1^\circ + RT \ln x_{A1} \tag{1-32}$$

$$\mu_{s'} = \mu_{s'}^\circ + RT \ln x_{s'} \tag{1-33}$$

It can be deduced from equations (1-28), (1-31) and (1-32) that,

$$\mu_A^\circ + RT \ln x_A f_A = \mu_{A1}^\circ + RT \ln x_{A1} \qquad (1\text{-}34)$$

Similarly,

$$\mu_S^\circ + RT \ln x_S f_S = \mu_{S'}^\circ + RT \ln x_{S'} \qquad (1\text{-}35)$$

From (1-34) and (1-35),

$$f_A = \left(\frac{x_{A1}}{x_A} \right) \exp \left(\frac{\mu_{A1}^\circ - \mu_A^\circ}{RT} \right) \qquad (1\text{-}36)$$

and $$f_S = \left(\frac{x_{S'}}{x_S} \right) \exp \left(\frac{\mu_{S'}^\circ - \mu_S^\circ}{RT} \right) \qquad (1\text{-}37)$$

It is convenient to regard a micelle forming system as a dilute solution of A in S, and to employ as a reference state an infinitely dilute solution of A in S. As $x_A \longrightarrow 0$, $x_{A1}/x_A \longrightarrow 1$ since A is only present as monomers at infinite dilution. From equation (1-34) it follows that for this reference system $\mu_{A1}^\circ = \mu_A^\circ$ and hence from equation (1-36),

$$f_A = \frac{x_{A1}}{x_A} \qquad (1\text{-}38)$$

Also as $x_S \longrightarrow 1$, $f_S \longrightarrow 1$ and $x_{S'} \longrightarrow 1$ so that from equation (1-35) $\mu_{S'}^\circ = \mu_S^\circ$ and hence from equation (1-37),

$$f_S = \frac{x_{S'}}{x_S} \qquad (1\text{-}39)$$

Thus, for the ideal associated solution f_A and f_S depend only on the extent of the association. The number average degree of association ($\bar{N}$) is given by,

$$\bar{N} = \frac{\sum_N N n_{AN}}{\sum_N n_{AN}} = \frac{\sum_N N n_{AN}}{n_m} \qquad (1\text{-}40)$$

Since the solute monomers and the associated species behave ideally, and the effect of differences between sizes or shapes of associated species are neglected, the respective chemical potentials are given by,

$$\mu_{A1} = \mu^{\circ}_{A1} + RT \ln x_{A1} \qquad (1\text{-}41)$$

$$\text{and } \mu_m = \mu^{\circ}_m + RT \ln x_m \qquad (1\text{-}42)$$

$$\text{where } x_m = \frac{n_m}{(n_{A1} + n_m + n_s)}$$

μ_m defined by equation (1-42) will be an average value for all of the n_m associated species , which have the number average degree of association, $\bar{N}$. The average chemical potential for the associated species can also be defined as,

$$\mu_m = \frac{\sum_N n_{AN}\, \mu_{AN}}{\sum_N n_{AN}} \qquad (1\text{-}43)$$

Substitution of the expression for μ_{AN} from equation (1-30) into (1-43) gives,

$$\mu_m = \frac{\sum_N \mu_{A1}\, (N\, n_{AN})}{\sum_N n_{AN}}$$

which reduces to the following expression on combination with equation (1-40),

$$\mu_m = \bar{N}\, \mu_{A1} \qquad (1\text{-}44)$$

From equations (1-41), (1-42) and (1-44) it follows that the average standard free energy change per mole of monomer for the association process ($\Delta G^{\circ}_{\bar{N}}$) is given by,

$$\Delta G^{\circ}_{\bar{N}} \equiv \left(\frac{\mu^{\circ}_m}{\bar{N}} - \mu^{\circ}_{A1} \right) = -\left(\frac{RT}{\bar{N}} \right) \ln x_m + RT \ln x_{A1} \qquad (1\text{-}45)$$

Equation (1-45) is analogous to (1-22) derived from the simple mass action model but with N replaced by $\bar{N}$, thus allowing for polydispersity among the micelles. It will be convenient for later analysis of results to define an "average" equilibrium constant ($K_{\bar{N}}$) for the polydisperse system such that,

$$\Delta G^{\circ}_{\bar{N}} = -\left(\frac{RT}{\bar{N}} \right) \ln K_{\bar{N}} \qquad (1\text{-}46)$$

$$\text{where } K_{\bar{N}} = \frac{x_m}{x_{A1}^{\bar{N}}} \qquad (1\text{-}47)$$

The use of $K_{\bar{N}}$ implies that the polydisperse system can be regarded as a monodisperse system with micelles of size $\bar{N}$.

The heat of mixing for an ideal mixture of n_A moles of A and n_s moles of S is given by,

$$-\frac{\Delta H_{mix}}{RT^2} = n_A\left(\frac{\partial \ln f_A}{\partial T}\right)_p + n_s\left(\frac{\partial \ln f_s}{\partial T}\right)_p \qquad (1\text{-}48)$$

Combination of (1-48) with (1-38) and (1-39) gives for the ideal associated solution,

$$-\frac{\Delta H_{mix}}{RT^2} = n_A\left(\frac{\partial \ln x_{A1}}{\partial T}\right)_p + n_s\left(\frac{\partial \ln x_{s'}}{\partial T}\right)_p \qquad (1\text{-}49)$$

The heat of mixing in equations (1-48) and (1-49) will be equal to the sum of the heats of formation from their monomers of all the associated species present at equilibrium in the system, so that

$$\Delta H_{mix} = \bar{N}\, n_m\, \Delta H^{\circ}_{\bar{N}} \qquad (1\text{-}50)$$

where $\Delta H^{\circ}_{\bar{N}}$ is the average standard enthalpy change per mole of monomer for forming a micelle from its pure components. Substitution of equation (1-50) into (1-49) gives,

$$-\frac{\bar{N}\, n_m\, \Delta H^{\circ}_{\bar{N}}}{RT^2} = n_A\left(\frac{\partial \ln x_{A1}}{\partial T}\right)_p + n_s\left(\frac{\partial \ln x_{s'}}{\partial T}\right)_p \qquad (1\text{-}51)$$

Now consider the system in terms of n_{A1} moles of A monomers, n_m moles of associated species and n_s moles of solvent. According to the Gibbs-Duhem equation,

$$n_{A1}\left(\frac{\partial \ln x_{A1}}{\partial T}\right)_p + n_m\left(\frac{\partial \ln x_m}{\partial T}\right)_p + n_s\left(\frac{\partial \ln x_{s'}}{\partial T}\right)_p = 0 \qquad (1\text{-}52)$$

If it is noted that,

$$n_A = n_{A1} + \bar{N}\, n_m \qquad (1\text{-}53)$$

by eliminating n_s between equations (1-51) and (1-52) the following

expression for $\Delta H^{\circ}_{\bar{N}}$ is obtained,

$$\Delta H^{\circ}_{\bar{N}} = \left(\frac{RT^2}{\bar{N}}\right)\left(\frac{\partial \ln x_m}{\partial T}\right)_p - RT^2\left(\frac{\partial \ln x_{A1}}{\partial T}\right)_p \qquad (1\text{-}54)$$

Equation (1-54) can be used to evaluate $\Delta H^{\circ}_{\bar{N}}$ if the temperature coefficients of $\ln x_{A1}$ and $\ln x_m$ can be determined. In practice it is usually difficult to evaluate these coefficients experimentally very precisely and it is therefore preferable to determine $\Delta H^{\circ}_{\bar{N}}$ by calorimetric methods. It should be noted that differentiation of $\Delta G^{\circ}_{\bar{N}}/T$ with respect to T at constant P for the ideal associated solution model does not give expression (1-54) for $\Delta H^{\circ}_{\bar{N}}$ if $\bar{N}$ varies with temperature. Temperature variation of $\bar{N}$ has not been ruled out in this treatment since the only restrictions on the differentiation in equation (1-48) are those of constant P, n_A and n_s.

The temperature coefficient of $\Delta H^{\circ}_{\bar{N}}$ can be used to evaluate the change in the standard heat capacity at constant pressure (ΔC°_p), that is

$$\Delta C^{\circ}_p = \left(\frac{\partial \Delta H^{\circ}_{\bar{N}}}{\partial T}\right)_p \qquad (1\text{-}55)$$

The standard entropy of micelle formation ($\Delta S^{\circ}_{\bar{N}}$) can be determined from $\Delta G^{\circ}_{\bar{N}}$ and $\Delta H^{\circ}_{\bar{N}}$ by the following expression,

$$\Delta S^{\circ}_{\bar{N}} = \frac{\Delta H^{\circ}_{\bar{N}} - \Delta G^{\circ}_{\bar{N}}}{T} \qquad (1\text{-}56)$$

1.5 Present Work

The self-association of β-casein appears to have some of the characteristics of synthetic detergent systems. It was decided to examine the self-association of the detergent Brij 35 and to compare this behaviour with that of β-casein A[1]. Brij 35 is a polyoxyethylene dodecyl ether and its formula can be written as $CH_3(CH_2)_{11}O(CH_2CH_2O)_{23}H$. It consists of a straight 12-carbon chain linked to 23 oxyethylene

(CH_2CH_2O) units. A slight degree of heterogeneity is expected to occur in the length of the polyoxyethylene chain of this type of molecule (Ikeda and Kakuichi, 1967; Biaselle and Millar, 1975), however the hydrocarbon chain will have definite length. The formula molar mass of the monomer unit is 1198 g mol^{-1}. The polyoxyethylene chain is polar whereas the dodecyl hydrocarbon chain is nonpolar, hence Brij 35 is an amphiphile. The molecule is classed as a nonionic detergent since the polar section, or head group, does not carry any charge.

Brij 35 would be expected to associate to form micelles in aqueous solution owing to its amphiphilic nature. Light scattering studies (Becher, 1961) indicate that a micelle with a molar mass of about 48,000 g mol^{-1} is formed in aqueous solution giving a degree of association of 40. Brij 35 cannot be regarded as a close model system for β-casein because Brij 35 is uncharged whereas β-casein carries a net negative charge and is therefore anionic. However, both Brij 35 and β-casein have long chain head groups whereas most of the available synthetic ionic detergents have small head groups attached to a long hydrocarbon chain. Also, the ionic strength of the β-casein solutions used in this study was relatively high, and the behaviour of ionic amphiphiles approaches that of nonionic amphiphiles as the ionic strength of the solution is increased. The magnitude of the degree of association for the two systems is also similar.

By using the same techniques to study the behaviour of both Brij 35 and β-casein in solution it was hoped to be able to determine whether β-casein does in fact closely resemble a detergent in its association behaviour. The work carried out for this thesis involved establishing values for some of the thermodynamic parameters associated with the self-association of β-casein A^1 and Brij 35 using the techniques of microcalorimetry, ultracentrifugation, surface tension measurement and pycnometry. This allowed some conclusions to be drawn regarding the

nature of the self-association processes involved in these systems. Experience was also gained in the various experimental techniques by using the relatively abundant supply of Brij 35 before attempting similar studies on the limited quantity of purified β-casein A^1 available.

CHAPTER 2

PREPARATION

2. PREPARATION

2.1 Purification of β-Casein A^1

The solutions of β-casein A^1 used in this study were prepared from the milk of twin Friesan cows which had been typed by Dr L.K. Creamer, of the N.Z. Dairy Research Institute, as having the A^1 variant only. Whole casein was separated from the milk by isoelectric precipitation at pH 4.6 (McKenzie, 1971) and the β-casein was isolated from the α-, γ- and κ- caseins by the method of Thompson (1966) which involves DEAE-cellulose-urea column chromatography with salt gradient elution. The various proteins were detected in the column fractions by alkaline disc gel electrophoresis and the fractions containing only β-casein A^1 were exhaustively dialysed against deionized water to complete the procedure. The experimental details for the purification procedure are given in the following sections.

2.1.1 Preparation of Acid Casein

Two litres of skim milk were heated to 30°C and the pH reduced to 4.6 by the addition of 1M HCl with stirring. The precipitated acid casein was filtered off and washed several times with distilled water. Excess water was removed from the casein precipitate and the damp acid casein was stored frozen until required for the β-casein isolation procedure.

2.1.2 DEAE-Cellulose-Urea Chromatography

An anion-exchange column (height 40cm, diameter 2.5cm) was set up using Whatman DE-52 DEAE-cellulose resin. The column was equilibrated with a buffer solution containing 4.5M urea, 0.1% 2-mercaptoethanol and 0.01M imidazole-HCl buffer at pH 7.0. Approximately 2g (wet weight) of the acid casein was added to $15cm^3$ of the imidazole-HCl buffer and the casein was dissolved by the dropwise addition of 1M NaOH with stirring to adjust the pH to 7.0. Sample preparation was completed by the addition of 3 drops of 2-mercaptoethanol to the solution.

The casein sample was adsorbed on to the top of the anion-exchange column and a salt gradient was set up by connecting $500cm^3$ of 0.3M NaCl in the imidazole-HCl buffer with a siphon tube to $500cm^3$ of imidazole-HCl buffer only. A second tube was run from the buffer to the top of the column via a Pharmacia P-3 peristaltic pump. The buffer was stirred with a magnetic stirrer during chromatography to ensure uniform mixing of the NaCl-buffer solution which siphoned across. A Gilson fraction collector was used to collect the eluate from the column. The flow rate through the column was set at about $50cm^3$ per hour, and the fraction collector speed was set at 6 fractions per hour to give a volume of about $8cm^3$ for each fraction. The column was run at room temperature and a total of 120 fractions was collected. The absorbance at 280nm (A_{280}) was measured for each fraction using a Hilger and Watts Uvichem Spectrophotometer and the results were plotted against the fraction number to produce an elution profile as shown in Figure (2-1).

2.1.3 Disc Gel Electrophoresis

The type of casein present in the fractions corresponding to the various peaks of the elution profile was determined by alkaline poly-acrylamide disc gel electrophoresis (Davis, 1964) in the presence of 5.5M urea. 7.5% acrylamide gels were run in 0.1M Tris-glycine buffer at pH 8.9 containing $0.5cm^3$ of 0.1% bromophenol blue per litre as a marker for the progress of the electrophoretic front. Electrophoresis was carried out using 20µl samples of the fractions being tested. A sample of the casein solution taken prior to the column chromatography was also run as a reference. The gels took about $1\frac{1}{2}$ hours to run with a current of 5mA per tube. The gels were stained with 0.1% amido black in 7% acetic acid for a minimum of 1 hour. Destaining was carried out using destaining tubes in the electrophoresis apparatus by running the gels in 3% acetic acid at 7mA per tube for about 1 hour. The gels were stored in test tubes in 3% acetic acid.

Figure (2-1) Elution Profile for DEAE-Cellulose-Urea Chromatography of Whole Casein

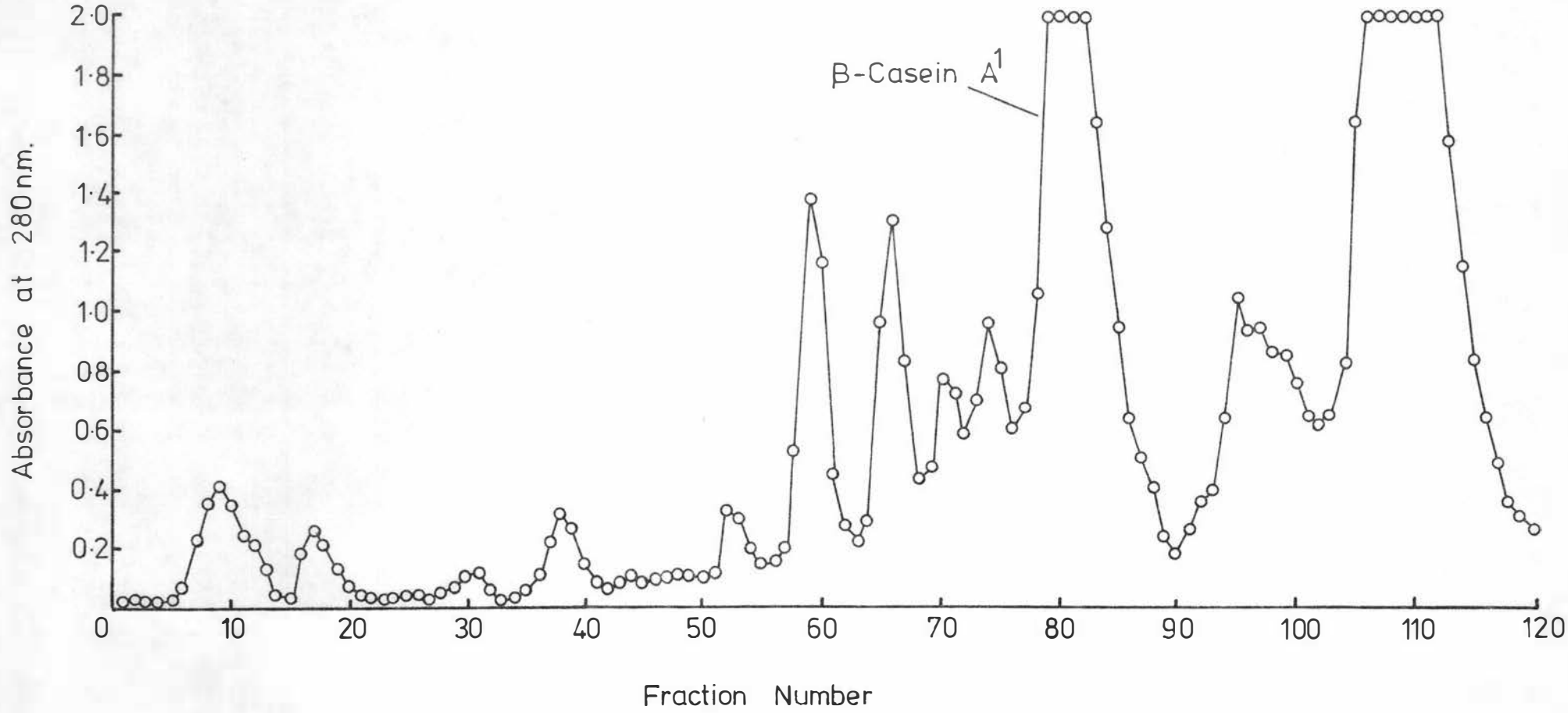

The type of casein present in each of the fractions tested was identified by comparing the electrophoretic bands with the bands observed for the reference sample. The identity of each of the bands in the reference sample was determined from McKenzie (1971) and Thompson (1971). In this way the peak labelled β-casein A^1 in the elution profile of Figure (2-1) was identified. The electrophoresis patterns for the fraction at the centre of this peak and for the whole casein sample are illustrated in Figure (2-2).

2.1.4 Dialysis

The fractions which exhibited a single electrophoretic band corresponding to β-casein A^1 were combined and exhaustively dialysed against distilled water at $4^{\circ}C$ for 1 to 2 days to remove the buffer and urea present in solution. At the completion of the dialysis an alkaline disc gel electrophoresis run was carried out on a sample of the protein solution to check that only a single band was still observed. The β-casein A^1 solution, which will be referred to as stock β-casein A^1 solution, was then stored frozen until required for further use.

2.1.5 Concentration Determination

The concentration of the β-casein A^1 solutions was determined from absorbance measurements using a Unicam SP 500 spectrophotometer. The absorbance at 280nm (A_{280}) was corrected for light scattering by subtracting 1.7 times the absorbance at 320nm (A_{320}) from A_{280} (Waugh et al., 1970). The absorbance measurements were converted to protein concentration in units of mg cm^{-3} by using the value of 0.46cm^{-1} mg^{-1} cm^3 for the absorptivity of β-casein A (Thompson and Pepper, 1964). For a cell of 1cm path length the concentration in mg cm^{-3} is therefore given by

$$C = \frac{A_{280} - 1.7A_{320}}{0.46} \qquad (2\text{-}1)$$

Figure (2-2) Alkaline Polyacrylamide Disc Gel Electrophoresis of Whole Casein and β-Casein A^1

The left hand gel contains a sample of the whole casein taken before the column chromatography. The right hand gel contains β-casein A^1 from the labelled peak of the elution profile of Figure (2-1). The gels were run in 0.1M Tris-glycine buffer at pH 8.9.

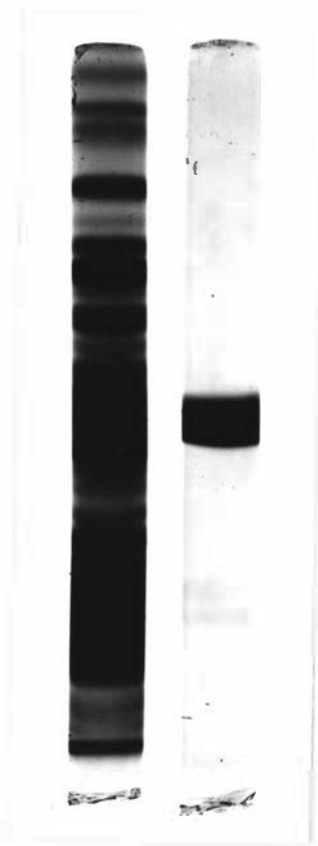

2.2 Preparation of Brij 35

Commercially manufactured Brij 35 (Koch-Light Laboratories) was used without further purification for making up the Brij 35 solutions used in this study. The Brij 35 (a solid at room temperature) was stored in a vacuum dessicator prior to weighing out, in order to minimize errors in the weight of the pure material which could arise from absorption of water from the atmosphere.

CHAPTER 3

MICROCALORIMETRY

3. MICROCALORIMETRY

3.1 Introduction

The standard enthalpy of micelle formation (ΔH_N°) can be determined from equation (1-54) if the temperature coefficients of the mole fractions of the solute species are known. However, for micelle forming systems it is preferable to determine ΔH_N° directly by using calorimetric methods (Benjamin, 1963; Holtzer and Holtzer, 1974; Franks and Reid, 1974; Fisher and Oakenfull, 1977). For a process occurring at constant pressure the enthalpy change (ΔH) is equal to the heat evolved or absorbed during the process (q), that is

$$\Delta H = q$$

The heat change can be measured directly by calorimetry. For processes which occur in solution the value of ΔH determined by calorimetry is very close to the value of the standard enthalpy change (ΔH°) if the solution is very dilute. Thus, for dilute solutions

$$\Delta H^\circ \simeq q$$

When a solution containing a micelle forming system is diluted with solvent, the equilibrium between the free monomers and the micelles is perturbed in such a way that some of the micelles dissociate to increase the proportion of free monomers and thus re-establish the equilibrium. Suppose that the system contained initially n_{A1}^i moles of monomers, n_m^i moles of micelles and n_s^i moles of solvent (the superscript i refers to the initial system, i.e. before dilution). The system is then diluted by the addition of solvent so that there are finally n_s^f moles of solvent, and n_{A1}^f and n_m^f moles of monomers and micelles respectively after the equilibrium is re-established (the superscript f referring to the final system, i.e. after dilution and dissociation). The total heat change which occurs during the above process will be denoted by q_{obs}. The process can be represented by,

$$n^i_{A1} + n^i_m + n^i_s \xrightarrow{q_{obs}} n^f_{A1} + n^f_m + n^f_s$$

There are two contributions to q_{obs}; the heat of dilution (q_{dil}) which accompanies the dilution of the solute species and the heat of dissociation (q_{diss}) which accompanies the dissociation process which occurs to re-establish the equilibrium. Thus, q_{obs} can be written as

$$q_{obs} = q_{diss} + q_{dil} \tag{3-1}$$

If the assumption is made that q_{dil} is negligible compared to q_{diss}, then

$$q_{obs} \simeq q_{diss} \tag{3-2}$$

The number of moles of monomer which become dissociated from the micelle state on dilution (Δn_{A1}) is given by,

$$\Delta n_{A1} = n^f_{A1} - n^i_{A1} \tag{3-3}$$

q_{diss} gives the overall heat change which accompanies the dissociation of Δn_{A1} moles of monomer. The enthalpy of micelle formation is the heat change per mole of monomer for the association process and is therefore opposite in sign to q_{diss}. For a dilute solution $\blacktriangle H^\circ_N$ is thus given by,

$$\Delta H^\circ_N = - \frac{q_{diss}}{\Delta n_{A1}} \tag{3-4}$$

q_{diss} can be measured by calorimetry, and Δn_{A1} is usually determined by some other technique. The determination of Δn_{A1} for the systems studied in this thesis is outlined in Chapter 8.

Special difficulties arise when calorimetric studies are attempted on macromolecular systems in solution. As previously noted, it is necessary to work with dilute solutions if the heat changes are to be directly related to standard enthalpy changes. This condition, coupled with the high molecular weights of macromolecules, generally results in a small heat change per unit volume of solution. Therefore, if the

heat changes are being measured in a conventional calorimeter (i.e. instruments that measure heat changes in the range of a few joules) large volumes of solution are required to produce a heat change of sufficient magnitude to be measured accurately. For many macromolecular systems, particularly those of biological origin, there is not a great amount of the purified material readily available and therefore it is not feasible to use large quantities. These problems have been largely overcome by the recent development of microcalorimeters (Wadso, 1970) which can measure heat changes in the microjoule range and require only small volumes of solution. In this study the heat changes associated with the dilution of small volumes of dilute Brij 35 and β-casein A[1] solutions were measured using an LKB 10700-2 Batch Microcalorimeter. The results were used to determine the standard enthalpy of association for these systems. A description of the microcalorimeter and the experimental techniques used is given in the following sections.

3.2 Description of the Microcalorimeter

In the batch calorimetric technique the two liquids which are to be mixed are placed in separate compartments of the calorimeter cell. After thermal equilibrium has been achieved the contents of the compartments are mixed by inverting the cell and the heat absorbed or released during this mixing process is recorded. The LKB 10700-2 Batch Microcalorimeter operates on the heat-leak principle; any heat change in the reaction vessel results in the conduction of heat to or from a surrounding heat sink of large heat capacity. This heat flow takes place through thermopiles where it is detected as a voltage. The overall heat change is proportional to the area under the voltage-time curve (Wadso, 1970). The microcalorimeter also operates on the twin principle, that is, there is a reference cell in addition to the reaction cell, and the thermopiles surrounding the reference cell are connected in opposition to those of the reaction cell. This cancels out the effect of external temperature

variations, and the voltage changes caused by the heat of friction during mixing in the reaction cell are largely offset by the similar changes produced by the reference liquids.

An LKB 10717 Calorimeter Unit was used which consists of a cylindrical aluminium heat sink containing two gold cells. The heat sink is insulated from the surrounding air by a layer of expanded polystyrene and also incorporates a heater to reduce the time taken to come to thermal equilibrium from a lower to a higher temperature. Each of the two cells contains two compartments; one holding a maximum volume of $4cm^3$ and the other a maximum volume of $2cm^3$. An electrical calibration heater is situated in the larger of the two compartments. The cells are connected to the heat sink by a series of thermopiles. The calorimeter unit can be rotated according to a set cycle which mixes and stirs the contents of the cell compartments.

The Calorimeter Unit was suspended in an LKB 10704 Thermostatic Air Bath, in which the air is circulated by means of a fan and the temperature is controlled by a thermistor. Water from an external water bath is circulated through a copper coil set in the air bath to produce a cooling effect, although this was not necessary for air bath temperatures more than $10^{\circ}C$ above room temperature. The range of controlled temperature available with this unit is from $20^{\circ}C$ to $40^{\circ}C$. The air bath temperature was measured with a Hewlett-Packard 2801A quartz thermometer.

An LKB 10746 Control Unit was used to operate the calorimeter. This unit contains the controls for the calibration current, calibration timer, mixing cycle and heat sink heater and also contains a calorimeter temperature indicator. A range of calibration currents from 1 to 100mA can be passed through either calibration heater for a time interval range from 1 to 9900 seconds.

The voltage produced in the thermopiles of the calorimeter was amplified using a Keithly Instruments 150 B Microvolt Ammeter which has

a full scale output voltage of ± 100mV. The full scale input voltage settings range from ± 1000mV down to ± 0.3μV. The voltage-time curves were recorded by a Servogor RE 512 Recorder-Integrator, which records the curves on chart paper. The full scale voltage settings available range from 20V to 2mV and the chart speeds range from 10mm per hour to 200mm per minute. The area under the curves is determined by a ball and disc integrator with the number of peaks produced by the integrator pen being proportional to the area under the curve.

Figure (3-1) shows schematically the interrelationship between the various units of the LKB Batch Microcalorimeter and also the form of the mixing cycle which rotates the Calorimeter Unit.

3.3 General Experimental Technique

A typical dilution experiment involved the addition of known volumes of solution and solvent to the relevant compartments of the reaction cell. Similar volumes of solvent only were added to the two compartments of the reference cell. The calorimeter was then allowed to come to thermal equilibrium at the required temperature, which usually took about 3 to 4 hours. Thermal equilibrium was considered to be achieved when the pen trace of the recorder was parallel to the time axis. The full scale voltage settings of the amplifier and recorder were determined from a trial run and the amplification which would give the largest possible peak on the chart recorder for the expected heat change was used. After thermal equilibrium was reached the mixing cycle was started and the heat absorbed or evolved during the dilution experiment was recorded as a peak by the recorder pen. When the pen had returned to a baseline the trace was allowed to continue for several minutes and then the mixing cycle was repeated to determine the uncompensated heat of friction which resulted from the mixing process. This was followed by an electrical calibration run which involved passing a known quantity of heat into the reaction cell via the calibration heater. The current and

Figure (3-1) Schematic Diagram of LKB Batch Microcalorimeter

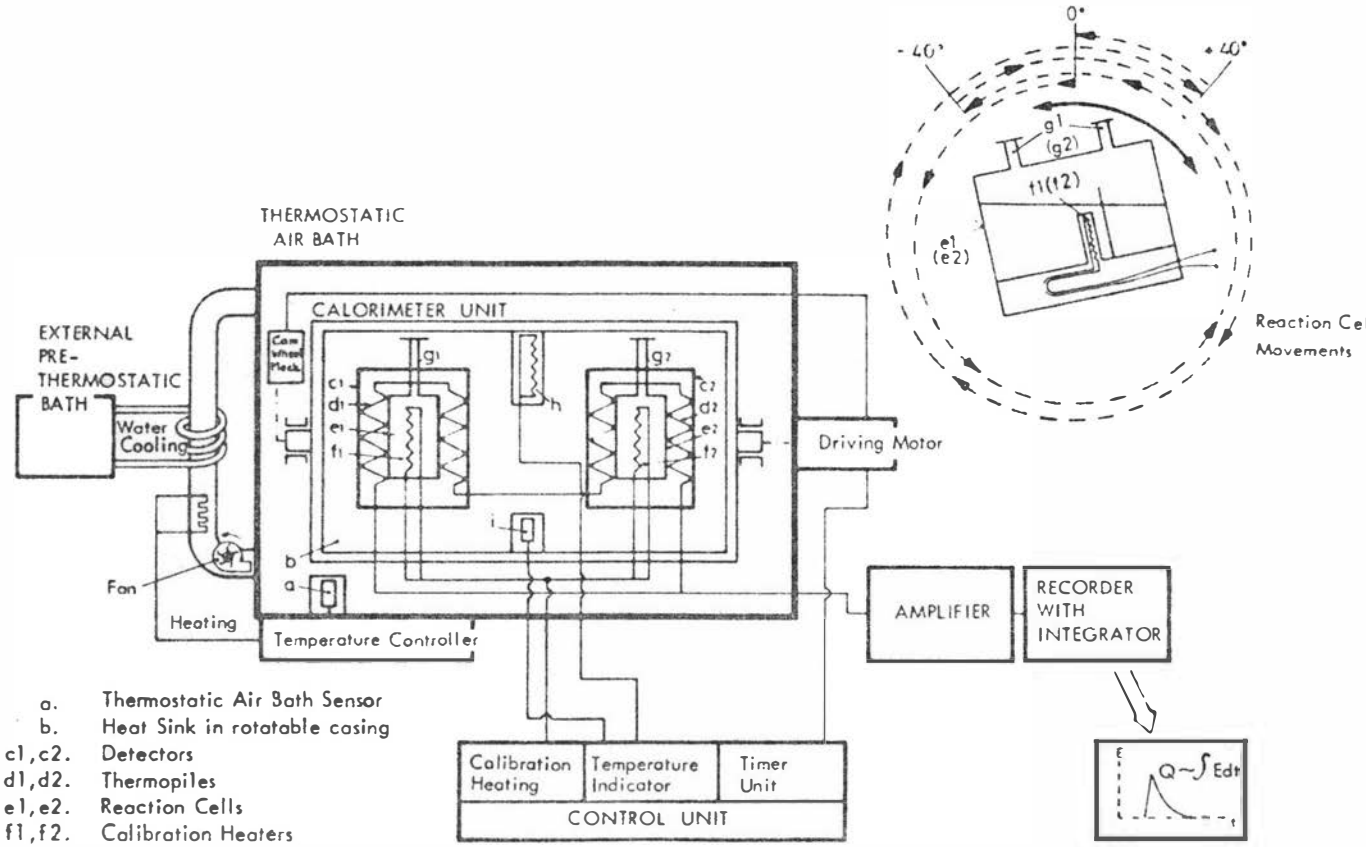

time settings were chosen to give a peak of similar shape and area to the reaction peak. The mixing cycle was usually operated during the calibration run to give equality of conditions with the reaction run. The baseline traces after both the friction and calibration peaks were allowed to continue as for the reaction peak.

The baseline position recorded after a run should be identical to that recorded before the run. However, in practice it was found that the following two different phenomena sometimes occurred.

(i) Baseline shift

This was characterized by the post-run baseline position being either higher or lower on the chart than the pre-run baseline. It was found that there was usually no significant variation in the heat of reaction value between "well behaved" runs and those involving a shifted baseline if the post-run baseline was used as the reference baseline. This procedure was the same as that followed by Wadsö (1968) who also observed baseline shift effects.

(ii) Baseline drift

This was indicated by a linear baseline which had a definite positive or negative gradient. Runs involving appreciable baseline drift were discarded owing to the uncertainty of establishing the true baseline position. Baseline drift is thought to result from an appreciable fluctuation in room temperature over the equilibration period (Wadsö, 1968).

The above phenomena became more of a problem at higher amplifications. For runs which involved relatively low amplifications both baseline shift and drift were negligible.

The heat change (q) associated with a calorimetric run is proportional to the net area (A) under the voltage-time curve recorded during the run, that is

$$q \propto \int_{t_1}^{t_2} E\,dt = A$$

where t_1 is the time at the start of the run, t_2 is the time at the end of the run and E is the recorder pen deflection (or voltage). The proportionality constant relating the heat change with the peak area is called the calibration constant ($\mathcal{E}$), thus

$$q = \int_{t_1}^{t_2} Edt = \mathcal{E}.A$$

The net area under a voltage-time curve was determined by subtracting the area under the baseline (A_b) from the total area (A_t). This is illustrated in Figure (3-2). Thus,

$$A = A_t - A_b \qquad (3\text{-}5)$$

The value of A_b is determined by means of the integrator using the following expression,

$$A_b = N_2 \left(\frac{l_1}{l_2} \right) \qquad (3\text{-}6)$$

where l_1 is the length of the reaction run, l_2 is the length of the baseline run and N_2 is the number of integrator peaks over l_2. If A_t in peak units is denoted by N_1 then from equations (3-5) and (3-6) A is given by

$$A = N_1 - N_2 \left(\frac{l_1}{l_2} \right)$$

Any run which involved the mixing cycle had the contribution from the uncompensated heat of friction included in the total heat evolved or absorbed. Therefore, the net area under the friction run curve (A_f) was subtracted from the net area under these reaction run curves. For dilution runs the contribution to A from the heat of reaction (A_r) is given by

$$A_r = A - A_f$$

Similarly, the contribution to A from the calibration heat (A_c) for calibration runs which involve the mixing cycle is given by

$$A_c = A - A_f$$

Figure (3-2) Voltage-Time Curve for a Typical Calorimetry Experiment

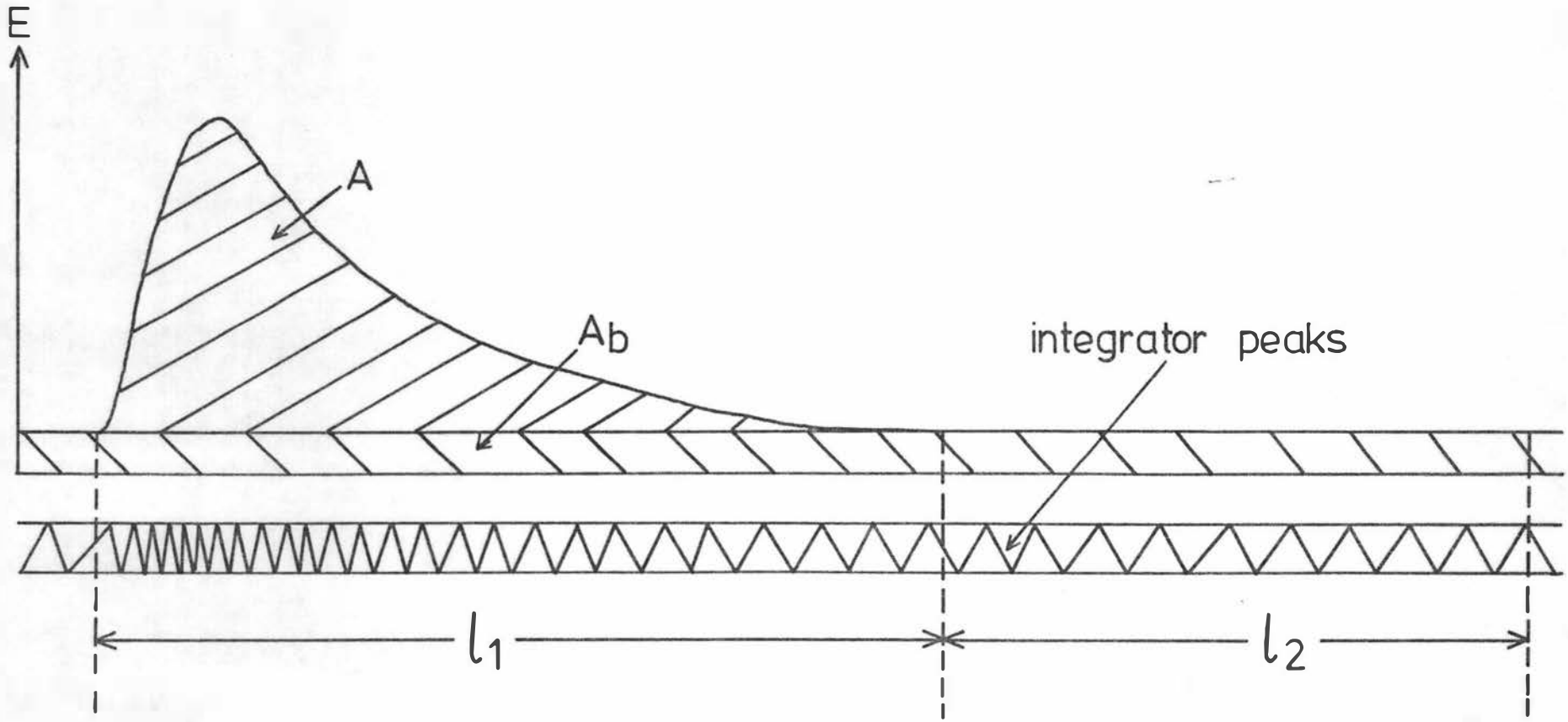

For calibration runs during which the mixing cycle is not operated no allowance for heat of friction is made, therefore,

$$A_c = A$$

The calibration constant ($\mathcal{E}$) for a reaction run is determined from the peak area of the calibration run (A_c) by the expression

$$\mathcal{E} = \frac{q_c}{A_c}$$

where q_c is the electrical calibration heat released by the calibration heater. q_c is related to the calibration current (i_c) and the time for which the calibration current runs (t_c) by

$$q_c = \frac{i_c^2 \cdot R_c \cdot t_c}{10^3} \qquad (3\text{-}7)$$

where R_c is the calibration heater resistance. Equation (3-7) gives q_c in mJ units if i_c is in mA, t_c in secs and R_c in ohms. The value of R_c for the calibration heater used in these experiments was 50.076 ohms (given by the specifications accompanying the instrument). The heat change associated with a reaction run (q_r) is given by the expression,

$$q_r = \mathcal{E} A_r$$

After the completion of each experiment the cell contents were sucked out with a syringe and the cells filled with deionized water. The mixing cycle was operated and the water was then sucked out. This washing procedure was repeated again using deionized water and then twice with acetone (Koch-Light AR). After most of the acetone had been removed the cells were dried by blowing dry air through each compartment for several minutes.

3.4 Calorimeter Calibration

The calibration constant for the calorimeter is related to the amplifier and recorder voltage settings and also to the chart speed of the recorder. The precision to which ε can be calculated determines the maximum precision to which the heat of any reaction run can be determined. The β-casein dilution runs gave heat changes close to the lower limit of the sensitivity of the instrument which is stated by the manufacturers to be about 0.2mJ. Therefore, it was decided to calculate ε values for a range of calibration heats in this energy region as this would give an indication of the maximum degree of precision which could be expected. A series of electrical calibration runs were carried out at 21, 25, 30 and 40°C. Both the reaction and reference cells were loaded with $2cm^3$ and $3cm^3$ of deionized water in the smaller and larger compartments respectively. The calorimeter was not rotated during these calibration runs so there was no contribution from uncompensated heat of friction. An amplifier setting of 10μV, a recorder setting of 20mV and a chart speed of 40mm min^{-1} were used for all of these runs. The precision in calorimetry is usually expressed as the standard deviation of the mean (s_x) (Skinner, 1969) where,

$$s_x = \sqrt{\frac{\sum_i^n (X_i - \bar{X})^2}{n(n-1)}}$$

where X_i is the value of the ith measurement, $\bar{X}$ is the mean value of n measurements and n is the total number of measurements. At any given temperature at least 5 runs were carried out for each value of q_c. The results are set out in Table (3-1).

It can be seen from Table (3-1) that there is no significant trend in the value of $\bar{\varepsilon}$ at any of the temperatures studied as q_c is varied in the range 0.25mJ to 2.50mJ. It is also apparent that $\bar{\varepsilon}$ does not show a significant variation as the temperature is increased from 21°C to 40°C. Therefore, it can be concluded that the value of $\bar{\varepsilon}$ is independent of

both the size of the calibration current and the temperature of the calorimeter. However, the precision to which $\bar{\mathcal{E}}$ can be measured significantly decreases as the magnitude of the calibration current decreases. When the standard deviation ($s_{\mathcal{E}}$) is expressed as a percentage of $\bar{\mathcal{E}}$ the precision can be determined from Table (3-1) to be about $\pm$ 1% for a q_c of 2.50mJ, whereas for a q_c of 0.25mJ the precision is about $\pm$ 5%.

The accuracy of the calorimeter was determined by measuring the heat of dilution of sucrose solutions at 25°C and comparing the results with values calculated from the literature. The heats of dilution were calculated from the data of Gucker et al. (1939) who gave the following expression for the apparent relative molal heat content (ϕL_2) for sucrose at 25°C,

$$\phi L_2 = 134.6m - 7.05m^2$$

where m is the molality of the sucrose solution. If m_i is the molality before dilution and m_f the molality after dilution then the calculated heat of dilution (q_{calc}) is given by the following equation,

$$q_{calc} = \phi L_2^f - \phi L_2^i$$

where $$\phi L_2^i = 134.6\, m_i - 7.05 m_i^2$$

and $$\phi L_2^f = 134.6\, m_f - 7.05 m_f^2$$

The sucrose solutions were prepared from either J.T. Baker "Baker Analysed" sucrose or National Bureau of Standards, standard sample 17, lot No. 6340 sucrose dissolved in water which had been twice distilled from alkaline potassium permanganate. The solutions were diluted in the calorimeter with distilled water. The liquids were added to the calorimeter using glass syringes with stainless steel needles. The weight of each liquid added was determined by weighing the syringe on a Mettler H20 five-figure balance both before and after the addition.

The difference (Δq) between the observed heat of dilution (q_{obs}) and q_{calc} is defined as,

$$\Delta q = q_{obs} - q_{calc}$$

The initial and final sucrose concentrations, the amounts of sucrose present, and the corresponding values of q_{obs}, q_{calc} and Δq are recorded in Table (3-2). It can be seen that the values of q_{obs} lie within 2% of the corresponding q_{calc} values over the concentration range studied. As the value of q_{obs} is decreased from -161mJ to -21.5mJ there does not appear to be any trend in Δq when expressed as a percentage of q_{calc}. The values of q_{obs} are on the average about 0.9% more exothermic than the q_{calc} values. The differences are within the expected uncertainty of both sets of data and compare favourably with those observed by Wadsö (1968). The accuracy of the instrument appears to be adequate for the systems studied in this thesis.

3.5 Brij 35 Dilution Experiments

3.5.1 Preparation

The initial concentration of the Brij 35 solutions used was 5.0 mg cm^{-3} for all the dilution runs. The appropriate weight of Brij 35 was added to a volumetric flask and distilled water (twice distilled from potassium permanganate) added to give the required total volume.

3.5.2 Calorimetry

1.0cm^3 of the 5.0 mg cm^{-3} Brij 35 solution was added to the smaller compartment of the reaction cell of the calorimeter and 4.0cm^3 of distilled water were added to the larger compartment. The small and large compartments of the reference cell had 1.0cm^3 and 4.0cm^3 respectively of distilled water added. All the liquids were added using a Micro-Metric SB-2 Syringe Microburet fitted with a stainless steel needle. The calorimeter was left to equilibrate at the required temperature and then rotated to mix the liquids, and thus give a 1 : 5 dilution of the Brij 35 solution resulting in a final concentration of 1.0 mg cm^{-3}. Dilution runs were carried out at 25° and 35°C and each run was followed by a friction run and an electrical calibration run. At 25°C an amplifier setting of 30μV and a recorder setting of 50mV was used whereas at 35°C the settings

Table (3-1) Electrical Calibration Constants

$q_c/\mu J$	T = 294.2K $\bar{\varepsilon}$ *	T = 298.2K $\bar{\varepsilon}$	T = 303.2K $\bar{\varepsilon}$	T = 313.2K $\bar{\varepsilon}$
250	59.0 ± 2.8	55.9 ± 2.8	55.2 ± 2.7	56.6 ± 2.2
501	56.0 ± 1.6	55.2 ± 1.8	54.3 ± 2.4	54.6 ± 1.6
1002	55.2 ± 1.2	54.4 ± 0.5	54.2 ± 1.0	55.1 ± 0.9
1502		54.8 ± 0.8	54.8 ± 0.9	55.8 ± 0.9
1803	55.6 ± 0.7			
2203			55.5 ± 0.6	
2504	55.4 ± 0.8	55.1 ± 0.6		54.8 ± 0.5

* The $\bar{\varepsilon}$ values are expressed in units of μJ (integrator unit)$^{-1}$

Table (3-2) Heats of Dilution of Sucrose Solutions at 298 K

m_i/mol kg^{-1}	m_f/mol kg^{-1}	Amount of Sucrose/mmol	$-q_{obs}$/mJ	$-q_{calc}$/mJ	Δq/mJ
0.5149	0.2041	0.9351	155.11	157.55	2.44
0.5121	0.2031	0.9412	160.85	157.65	-3.20
0.5121	0.1802	0.8030	145.22	144.65	-0.57
0.2810	0.0962	0.4121	42.69	42.05	-0.64
0.2708*	0.0975	0.4421	42.30	42.31	0.01
0.2338	0.0796	0.3475	30.15	29.68	-0.47
0.2231*	0.0569	0.2294	21.50	21.16	-0.34
0.2231*	0.0560	0.2280	21.54	21.14	-0.40

* NBS standard sample 17, lot 6340

were 10μV and 100mV respectively. A chart speed of 40 mm min^{-1} was used in all cases.

3.5.3 Results

The net heat change (q_{obs}) observed during the Brij 35 dilution experiments was exothermic at both 25°C and 35°C. A stable post-run baseline was generally reached after about 15 mins. The results are recorded in Table (7-1). It can be seen that the magnitude of q_{obs} was about -17mJ at 25°C and about -12mJ at 35°C. The uncompensated heat of friction was never greater than 1 to 2% of q_{obs}. Most of the dilution runs exhibited a baseline shift but this was very small in all cases. The standard deviation of the mean for q_{obs} (s_q) was approximately 0.5% of the mean value of q_{obs} ($\bar{q}_{obs}$) at both 25°C and 35°C.

3.6 β-Casein A^1 Dilution Experiments

3.6.1 Preparation

Stock β-casein A^1 solution (Section (2.1.4)) was further treated for use in the calorimetry experiments as follows. Phosphate buffer solution was prepared containing 0.0025M Na_2HPO_4 (May & Baker AR), 0.0025M KH_2PO_4 (May & Baker AR) and 0.1M KCl (May & Baker AR) in freshly boiled distilled water. This buffer solution had a pH of 6.8 and an ionic strength of 0.11. About $10cm^3$ of stock β-casein A^1 solution was dialysed for 24 hours against 2 litres of the phosphate buffer in a cold room at 4°C. Two changes to fresh buffer solution were made during this period. The buffer was stirred using a magnetic stirrer during the dialysis.

A final dialysis was carried out using fresh buffer solution at the temperature of the calorimetric experiment which was to follow. This was to allow the protein solution in the dialysis bag to equilibrate with the phosphate buffer at the temperature of the calorimetric experiment. Any contribution to the overall heat change by ionization of the buffer on the dilution of the protein solution with the dialysate would therefore be minimized. The initial dialysis at 4°C enabled the dialysis time at the

higher temperatures to be shortened, which reduced the possibility of bacterial growth or enzymic degradation occurring during the dialysis period. The dialysis at the higher temperature was carried out for about 2 hours in a water bath. A water-tight magnetic stirring apparatus was built for this purpose and was immersed in the water bath along with the dialysis flask.

After completion of the final dialysis the β-casein A^1 concentration was determined spectrophotometrically (Section (2.1.5)) and the protein solution diluted with the dialysate to give a final concentration of 1.8 mg cm^{-3}. The diluted solution was separated into approximately 2.5cm^3 aliquots which were stored frozen until required for calorimetry. The dialysate was stored in a cold room at 4°C. It was observed in trial runs that cloudiness sometimes had occurred in the β-casein solutions in the calorimeter after the run, particularly at 40°C. This was attributed to bacterial growth in the solution. It was found that this could be prevented by heating the protein solution for 10 minutes at 65°C before storing the solutions in the freezer. Pearce (1975) observed that β-casein solutions which had been subjected to temperatures in this range still exhibited reproducible reversible association behaviour.

3.6.2 Calorimetry

Each calorimetric experiment involved a 2.5 times dilution of the 1.8 mg.cm^{-3} β-casein solution with dialysate to give a final concentration of 0.72 mg cm^{-3}. The β-casein solution (2.0cm^3) was added to the smaller compartment of the reaction cell, and dialysate (3.0cm^3) was added to the larger compartment. 2.0cm^3 and 3.0cm^3 of dialysate were added to the smaller and larger compartments respectively of the reference cell. All the additions were made using a Micro-Metric SB-2 Syringe Microburet. The calorimeter was allowed to come to thermal equilibrium at the required temperature,and then the dilution run was carried out followed by the friction and electrical calibration runs. Experiments were carried out at

21, 25, 30 and 40°C. An amplifier setting of 10μV, a recorder setting of 20mV and a chart speed of 40 mm min^{-1} was used for all the dilution runs.

3.6.3 Results

The net heat change observed for each dilution run was exothermic at all the temperatures studied, with values of q_{obs} ranging from about -1.0mJ to -2.7mJ, and the uncompensated heat of friction ranging from 10 to 15% of q_{obs}. The results are recorded in Table (7-2). The relatively high amplification required to record heat outputs in this range resulted in a magnification of any baseline instability which occurred during the run. The post-run baseline was generally reached after about 10 mins. Baseline shift was more significant at the amplification used for the β-casein runs than for the Brij 35 runs but it rarely exceeded 2% of the peak height. It was found that the baseline would often remain relatively stable for the duration of the dilution and friction runs but would begin to drift by the time a calibration run was started. Therefore, instead of a separate calibration being made for each run, it was decided to use a mean value of the calibration constant ($\bar{\varepsilon}$) at each temperature. The value of $\bar{\varepsilon}$ was chosen from those recorded in Table (3-1) at the same temperature as the dilution run and corresponding to a calibration heat close to the magnitude of $\bar{q}_{obs}$. This $\bar{\varepsilon}$ value was used to determine q_{obs} for all the dilution runs at the given temperature. The overall standard deviation of the value of $\bar{q}_{obs}$ (s_q) was calculated from the following expression (Skinner, 1969).

$$s_q = \bar{q}_{obs} \sqrt{\left(\frac{s'_q}{\bar{q}_{obs}}\right)^2 + \left(\frac{s_\varepsilon}{\bar{\varepsilon}}\right)^2}$$

where s'_q is the standard deviation of the set of q_{obs} values and s_ε is the standard deviation of $\bar{\varepsilon}$. The values of s_q were in the range of 0.05 - 0.08mJ which is close to the standard deviations observed for the Brij 35 runs. For the β-casein runs the standard deviations ranged from about 3% (at 25°C) to 7% (at 40°C) of the value of $\bar{q}_{obs}$.

CHAPTER 4

ULTRACENTRIFUGATION

4. ULTRACENTRIFUGATION

4.1 Introduction

The technique of ultracentrifugation involves the study of the behaviour of macromolecules in solution as they sediment under the influence of a high gravitational field. Analytical ultracentrifugation was originally developed by Svedberg (Svedberg and Nicols, 1923). Lamm (1929) was the first to derive a differential equation which described the rate of change of solute concentration with time during ultracentrifugation at any radial distance from the centre of rotation (r). For an ideal two component system (i.e. the solvent and one solute) in which the partial specific volumes of the components are constant the Lamm equation can be written as follows (Fujita, 1962),

$$\frac{\partial c}{\partial t} = \frac{1}{r} \frac{\partial}{\partial r} \left[rD \left(\frac{\partial c}{\partial r} \right) - s\omega^2 r^2 c \right]$$

where c is the solute concentration, D is the diffusion coefficient, s is the sedimentation coefficient and ω is the angular velocity of the rotor. The Lamm equation can be solved to describe the sedimentation behaviour of the solute for a variety of ultracentrifuge techniques providing certain simplifying assumptions are made. Fujita (1962) provides a summary of the attempts to derive analytical solutions to the Lamm equation.

Ultracentrifuge experiments were carried out in this study using a Beckman Model E Analytical Ultracentrifuge. This instrument allows visual monitoring of the sedimentation process which occurs during ultracentrifugation. The two optical systems used in this study were the Rayleigh interference system and the schlieren system. A description of these optical systems can be found in the literature (e.g. Schachman, 1963). A brief description follows of the visual patterns observed with each of these optical systems.

The Rayleigh interference pattern consists of a series of alternating light and dark parallel interference fringes. If no concentration

gradient exists in the ultracentrifuge cell then these fringes are horizontal, but the fringes are displaced vertically where a concentration gradient occurs. This vertical displacement is proportional to the concentration increment, so that the variation of the position of an interference fringe with the distance from the centre of rotation is proportional to a plot of solute concentration against r. The interference pattern for a single sedimenting solute will have a horizontal region where only the solvent is present, and will slope upwards across the solvent-solution boundary to a plateau where the solution is present (Figure (4-1)). The fringe displacement across the boundary is proportional to the solute concentration in the plateau region.

The schlieren pattern consists of a single line with the vertical displacement of this line being proportional to the concentration gradient at each radial position in the cell. Thus, the variation of the schlieren pattern with the distance from the centre of rotation is proportional to a plot of the concentration gradient (dc/dr) against r. The schlieren pattern exhibits a peak across the solvent-solution boundary for a single sedimenting solute (Figure (4-1)). The area under this peak is proportional to the solute concentration in the region after the boundary.

The Beckman Model E ultracentrifuge normally uses an AH-6 mercury discharge light source. However, the instrument used in this study had been modified by Dr J.A. Lewis to enable a helium-neon gas laser light source to be used in addition to the conventional mercury lamp (Lewis and Lyttleton, 1973). The laser light source has two principle advantages over the mercury discharge source when interference optics are used; improved clarity of the meniscus and base positions, and increased illumination intensity of the interference pattern.

There are several different methods of analytical ultracentrifugation those used in this study being low and high speed sedimentation equilibrium and sedimentation velocity. The self-association of both Brij 35 and bovine β-casein A[1] was studied using these methods in order to determine values

Figure (4-1) Typical Interference and Schlieren Patterns for a Single Sedimenting Solute

Double exposure of the interference (upper) and schlieren (lower) patterns for a synthetic boundary run with 2.5mg cm^{-3} bovine serum albumin solution using a 12mm double sector cell. The photograph was taken using the mercury light source.

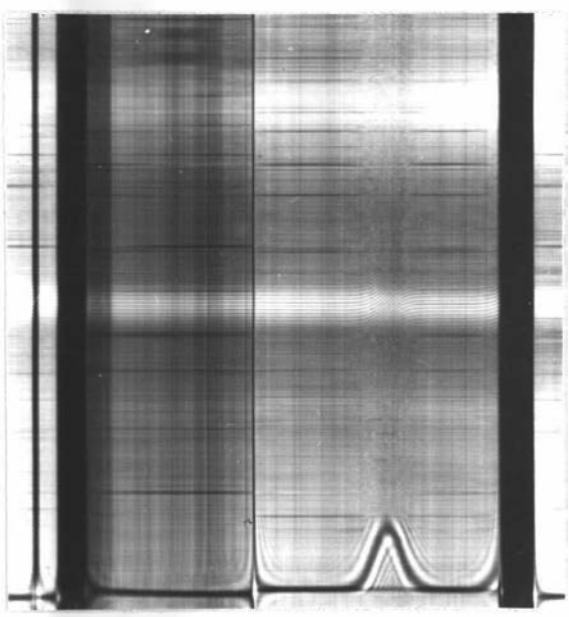

for some of the thermodynamic parameters involved in the processes. The following sections outline the theory behind the methods and their application to the study of reversible self-associating systems.

4.2 Sedimentation Equilibrium

4.2.1 General Theory

During the ultracentrifugation at constant temperature of a two-component system the sedimenting component moves towards the bottom of the ultracentrifuge cell under the influence of the centrifugal field. This results in a concentration gradient being set up with increasing solute concentration towards the bottom of the cell. Diffusion of the solute occurs along this gradient in the opposite direction to sedimentation. At certain rotor speeds (which depend on the molar mass of the solute) the rate of back diffusion eventually equals the rate of sedimentation and there is no net movement of solute within the cell. When this situation has been reached the concentration gradient does not change with time and thermodynamic equilibrium exists in which the total potential of each component in the cell is constant. This situation is called sedimentation equilibrium. Goldberg (1953) treated sedimentation equilibrium from a rigorous thermodynamic viewpoint and derived expressions which allowed for deviations from ideality. For a two-component system at sedimentation equilibrium the solute is distributed according to

$$\frac{dc}{dr} = M(1 - \bar{v}\rho)\omega^2 r\left(\frac{\partial c}{\partial \mu}\right) \qquad (4\text{-}1)$$

where M is the molar mass of the solute, $\bar{v}$ is the partial specific volume of the solute, ρ is the density of the solution and μ is the chemical potential of the solute. When μ in equation (4-1) is expressed in terms of c and y (where y is the activity coefficient of the solute on the same concentration scale as c) the fundamental expression for the distribution of solute in the cell for sedimentation equilibrium of a nonideal two-component system can be written as

$$\frac{dc}{dr} = \frac{M(1 - \bar{v}\rho)\omega^2 r c}{RT\left(1 + c\frac{\partial \ln y}{\partial c}\right)} \qquad (4\text{-}2)$$

The activity coefficient can be related to the molar mass of the solute by the following expression (Goldberg, 1953),

$$\ln y = BMc + \ldots. \qquad (4\text{-}3)$$

where higher order terms in c are usually neglected. B is the second virial coefficient and is a measure of the nonideality of the system. Differentiation of equation (4-3) with respect to c gives

$$\frac{\partial \ln y}{\partial c} = BM \qquad (4\text{-}4)$$

Substitution of equation (4-4) into (4-2) results in the following expression,

$$\frac{dc}{dr} = \frac{(1 - \bar{v}\rho)\omega^2 r c}{RT}\left(\frac{M}{1 + BMc}\right) \qquad (4\text{-}5)$$

A quantity called the apparent molar mass (M_{app}) is defined as

$$M_{app} = \frac{M}{(1 + BMc)} \qquad (4\text{-}6)$$

It is evident that M_{app} is equal to the actual molar mass in an ideal solution, for which B = 0. Equation (4-5) can thus be written as

$$\frac{dc}{dr} = \frac{M_{app}(1 - \bar{v}\rho)\omega^2 r c}{RT} \qquad (4\text{-}7)$$

It is useful to express equation (4-7) in the following form,

$$M_{app} = \frac{2RT}{(1 - \bar{v}\rho)\omega^2} \cdot \frac{d \ln c}{d(r^2)} \qquad (4\text{-}8)$$

It can be seen from equation (4-8) that the slope of a plot of ln c against r^2 is proportional to M_{app}. For an ideal solution M_{app} equals M, and the molar mass of the solute is therefore given by

$$M = \frac{2RT}{(1 - \bar{v}\rho)\omega^2} \cdot \frac{d \ln c}{d(r^2)} \qquad (4\text{-}9)$$

4.2.2 Self-Associating Systems

The first theoretical treatment of sedimentation equilibrium involving self-associating systems was presented by Tiselius (1926) although only ideal systems were considered. Adams and Fujita (1963) presented an extended mathematical analysis of these systems which allows for the effects of nonideality. Adams and Williams (1964), Adams (1965, 1967) and Adams and Filmer (1966) have published methods for the analysis of the data from sedimentation equilibrium experiments on nonideal self-associating systems. The analysis assumes that the partial specific volumes and the refractive index increments of all the associating species are equal, and also that in dilute solutions the activity coefficients of each of the associating species (y_{Ai}) are related to the total solute concentration (c_A) by,

$$\ln y_{Ai} = i\, BM_{A1}\, c_A \quad (i = 1, 2, \ldots\ldots) \tag{4-10}$$

where M_{A1} is the molar mass of the monomer and higher terms in c are assumed to be negligible. The fundamental sedimentation equilibrium expression can be written for self-associating systems as follows (Adams and Fujita, 1963; Adams and Williams, 1964),

$$M_{w,app} = \frac{2RT}{(1 - \bar{v}\rho)\omega^2} \cdot \frac{d \ln c_A}{dr^2} \tag{4-11}$$

where $M_{w,app}$ is the apparent weight average molar mass of the associating species. Also, by comparison with equation (4-6)

$$M_{w,app} = \frac{M_w}{(1 + BM_w c_A)} \tag{4-12}$$

where M_w is the weight average molar mass defined by,

$$M_w = \frac{\sum_N c_{Ai} M_{Ai}}{\sum_i c_{Ai}} = \frac{\sum_i c_{Ai} M_{Ai}}{c_A} \tag{4-13}$$

The concentration of each associating species of molar mass M_{Ai} is denoted by c_{Ai}. $M_{w,app}$ for a self-associating system is a unique function of the total concentration of the interacting solute, that is,

for a given value of c_A there is a single value for $M_{w,app}$. Therefore, the magnitude of $M_{w,app}$ continually alters down the ultracentrifuge cell as r changes.

Self-associating systems are nonideal owing to the presence of solute-solute interactions and therefore both the equilibrium constant and the second virial coefficient are measures of nonideality. These systems are usually analysed by evaluating the self-association interactions as the equilibrium constant and including the remaining interactions in the second virial coefficient. Some examples of systems which have been studied in this way are sodium dodecyl sulphate and dodecyltrimethylammonium bromide (Anacker et al., 1964), polyoxyethylene octylphenylether (Ikeda and Kakiuchi, 1967) and the isoethylphenoxy polyethoxyethanol, Triton X-100 (Biaselle and Millar, 1975). A sedimentation equilibrium study was carried out on β-casein B by Noelken and Reibstein (1968) but the experimental conditions used were such that essentially only the monomer was present in the solution. The treatment of the primary data obtained from the sedimentation equilibrium experiments carried out in this present study is described in chapter 8.

4.2.3 Polyelectrolytes

Tiselius (1932) has shown that during sedimentation equilibrium a protein with a net charge Z in the presence of its counterions only will distribute in the cell as if it had a molar mass of $(1/(Z + 1))$ times the true molar mass. In practice this effect can be reduced to negligible proportions by the addition of a supporting electrolyte of low molar mass in a concentration of at least 0.1M.

If the concentration of buffer ions, counterions and supporting electrolyte present in the protein solution changes through the ultracentrifuge cell owing to interaction with the protein component then the basic sedimentation equilibrium expressions no longer hold. However, Cassasa and Eisenberg (1964) have shown that this problem can be avoided

if the protein solution is dialysed to osmotic equilibrium against a large excess of the multicomponent solvent.

4.2.4 Low Speed Sedimentation Equilibrium

The low speed sedimentation equilibrium method requires the rotor speed to be low enough to allow a finite concentration of the sedimenting solute to be present at the meniscus of the solution column in the cell after equilibrium has been achieved. A concentration ratio of about 4 : 1 between the ends of the sample column is considered suitable for low speed experiments (Van Holde, 1967). If an approximate value for the molar mass of a monodisperse solute is known, the rotor speed which should give the above condition can be found from equation (4-14) below, which is derived by integrating equation (4-9),

$$\ln 4 = 1.386 = \frac{M(1 - \bar{v}\rho)\omega^2}{RT}\left(\frac{r_b^2 - r_m^2}{2}\right) \qquad (4\text{-}14)$$

where r_b and r_m are the distances from the centre of rotation to the bottom and meniscus of the sample column respectively. For this estimate in an interacting system, attention is focussed on the concentration ratio of the associated species so that M is taken as the molar mass of the associated species. Equation (4-14) can be solved for ω but this is used as a guide only and the final choice of rotor speed depends on the appearance of the interference fringe pattern during the course of the experiment. Theoretically, sedimentation equilibrium is never completely attained but in practical terms it can be said to be attained when the concentration difference down the sample column is within 0.1% of the equilibrium value (Van Holde, 1967). The time taken to reach this condition ($t_{0.1\%}$) is given by

$$t_{0.1\%} \simeq 0.7\,\frac{(r_b - r_m)^2}{D} \qquad (4\text{-}15)$$

A disadvantage of the low speed method is the long time period required before sedimentation equilibrium is attained for macromolecules

of high molar mass (e.g. about 60 hours using a 3mm column if $D = 3 \times 10^{-7}$ cm^2 sec^{-1}). Various methods have been suggested to shorten the time required to reach low speed sedimentation equilibrium (Richards et al., 1968; Hexner et al., 1961; Chervanka, 1969). The final check on whether equilibrium has been reached is carried out by taking several photographs of the fringe pattern at suitable time intervals. When there is no detectable change in the fringe pattern between successive photographs it can be assumed that equilibrium has been attained.

4.2.5 High Speed Sedimentation Equilibrium

The high speed sedimentation equilibrium method, also known as the Yphantis or meniscus depletion method, was developed by Yphantis (1964). For a solute of a given molar mass this method uses rotor speeds 2 to 3 times greater than those used in the low speed method. This causes the solute to sediment completely away from the meniscus resulting in zero concentration in the meniscus region at sedimentation equilibrium. The recommended rotor speed for high speed runs can be determined from the following expression (Yphantis, 1964),

$$\frac{\omega^2 M(1 - \bar{v}\rho)}{RT} \simeq 5 \qquad (4\text{-}16)$$

The time required to reach sedimentation equilibrium is considerably shorter for the high speed than for the low speed method (Yphantis, 1964) and the attainment of equilibrium is checked by a series of photographs of the fringe pattern as for the low speed method. However, the high speed method is subject to a disadvantage if there is more than one sedimenting species and if there is also a wide molar mass range covering these species. In systems where there is a large difference between the molar masses of the smallest and largest species the rotor speed which gives meniscus depletion for the lightest species may cause the heaviest species to accumulate at the bottom of the cell. This particularly applies to self-associating systems with a high degree of association. In this

situation the high speed method can only be used to determine the molar mass of the monomer species. However, this does allow the monomer molar mass to be determined without interference from the aggregated species, as the high molar mass species is packed on the cell bottom.

4.3 Sedimentation Velocity

4.3.1 Basic Theory

The sedimentation velocity technique uses rotor speeds high enough to overcome the effects of back diffusion, thus causing the solute eventually to sediment completely to the bottom of the cell. It has been shown by Svedberg (1925) that the molar mass of an ideal solute is related to the sedimentation and diffusion rates by the following expression,

$$M = \frac{RT}{(1 - \bar{v}\rho)\, D}\left(\frac{1}{\omega^2 r}\right)\frac{dr}{dt} \qquad (4\text{-}17)$$

The sedimentation coefficient(s) is defined as

$$s = \left(\frac{1}{\omega^2 r}\right)\frac{dr}{dt} \qquad (4\text{-}18)$$

Substitution of s from equation (4-18) into equation (4-17) gives the well-known Svedberg equation,

$$M = \frac{RT}{(1 - \bar{v}\rho)}\left(\frac{s}{D}\right) \qquad (4\text{-}19)$$

If values for s and D are determined then equation (4-19) can be used to obtain a value for the molar mass of the sedimenting species.

The sedimentation velocity technique can also be used to determine the relative concentration of each component in a multi-component system (Svedberg and Pederson, 1940). When more than one sedimenting species is present a sedimentation boundary should be observed for each species. Each boundary will sediment at a rate proportional to the molar mass of the corresponding component. If the rates of sedimentation of the various species are sufficiently different and schlieren optics are used, the area under each peak is proportional to the concentration of the

corresponding species. If interference optics are used the fringe displacement across each boundary is proportional to the concentration of the corresponding component in the initial mixture. In both cases corrections must be made for the effect of radial dilution (Trautman and Schumaker, 1954). However, the Johnston-Ogston effect (Johnston and Ogston, 1946) can cause the relative area of a slower peak to be increased at the expense of a faster peak in front of it. When this effect occurs the relative concentration of each species is not proportional to the corresponding peak area. However, the Johnston-Ogston effect decreases with decreasing total concentration and is negligible at low solute concentrations.

4.3.2 Self-Associating Systems

In favourable cases the sedimentation velocity technique can be used for the determination of the relative concentration of each component in a reversible self-associating system. Reviews of this application of the technique have been given by Cann (1970) and Nichol *et al.* (1964). If the rate of attainment of equilibrium between the interacting species is very slow relative to their rate of separation by sedimentation the system essentially behaves in the same way as a non-interacting system (Schachman, 1959). In this case the concentration change across each boundary (corrected for radial dilution) should correspond to the concentration of each species before sedimentation. If the equilibrium is fast compared to the sedimentation rate chemical equilibrium is maintained between the species at all points in the cell during the sedimentation process (Schachman, 1959). The sedimentation boundaries observed in this case are part of a single reaction boundary in which dynamic processes are continually occurring as the boundary moves down the sample column (Cann, 1970). If schlieren optics are used, a single peak will be observed for dimerization whereas a bimodal peak occurs for higher degrees of association, in which case the area of the slow peak remains constant

whereas the area of the faster peak increases as the total solute concentration is increased (Gilbert, 1955, 1959; Nichol et al., 1964). Also, the value of the sedimentation coefficient for the slower peak corresponds to that of the monomer whereas the sedimentation coefficient of the faster peak increases with total concentration. However, in the limiting case of rapid reversible self-association involving a large equilibrium constant and a high degree of association the areas under the slow and fast peaks are proportional to the monomer and N-mer concentrations respectively (Cann, 1970). In this case the sedimentation coefficients associated with the slow and fast boundaries closely approximate those of the monomer and N-mer respectively. Although two apparently discrete boundaries are observed, both of these are part of a single reaction boundary which has a finite, but virtually undetectable, concentration gradient between the observed peaks. The self-association reaction of myosin appears to be an example of the above type of system (Josephs and Harrington, 1967, 1968). A third type of system occurs when the rate of equilibration is of the same order as the sedimentation rate. In this case a complicated relationship exists between the peak areas and the concentrations of the individual species, and also between the observed sedimentation coefficients and those of the individual species (Cann, 1970; Coates, 1970; Schachman, 1959). Thus, there is no direct proportionality between the peak areas and the individual component concentrations. A satisfactory method of analysis of such systems has apparently not yet been devised.

4.4 Optical Alignment

The following sections will describe the experimental procedures and results for the low and high speed sedimentation equilibrium runs and the sedimentation velocity runs carried out in this study on the Brij 35 and β-casein A^1 systems. However, the Rayleigh interference optical system requires precise alignment if accurate results are to be obtained.

Accordingly, the optical alignment test described by Dyson (1970) was carried out on the Beckman Model E ultracentrifuge used in this study and the required adjustments to the condensing lens mask and the cylinder lens positions were made. The appearance of the fringe pattern during a boundary cancelling run carried out after the alignment procedure had been completed is illustrated in Figure (4-2).

4.5 Low Speed Sedimentation Equilibrium Experiments

4.5.1 General Procedure

The experimental procedure used for the low speed runs was based on Chervanka (1969). A 12mm double sector synthetic boundary cell was used with sapphire windows and an aluminium-filled Epon synthetic boundary centrepiece. The screw ring of the cell was torqued to 13.5 m-N with a Beckman 1460 Torquometer. FC-46 fluorocarbon oil ($0.03cm^3$) followed by a $0.12cm^3$ of the sample solution was added to the sample sector of the cell and $0.17cm^3$ of the reference solution was added to the reference sector. The runs were carried out using an An-D rotor with an interference counterbalance. Interference optics were used with a symmetrical 0.75mm double slit interference aperture mask. The fringe patterns were photographed using Ilford HP3 panchromatic plates in conjunction with the laser light source, and Kodak II-G plates with the mercury light source. Immediately after the rotor had reached full speed, and before sedimentation could be detected, a baseline reference photograph was taken to record the extent of any underlying fringe shift caused by window distortion. This photograph was also a useful aid in determining the true meniscus and base positions for the sample column in the photographs taken later at sedimentation equilibrium.

The low speed method requires the determination of the initial solute concentration in the sample in terms of interference fringes (j_o). This determination was carried out by a synthetic boundary run after the completion of the sedimentation equilibrium run as follows. The solution

Figure (4-2) Interference and Schlieren Patterns During a Boundary Cancelling Test

The boundary cancelling test (Dyson, 1970) was carried out using a 12mm cell with a 7° single sector centrepiece containing a solution of bovine serum albumin (5mg cm^{-3}). The mercury light source was used for the photographs.

Photograph A

Double exposure of interference pattern and aperture mask slits showing no detectable slope in the interference fringes.

Photograph B

The schlieren pattern for the same run showing the steep concentration gradients at the meniscus and base of the sample column.

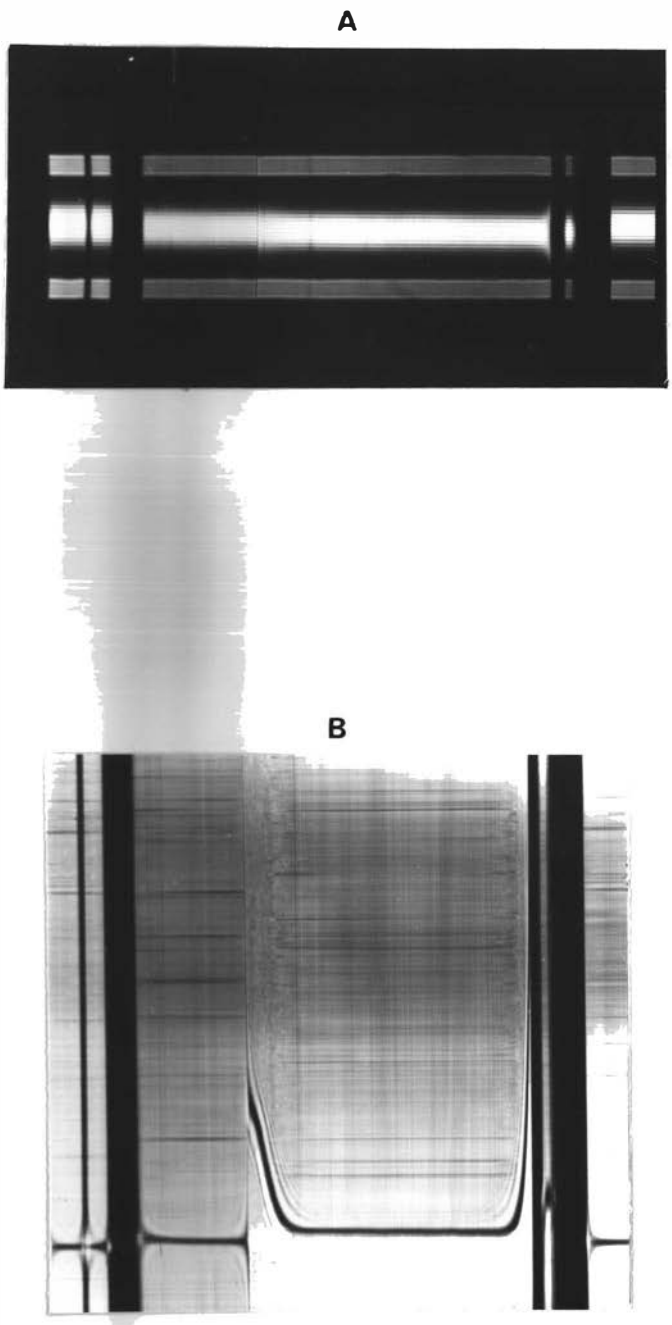
A
B

in the cell used in the equilibrium run was shaken gently to remix the solute then reference solution was added to the reference column to give a total volume of 0.46cm^3. The rotor was then spun at about 8,000 rpm so that the reference solution layered over the sample column. A photograph was taken as soon as the two menisci were equalized and further photographs were taken at appropriate time intervals after the interference fringes could be resolved.

The photographic plates were developed according to the manufacturer' instructions. A Topcon PP-30E Profile Projector fitted with a Type-D two-dimensional object table was used to take the required measurements from the photographic plates. The plate reading procedure and associated calculations for low speed runs is well established (Chervanka, 1969; Van Holde, 1967) and therefore will not be repeated in this thesis. The calculations were carried out on a Hewlett-PackardModel 30 calculator equipped with a printer and a plotter.

4.5.2 Brij 35 Runs

4.5.2.1 Preparation and Procedure

Brij 35 solutions were prepared as described in section (3.5.1). Low speed runs were carried out at 25° and 35°C with initial concentrations of 1.00, 2.00 and 5.00 mg cm^{-3} using distilled water as the reference solvent. A rotor speed 20,000 rpm was used in all cases. Sedimentation equilibrium was reached typically after about 24 hours without overspeeding procedures being used.

4.5.2.2 Results

Photographs of the interference fringe patterns taken at sedimentation equilibrium using the laser light source are illustrated in Figure (4-3) for the Brij 35 low speed runs. The primary data from these runs are recorded in Tables (7-3), (7-4) and (7-5) along with the relevant experimental details. With laser optics it was found that at 25°C a concentration change of 1 mg cm^{-3} resulted in a fringe displacement of

2.49 fringes, whereas at 35°C the displacement was 2.38 fringes. The analysis of the primary data is described in Chapter 8.

4.5.3 β-Casein A^1 Runs

4.5.3.1 Preparation and Procedure

Solutions of β-casein A^1 in phosphate buffer were prepared as described in section (3.6.1). From the observations of Waugh et al. (1970) it is expected that the β-casein monomer will carry a net negative charge of about -13 at the pH of 6.8 used for the solutions. The effect, noted in section (4.2.3), that this charge would have on the sedimentation behaviour of the protein should be counteracted by the solution ionic strength of 0.11. The dialysis of the β-casein solution against the buffer would counteract the second effect noted in section (4.2.3). The dialysate was used as the reference solvent in all the ultracentrifuge runs.

Estimates of the molar mass of β-casein micelles vary considerably as can be seen from Table (1-1) on page 9. If a molar mass of 7×10^5 g mole^{-1} is assumed as a rough guide, and the factor $(1 - \bar{v}\rho)$ is given the value of 0.268 (Payens and van Markwijk, 1963), then from equation (4-14) a suitable rotor speed for low speed runs on β-casein solutions using a 3mm sample column should be about 2,800 rpm. An An-J rotor should be used for speeds as low as this (Chervanka, 1969), particularly as the An-D rotor was found to precess at rotor speeds under 2,800 rpm. However, an An-J rotor was not available for use in this study and therefore the runs had to be carried out using an An-D rotor. Proteins of a molar mass similar to that estimated for the β-casein micelle have diffusion coefficients near 3×10^{-7} cm^3 sec^{-1} in value (Svedberg and Pederson, 1940) and therefore from equation (4-15) the time required for the micelle to reach sedimentation equilibrium can be estimated to be about 60 hours under normal low speed conditions. However, the overspeeding method of Chervanka (1969) was used to reduce

Figure (4-3) Interference Patterns for Brij 35 Solutions at Low Speed Sedimentation Equilibrium

Photograph A

Initial concentration = 0.74mg cm^{-3}

Rotor speed = 20,180 rpm

Temperature = 25°C

Photograph B

Initial concentration = 0.74mg cm^{-3}

Rotor speed = 20,230 rpm

Temperature = 35°C

Photograph C

Initial concentration = 1.59mg cm^{-3}

Rotor speed = 20,240 rpm

Temperature = 25°C

Photograph D

Initial concentration = 1.59mg cm^{-3}

Rotor speed = 20,140 rpm

Temperature = 35°C

Photograph E

Initial concentration = 4.12mg cm^{-3}

Rotor speed = 20,280 rpm

Temperature = 25°C

Photograph F

Initial concentration = 4.12mg cm^{-3}

Rotor speed = 20,290 rpm

Temperature = 35°C

The laser light source was used for all the photographs.

A

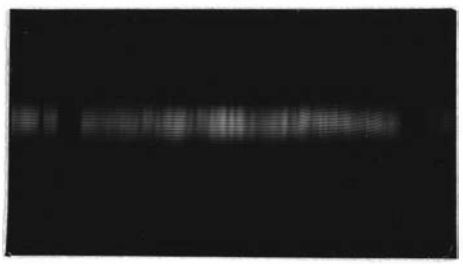

B

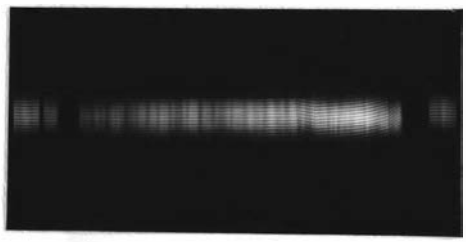

C

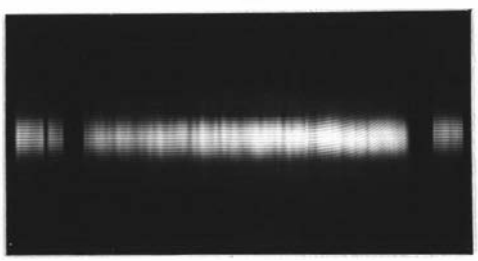

D

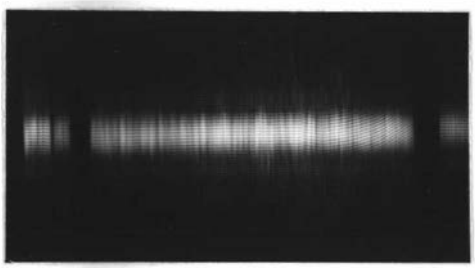

E

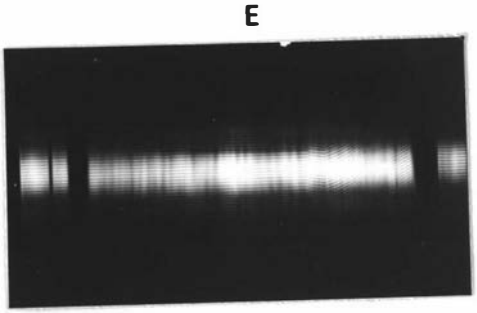

F

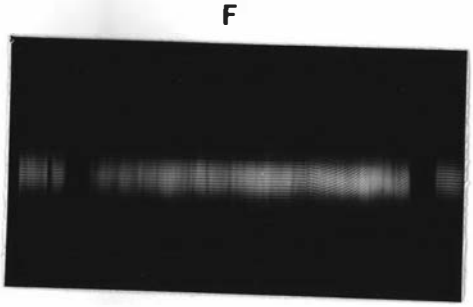

the time required.

A low speed run was initially carried out at 21°C using a rotor speed of 3,000 rpm with an initial β-casein A^1 concentration of 1.8 mg cm^{-3}. However, after the run had continued for 1 to 2 days, and before sedimentation equilibrium had been reached, a pellet of material was observed to have formed at the bottom of the sample column as illustrated in Figure (4-4). The amount of material packed at the bottom of the cell appeared to increase as time went on. The run was stopped and the solute was redistributed by gentle shaking of the cell and the run was then restarted. A pellet was observed to form at the bottom of the cell a short time after the final rotor speed of 3,000 rpm had been reached. It was therefore assumed that irreversible aggregation of the protein had occurred. Adams (1967) reported that the FC 43 fluorocarbon oil used in the ultracentrifuge cell will precipitate β-lactoglobulin A. Therefore, a low speed run was carried out on a fresh sample of the β-casein solution without the addition of oil to the cell. However, the β-casein exhibited similar behaviour to that observed in the run carried out in the presence of oil.

A slow irreversible aggregation process was also observed to occur in β-casein solutions by Holt (1974) in addition to the reversible process. Noelken and Reibstein (1968) observed protein degradation in dilute neutral salt solutions of β-casein B at temperatures above 15°C, with degradation occurring after 24 hours at 25°C. Therefore, in the present study it was decided to carry out alkaline polyacrylamide disc gel electrophoresis on samples of β-casein A^1 taken both before and after a low speed run which had exhibited irreversible aggregation. The results are illustrated in Figure (4-4). Only a single electrophoretic band was observed for the protein sample taken before the run whereas more than one band was observed to be present in the sample taken after the run. It was therefore concluded that degradation of β-casein A^1 was occurring during

Figure (4-4) Interference Patterns and Electrophoresis Gels Showing Degradation in β-Casein A^1 Solutions

(a) Low Speed Equilibrium Run

The run was carried out on 1.8mg cm^{-3} β-casein A^1 solution at 21°C using a rotor speed of 3,000 rpm. Overspeeding was carried out as described in Chervanka (1969).

Photograph A

Interference pattern after 20 mins showing the positions of the meniscus and base of the sample column.

Photograph B

Interference pattern after 12 hours. No degradation is apparent at this stage.

Photograph C

Interference pattern after 40 hours. Degradation is indicated by the opaque band at the bottom of the sample column.

The photographs were taken with the mercury light source.

(b) Alkaline Polyacrylamide Gel Electrophoresis

Photograph D

The right hand gel contains a sample of the β-casein A^1 solution taken before the low speed run. The left hand gel contains a sample taken after the run. Degradation is indicated by the additional bands observed for the latter sample.

A

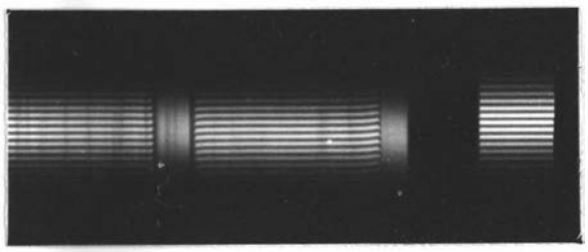

B

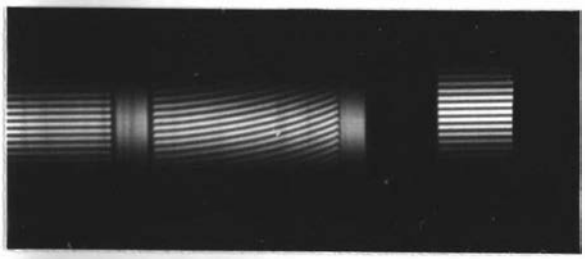

C

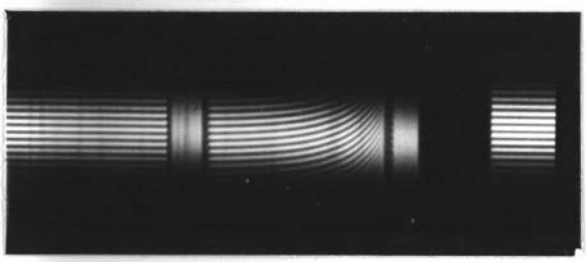

D

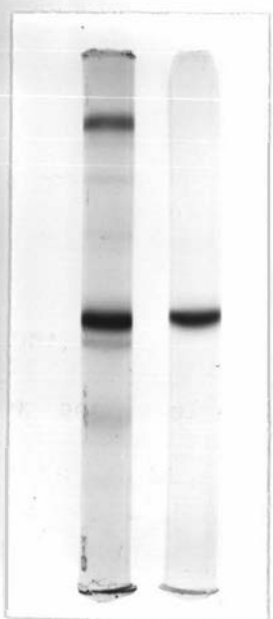

the low speed sedimentation equilibrium runs. Unsuccessful attempts were made by Noelken and Reibstein (1968) to stabilize β-casein B but the nature of these attempts was not reported.

Attempts were made in the present study to eliminate the possibility of bacterial growth being the source of the degradation by passing a fresh sample of β-casein A[1] solution through an autoclaved 0.22μ MF-Millipore Filter (GSWP 01300) into small autoclaved screwtop glass bottles. Each bottle contained enough of the protein solution for a low speed run and was stored in a freezer until required. Before a low speed run was carried out the cell windows and centrepiece were sterilized both before and after cell assembly by using a high intensity ultra-violet lamp. The cell was filled using a commercially available sterilized infusion syringe needle attached to a 30cm long polyethylene tube (Surflo SV-23BL). The sterile tubing could hold a 0.3cm^3 volume of liquid therefore no protein solution entered the syringe barrel. However, irreversible aggregation was still observed during low speed runs despite these precautions. A run was also carried out with sodium azide (BDH) present as an antibacterial agent in the sample and reference columns at a concentration of 0.2 mg cm^{-3}, without success. It was concluded that bacterial growth was not the cause of the irreversible aggregation of the protein.

It is known that an enzyme, milk protease, accompanies the casein precipitated under acid conditions (Warner and Polis, 1945). Milk protease exhibits tryptic activity, has a pH optimum between 6.5 and 9.0 and is relatively stable at high temperatures ($>60^{\circ}$C) at neutral pH (Shahani et al., 1973). β-casein is the most susceptible of the caseins to proteolysis by milk protease and the degradation products migrate as bands of lower mobility than β-casein during alkaline polyacrylamide gel electrophoresis (Yamauchi and Kaminogawa, 1972; Chen and Ledford, 1971). The electrophoretic pattern for the sample from the low speed run in the

present study exhibited bands which moved slower than β-casein, providing evidence that the stock β-casein A[1] solution may have been contaminated by milk protease. The solution pH of 6.8 is within the range of the optimum for the enzyme. Milk protease is known to be inhibited by Soya bean trypsin inhibitor, STI (Chen and Ledford, 1971). It was therefore decided to add STI (Sigma II-S) at a concentration of 0.02 mg cm^{-3} to the β-casein solutions used for the low speed runs but this was not found to be successful in stabilizing the β-casein during the ultracentrifuge experiments. The possibility was then considered that a stable STI-enzyme complex could not be formed under the conditions encountered in the ultracentrifuge. Therefore, an attempt to remove any enzyme with tryptic activity which may have been present in the β-casein solution was carried out by preparing an affinity column containing bound STI. It was hoped that by passing the β-casein solution down such a column the enzyme would become bound to the column while the β-casein passed through. The preparation of the affinity column was based on the method of Cuatrecasas (1970) and is described as follows.

9g (wet weight) of Sepharose 4B resin (Pharmacia) was added to 30cm^3 of distilled water and 1g of cyanogen bromide (Riedal-De Haen Prosynth) was slowly added to the mixture with stirring. During the addition the pH was kept constant at 11.0 with 1M NaOH and the temperature was kept at 20°C with the addition of small pieces of ice. After the reaction with cyanogen bromide had been completed (indicated by a stable pH) the resin was filtered through sintered glass and washed three times with ice water. The resin was then transferred into a solution of 100mg STI (Sigma II-S) in 20cm 0.1M $NaHCO_3$ and gently stirred in a cold room at 4°C overnight. After the reaction with the STI had been completed, the resin was washed several times with water to remove excess STI.

A column 3cm in height and 1cm in diameter was formed with the STI-sepharose in a small glass column holder. It has been shown that

tryptic enzymes are bound to STI-sepharose affinity columns at neutral pH and dissociate at low pH values (Feinstein, 1970). The column was equilibrated with 0.1M Tris-HCl buffer at pH 7.1, and the effectiveness of the column in binding enzymes which exhibit tryptic activity was then tested by adsorbing a solution of 1 mg of bovine trypsin (Sigma XI) in the Tris-HCl buffer onto the column. This was followed by eluation with Tris-HCl buffer at pH 7.1 followed by eluation with 3mM HCl at pH 2.8. Any protein present in the eluate was detected by monitoring the absorbance at 280nm using an LKB Uvicord II apparatus with chart recorder. Trypsin should have become bound to the affinity column at pH 7.1 and have come off when the pH was reduced to 2.8. This was in fact observed and, as the resin had been shown to be successful in binding trypsin, a similar column was formed using a fresh sample of the STI-sepharose resin. This column was then equilibrated with phosphate buffer dialysate from the β-casein A^1 solution preparation and $2cm^3$ of undiluted β-casein solution was adsorbed onto the column. This was followed by eluation with the dialysate, and the eluate containing the protein was stored frozen for use in low speed sedimentation equilibrium runs. Eluation of the column at pH 2.8 did not show any evidence of protein material in the eluate but it would be expected that the concentration of any tryptic enzyme present in the β-casein solution would be too low for spectrophotometric detection.

A further low speed sedimentation equilibrium run was carried out on the β-casein A^1 solution which had been passed through the STI-affinity column but it was found that the above procedure had not been successful in stabilizing the protein during the time period of the ultracentrifuge experiment. It was decided to abandon any further attempts to carry out low speed sedimentation equilibrium runs on β-casein A^1 solutions.

4.6 High Speed Sedimentation Equilibrium Experiments

4.6.1 β-Casein A^1

The high speed method was used to determine the molar mass of the β-casein A^1 monomer. Although the value has been well established in the literature it was decided to carry out the determination as further evidence that the protein solution used did in fact contain β-casein. Noelken and Reibstein (1968) have used high speed sedimentation equilibrium to determine the molar mass of the β-casein B monomer under a variety of experimental conditions. The molar mass of the Brij 35 monomer can not be determined using the high speed method as the rotor speeds required for molecules of molar mass under 10,000 g $mole^{-1}$ are outside the range of the instrument.

4.6.1.1 Procedure

β-casein A^1 solution was prepared as previously described in section (3.6.1). The procedure of Chervanka (1969) was used to carry out the high speed run. This was essentially the same procedure as for the low speed runs (section (4.5.1)) except for a higher rotor speed and different column volumes in the cell. The sample column for the high speed run consisted of 0.12cm^3 β-casein A^1 solution and 0.01cm FC-43 oil. The reference column contained 0.14cm^3 of dialysate. The run was carried out at 15°C using a rotor speed of 32,000 rpm. A reference photograph was taken as soon as the rotor had reached full speed, and further photographs were taken at appropriate time intervals to determine when sedimentation equilibrium was attained. A synthetic boundary run is not required in conjunction with a high speed run as the meniscus concentration is known to be zero, hence the concentration at other radial positions in the cell can be determined by using the meniscus region as the concentration reference. The plate reading procedure and calculations which were carried out for the high speed run are described in Chervanka (1969) and Van Holde (1967).

4.6.1.2 Results

A photograph of the interference fringe pattern taken at sedimentation equilibrium for the high speed run on the β-casein A^1 solution is illustrated in Figure (4-5). The primary data obtained from this run are recorded in Table (7-6) and the calculations required for the determination of the molar mass of the β-casein A^1 monomer are set out in Chapter 8.

4.7 Sedimentation Velocity Experiments

4.7.1 β-Casein A^1

The self-association of β-casein has been studied using the sedimentation velocity technique by Sullivan *et al.* (1955), McKenzie and Wake (1959), Payens and van Markwijk (1963), Hoagland (1966), Payens *et al.* (1969) and Waugh *et al.* (1970). Payens and van Markwijk interpreted their results as indicating that the rate of equilibration of the β-casein self-association process is very slow compared to the rate of separation of the monomer and N-mer species by sedimentation. They used the areas under the peaks of the schlieren pattern to evaluate the concentrations of monomer and N-mer in β-casein solutions at 8.5° and 13.5°C. Payens *et al.* also used this method to determine the relative concentrations of β-casein monomer and N-mer in solution at 21°C.

Owing to the lack of success experienced in this present study in obtaining useful data from sedimentation equilibrium experiments on the self-association of β-casein A^1, it was decided to attempt to determine the relative concentrations of the monomer and N-mer forms of the protein in solution using the sedimentation velocity technique. The following sections describe the experimental procedure used for the experiments and a discussion of the results obtained.

4.7.1.1 Procedure

β-casein A^1 solutions were prepared as described in Section (3.6.1). Double sector cells were used for all runs as this allowed both interference

Figure (4-5) Interference Pattern for β-Casein A^1 Solution at High Speed Sedimentation Equilibrium

Initial concentration = 0.72mg cm^{-3}

Rotor speed = 32,410 rpm

Temperature = 15°C

The laser light source was used for this photograph.

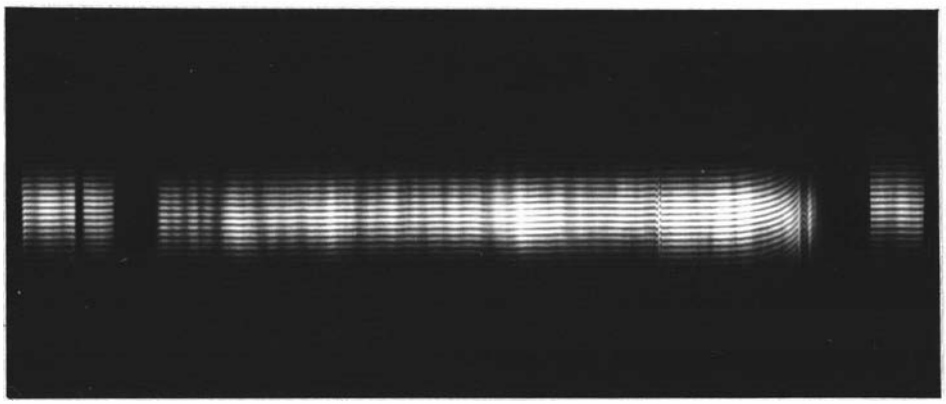

and schlieren optics to be used during a single run. An additional advantage occurs when double sector cells are used in conjunction with schlieren optics in that a baseline is recorded along with the schlieren pattern. For low β-casein concentrations (below 2mg cm^{-3}) the schlieren pattern could not be satisfactorily resolved and only interference optics could be used.

Runs were carried out using initial β-casein A^1 concentrations of 4.0, 1.8 and 0.72mg cm^{-3} using a procedure based on that of Chervanka (1969). For protein concentrations of 1.8mg cm^{-3} and above, 12mm aluminium-filled Epon centrepieces of both the standard and synthetic boundary types were used. A 30mm centrepiece was used when the protein concentration was 0.72mg cm^{-3} as the increased light path gave a corresponding increase in the displacement of the interference fringes. The fringe displacement observed with a 0.72mg cm^{-3} concentration in a 12mm cell was too small to be clearly resolved. Sapphire windows were used in conjunction with both the 12mm and 30mm centrepieces. Rotor speeds above 50,000 rpm cannot be used with sapphire windows therefore all runs were carried out at 48,000 rpm. Although rotor speeds greater than 50,000 rpm can be tolerated if quartz windows are used, these windows give a distorted interference pattern at high rotor speeds. The cells were torqued to 13.5 m-N and the standard 12mm cells were filled with 0.45cm^3 of β-casein solution in the sample sector and 0.46cm^3 of dialysate in the reference sector. The 12mm synthetic boundary cell had 0.16cm^3 of protein solution added to the sample sector and 0.46cm^3 of dialysate added to the reference sector. 1.0cm^3 of solution and 1.02cm^3 of dialysate were added to the sample and reference sectors respectively of the 30mm cell. An An-D rotor was used with the 12mm cells whereas an An-E rotor was used with the 30mm cell. Interference counterbalances were used with both rotors. A symmetrical 0.75mm double slit interference aperture mask was used in conjunction with both interference and schlieren optics. Runs were carried out over a temperature

range of 14° to 30°C. A baseline reference run was carried out, using dialysate in both cell sectors, after each sedimentation velocity run to determine the extent of the fringe shift caused by window distortion.

4.7.1.2 Results and Discussion

A qualitative picture of the temperature dependence of the β-casein self-association process was provided by runs carried out using the synthetic boundary cell with an initial concentration of 4.0mg cm^{-3} at 14° and 25°C. The schlieren patterns are illustrated in Figure (4-6(a)) for the run at 14°C and Figure (4-6(b)) at 25°C. At 14°C the boundary consisted of a single peak with a small shoulder which moved towards the cell bottom at a faster rate than the main peak. At 25°C two peaks of similar size were observed, indicating that the faster moving shoulder had increased in size to form a peak at the expense of the area of the slower peak. If the faster peak is attributed to the N-mer species and the slower peak to the monomer species then the observed change in the schlieren pattern between 14°C and 25°C could be interpreted as a shift in the equilibrium in favour of the N-mer species. This is consistent with the observations of Sullivan et al. (1955), von Hippel and Waugh (1955) and Payens and van Markwijk (1963).

If the peaks are assumed to represent two independent and discrete sedimenting boundaries it would be expected that the areas of the slower and faster peaks would be proportional to the concentrations of the β-casein monomer and N-mer species respectively (Payens and van Markwijk, 1963; Payens et al., 1969). If this assumption is valid there should be a zero concentration gradient between the two peaks when they are widely separated. Owing to the nature of the synthetic boundary cell a large degree of peak separation cannot be achieved. A sedimentation velocity run was therefore carried out at 21°C with an initial concentration of 4.0mg cm^{-3}, using a standard 12mm cell to study the region between the peaks. A combined schlieren and interference pattern for this run is illustrated in

Figure (4-6) Schlieren Patterns for β-Casein A^1 Solutions During Sedimentation Velocity Runs at 14°C and 25°C

(a) Schlieren Pattern at 14°C

Photograph A

Initial concentration = 4.0mg cm^{-3}

Run time = 34 min

Rotor speed = 48,000 rpm

(b) Schlieren Pattern at 25°C

Photograph B

Initial concentration = 4.0mg cm^{-3}

Run time = 14 min

Rotor speed = 48,000 rpm

The runs were carried out using a 12mm double sector synthetic boundary cell.

A

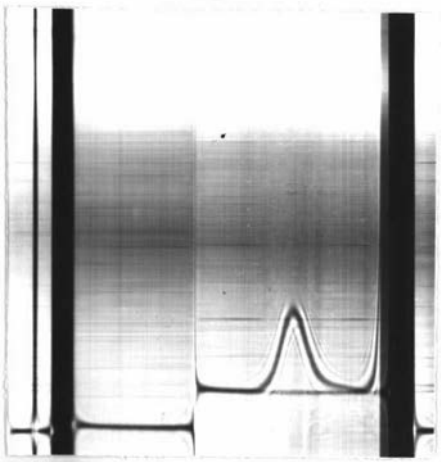

B

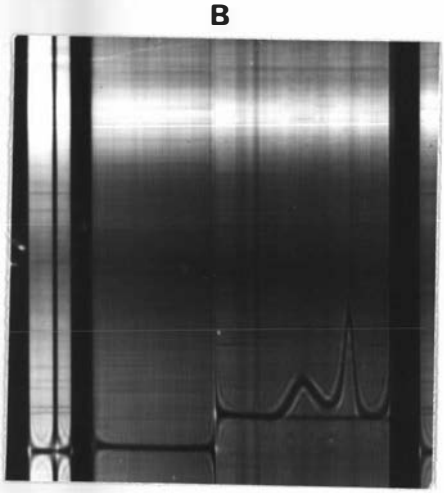

Figure (4-7). It can be seen that there is a positive slope in the interference fringes corresponding to the region between the two schlieren peaks, even though the peaks are widely separated. This indicates that a definite concentration gradient exists between the sedimenting boundaries. A concentration gradient was observed to exist from the slow boundary to the cell bottom even after the fast boundary had completely sedimented onto the bottom. Similar runs were carried out at 21°C using initial β-casein concentrations of 1.80 and 0.72mg cm^{-3}. The interference patterns from these runs are illustrated in Figure (4-8). Two boundaries were observed at both of these lower concentrations with a small, but significant, concentration gradient existing between the boundaries for 1.80mg cm^{-3}. Owing to the small size of the faster boundary for the initial concentration of 0.72mg cm^{-3} it was difficult to detect whether the fringes sloped to a significant extent between the boundaries. The interference patterns for sedimentation velocity runs at 25° and 30°C with initial concentrations of 1.80 and 0.72mg cm^{-3} gave similar results to those at 21°C, except that the faster boundary increased and the slower boundary decreased in size as the temperature was increased.

If the rate of equilibration of the β-casein self-association was very slow in comparison with the rate of separation of the monomer and N-mer species by sedimentation it would be expected that the system could be treated as non-interacting as discussed in Section (4.3.2). However, the observation in this study of a concentration gradient between the two sedimenting boundaries is at variance with the above point of view. It is apparent from the photographs of the sedimentation velocity patterns for β-casein published by Payens and van Markwijk (1963) and Payens *et al.* (1969) that these runs were carried out using single sector cells. In the case of single sector cells a reference baseline is not present in the schlieren pattern, thus making the detection of small concentration gradients very difficult. When the lack of a reference baseline is coupled

Figure (4-7) Combined Interference and Schlieren Patterns for 4.0mg cm^{-3} β-Casein A^1 Solution During Sedimentation Velocity Run at 21°C

Double exposure showing both interference pattern (upper) and schlieren pattern (lower) for the run after about 60 min at 21°C. A 12mm double sector cell was used and the rotor speed was 48,000 rpm. The mercury light source was used for the photograph.

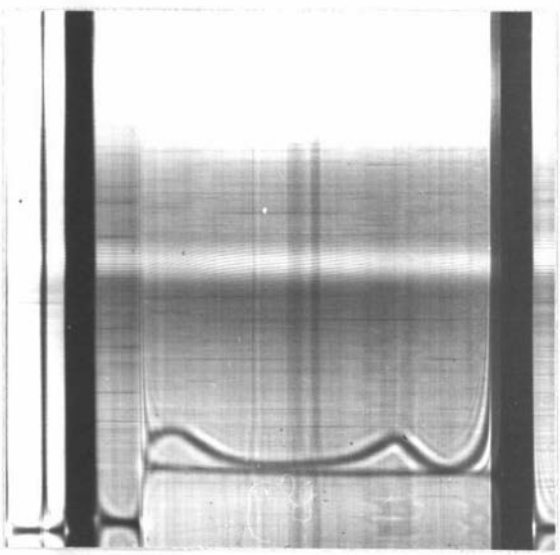

Figure (4-8) Interference Patterns for β-Casein A[1] Solutions During Sedimentation Velocity Runs at 21°C

Photograph A

Initial concentration = 1.8mg cm^{-3}

Run time = 73 min

Rotor speed = 48,000 rpm

The 12mm double sector cell was used for this run.

Photograph B

Initial concentration = 0.72mg cm^{-3}

Run time = 60 min

Rotor speed = 48,000 rpm

The 30mm double sector cell was used for this run.

The photographs were taken using the mercury light source.

A

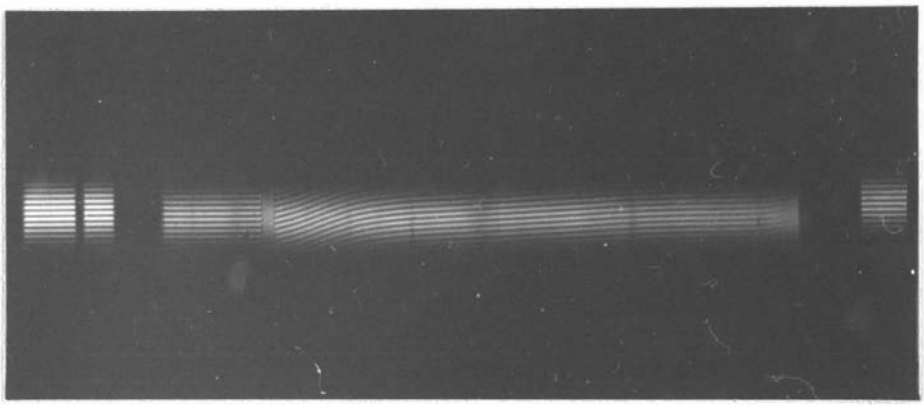

B

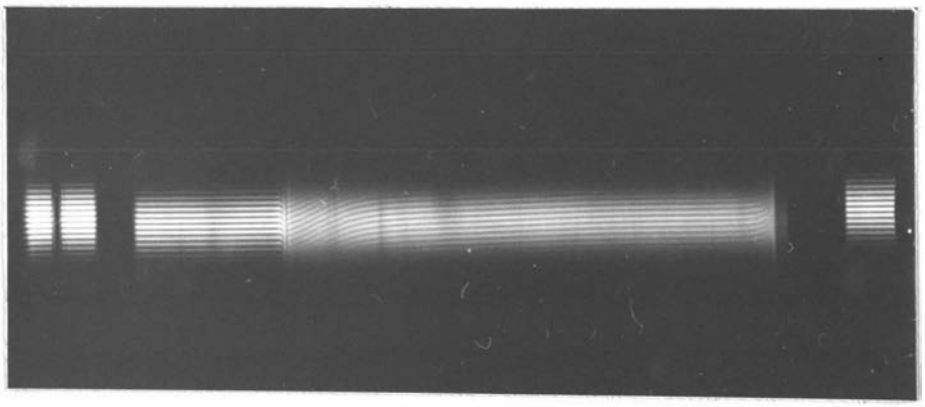

with the relatively low sensitivity of the schlieren system, even moderate concentration gradients can go undetected.

Pearce (1975) and Garnier (1966) have published evidence which indicates that the rate of equilibration of the self-association of β-casein may in fact be quite fast. As noted in Section (4.3.2), if the equilibration rate is considerably faster than the sedimentation rate a small concentration gradient would be expected to exist between the two boundaries of a monomer-N-mer system. In this case the area of the slow peak of the schlieren pattern should remain constant as the total concentration is increased. However, Paynes and van Markwijk (1963) found that the area of the slow peak significantly increased with increasing total β-casein concentration.

A reasonable conclusion can be made, on the basis of the evidence available, that the rate of equilibration of β-casein self-association is similar to the rate of separation of the monomer and N-mer species by sedimentation. In this situation the two sedimenting boundaries would be part of a single reaction boundary. It was noted in Section (4.3.2) that the concentration changes across the slow and fast components of this boundary do not bear a simple relationship to the concentrations of the monomer and N-mer forms of β-casein which were present before sedimentation began. Owing to the considerable difficulty in analysing systems of the above type it was decided not to continue with further sedimentation velocity studies on β-casein A^1 solutions.

CHAPTER 5

DENSITY MEASUREMENTS

5. DENSITY MEASUREMENTS

5.1 Apparent and Partial Specific Volume

The determination of molar mass using the sedimentation equilibrium technique requires a value for the bouyancy term $(1 - \bar{v}\rho)$ where $\bar{v}$ is the partial specific volume of the sedimenting solute and ρ is the density of the solution. The partial specific volume of solute A is defined as

$$\bar{v} = \left(\frac{\partial V}{\partial g_A} \right)_{g_s,\, T,\, p} \tag{5-1}$$

where V is the volume of the solution and g_A and g_s are the masses of the solute A and the solvent respectively. It is convenient to define a quantity called the apparent specific volume $(\bar{v}_{app})$ as

$$\bar{v}_{app} = \frac{V - V_s}{g_A} = \frac{1}{\rho_s} \left[1 - \frac{10^3(\rho - \rho_s)}{C_A} \right] \tag{5-2}$$

where V_s is the volume of the solvent, ρ_s is the density of the solvent and C_A is concentration of solute A in units of mg cm^{-3}. From equations (5-1) and (5-2) the relation between $\bar{v}$ and $\bar{v}_{app}$ is given by

$$\bar{v} = \bar{v}_{app} + g_A \left(\frac{\partial \bar{v}_{app}}{\partial g_A} \right)_{g_s,\, T,\, p} \tag{5-3}$$

At low solute concentrations the apparent specific volume is usually independent of concentration and is therefore equal in value to the partial specific volume. Rearrangement of equation (5-2) gives the following expression

$$\rho = \rho_s + \frac{(1 - \bar{v}_{app}\rho_s)C_A}{10^3} \tag{5-4}$$

A plot of ρ against C_A will give a straight line of slope $(1 - \bar{v}_{app}\rho_s)/10^3$ if $\bar{v}_{app}$ is independent of concentration over the range of C_A employed. The value of the slope can be used to calculate the value of $\bar{v}_{app}$ and hence the value of $\bar{v}$.

Density measurements were made on Brij 35 solutions at several concentrations to obtain values for $\bar{v}$ and $(1 - \bar{v}\rho)$ by using the technique of pycnometry. Similar measurements were not made on β-casein A[1] solutions as values are available in the literature (McMeekin et al., 1949; Payens and van Markwijk, 1963; Noelken and Reibstein, 1968).

5.2 Experimental Procedure

The Brij 35 solutions were made up by weighing out the required amount of Brij 35 into a $100cm^3$ volumetric flask using a Mettler H20 five-figure balance, adding distilled water to the mark, and then reweighing. The concentration was determined in terms of the weight fractions of solute (w_A) where

$$w_A = \frac{g_A}{g_A + g_s}$$

The weight fraction was converted to concentration in units of mg cm^{-3} by

$$c_A = 1000 \rho w_A$$

Density determinations were carried out at 25° and 35°C, over a concentration range of about 5 to 20mg cm^{-3}, using a specific gravity bottle of approximately $25cm^3$ capacity which was closed with a ground glass stopper. The bottle was cleaned before use with chromic acid, rinsed with water, A.R. acetone and A.R. ether and then dried. The specific gravity bottle was first weighed empty on a Mettler H20 balance, filled with the solution and suspended for at least 30 minutes in a thermostatted water bath controlled to within ± 0.01°C. The bottle was then removed from the bath, wiped dry and weighed after it had been allowed to stand for a constant period of 20 minutes in the balance case in a constant temperature room. At least three repeat density determinations were carried out at each concentration. The volume of the bottle was determined by carrying out the above procedure using distilled water.

5.3 Calculation of Density

The mass of the liquid in the specific gravity bottle (g_l) was corrected for the effect of air bouyancy during weighing by using the following equation,

$$g_l = \left\{ g_f(1 - \rho_a'/\rho_w) - g_i \left[\frac{(1 - \rho_a/\rho_w)(1 - \rho_a'/\rho_b)}{(1 - \rho_a/\rho_b)} \right] \right\} \frac{1}{1 - \rho_a/\rho_l} \quad (5\text{-}5)$$

where g_i and g_f are the masses of the empty and full bottle respectively, ρ_a and ρ_a' are the densities of air during the weighing of the empty and full bottle respectively, ρ_b is the bottle density, ρ_w is the density of the weights and ρ_l is the density of the liquid in the bottle which only requires an approximate value for the purposes of the bouyancy correction. The volume of the bottle (V_b) was determined from

$$V_b = \frac{g_{H_2O}}{\rho_{H_2O}}$$

where g_{H_2O} is the mass of distilled water in the filled bottle and ρ_{H_2O} is the literature value for the density of water at the temperature at which the calibration was carried out. The value of ρ_{H_2O} was taken as 0.99707g cm^{-3} at 25°C and 0.99406g cm^{-3} at 35°C. The solution densities are given by

$$\rho = \frac{g_{sol}}{V_b}$$

where g_{sol} is the mass of the solution in the filled bottle.

The values calculated for the densities of the Brij 35 solutions are given in Table (7-7). The densities were determined to within a precision of $\pm$ 0.003%. The calculations carried out to determine values for the partial specific volume and the bouyancy term are given in Chapter 8.

CHAPTER 6

SURFACE TENSION MEASUREMENTS

6. SURFACE TENSION MEASUREMENTS

6.1 Surface Tension and Critical Micelle Concentration

Where a particular physical property of a micelle forming system depends on the free monomer concentration, but not on that of the micelles, the cmc can be determined from the abrupt change in slope when the property is plotted against total amphiphile concentration. As noted in section (1.3) at low concentrations the amphiphile monomers in aqueous solution tend to migrate to the solution-air interface. The effect of these solute molecules at the surface of the aqueous phase is to lower the value of the surface tension below that of pure water. For this reason such molecules are often referred to as surface active substances or surfactants. However, when the amphiphiles form micelles they tend to remain in the bulk solution rather than migrating to the surface, thus only the monomer form is surface active. The relationship between the concentration of the free surface active component (C_{A1}) and the surface tension (γ) is given by the Gibbs adsorption isotherm which can be expressed as

$$\Gamma_{A1} = -\frac{1}{RT}\left(\frac{\partial \gamma}{\partial \ln C_{A1}}\right)_{T,p} \qquad (6\text{-}1)$$

The parameter Γ_{A1} is called the surface excess of component A_1 and can also be defined as

$$\Gamma_{A1} = \frac{n_{A1} - n_{A1}^{(b)}}{A^{(s)}} = \frac{n_{A1}^{(s)}}{A^{(s)}} \qquad (6\text{-}2)$$

where n_{A1} is the total number of moles of A_1 present in all phases, $n_{A1}^{(b)}$ is the number of moles of A_1 in the bulk solution, $n_{A1}^{(s)}$ is the number of moles at the air-solution interface and $A^{(s)}$ is the area of the interface. Γ_{A1} is positive if the interface is richer in A_1 than the bulk aqueous phase. Therefore, from equation (6-1) it can be seen that an increase in C_{A1} will result in a reduction in the surface tension.

At total amphiphile concentrations below the cmc, $C_A \simeq C_{A1}$ and hence a plot of γ against $\ln c_A$ is essentially the same as a plot of γ

against $\ln c_{A1}$. From equation (6-1) the slope of such a plot will be equal to $-RT\Gamma_{A1}$. If the slope of the plot is constant in this region then the excess concentration of amphiphile at the interface is also constant, which implies that the surface has been covered by a monolayer of amphiphile molecules. In this case the following equation can be used to determine the effective surface area of a monomer molecule at the interface (A_{A1}),

$$A_{A1} = \frac{1}{\Gamma_{A1} N_o} \qquad (6\text{-}3)$$

where N_o is Avagadro's number. At values of c_A above the cmc the value of C_{A1} remains relatively constant hence the slope of a plot of γ against $\ln c_A$ will be close to zero in this region. The value of the cmc can be determined from the point of intersection of the slopes observed before and after the cmc.

6.2 Drop Volume Technique

The surface tension of both pure liquids and solutions can be conveniently measured by the drop volume (or drop weight) technique developed by Harkins and Brown (1919). The method involves the measurement of the volume (or weight) of the drops of liquid which fall from the tip of a vertical glass or metal capillary tube. The drops must be formed in equilibrium with an atmosphere saturated with the vapour of the solvent to prevent evaporation from the surface of the drop. The surface tension is related to the mass of the drop (m) which falls from a tip of radius r by the following expression (Harkins and Brown, 1919),

$$\gamma = \frac{mg}{2\pi r\, \psi(r/v^{1/3})} = \frac{mg}{2\pi r\, f(r/a)} \qquad (6\text{-}4)$$

where g is the acceleration due to gravity and $\psi(r/v^{1/3})$ and $f(r/a)$ are empirical correction factors related to the geometry of the drop formation. The correction factors allow for the fact that only a portion of the drop which forms at the tip actually falls. Both $\psi(r/v^{1/3})$ and $f(r/a)$ are equal in value but are related to different parameters. $\psi(r/v^{1/3})$ is a function

of $r/v^{1/3}$ where V is the volume of the drop which falls, whereas f(r/a) is a function of r/a where a is the capillary constant defined by

$$a^2 = \frac{2\gamma}{\Delta\rho g} \tag{6-5}$$

$\Delta\rho$ is the difference in density between the two phases at the drop interface. The advent of the micrometer syringe has allowed the accurate measurement of drop volumes as opposed to drop weights (Kaufman, 1976; Wilkinson, 1972; Parreira, 1965; Gaddum, 1931). Equation (6-4) can be rewritten in terms of the drop volume as follows,

$$V = \frac{V\Delta\rho g}{2\pi r\,\psi(r/V^{1/3})} = \frac{V\Delta\rho g}{2\pi r\, f(r/a)} \tag{6-6}$$

The values of $\psi(r/V^{1/3})$ and f(r/a) can be determined from the tables of Harkins and Brown (1919), which were extended by Wilkinson (1972) to allow dropping tips of small radius to be used. An advantage of the $\psi(r/V^{1/3})$ correction factors over the f(r/a) factors is that $r/V^{1/3}$ can be directly measured. However, Harkins and Brown (1919) considered that the f(r/a) values were more accurate.

An alternative method of calculating the surface tension from drop volume measurements was suggested by Wilkinson (1972). In this approach equation (6-5) is rearranged to give the following expression,

$$\gamma = \frac{r^2\Delta\rho g}{2(r/a)^2} \tag{6-7}$$

The value of $r/V^{1/3}$ is calculated from the drop volume, the corresponding value of r/a is determined from tables published by Wilkinson and γ is calculated from equation (6-7).

The drop volume technique was used in the present study to measure the surface tension of Brij 35 solutions in order to determine cmc values. Similar measurements were also carried out on β-casein A^1 solutions to determine whether the phenomenon of a cmc could be observed for this system. Pierson and Whitaker (1976) have reported that the technique is

theoretically justified for use with surfactant solutions and they provided supporting experimental evidence.

6.3 Drop Volume Apparatus

Wilkinson (1972) has reported that very good results can be obtained using stainless steel hypodermic syringe needles as dropping tips. Therefore, the dropping tip used in this study was formed from an 18 gauge stainless steel syringe needle with the tip ground to give a flat level surface. The tip diameter was measured with a Mitutaya micrometer screw gauge and found to be 0.1254cm. The dropping tip was attached to an Agla MS 01 micrometer syringe (Wellcome Reagents Ltd.) of $0.5cm^3$ capacity. This syringe can deliver volumes down to $0.0001cm^3$ with a precision of $0.00005cm^3$. The syringe barrel was fitted through a Quickfit ST 52/18 screw cap adapter which was connected to an MF 17/1 'T' adapter attached to an FR 5/1S round bottom flask. A 23 gauge hypodermic needle attached to a 40cm length of PVC tubing was connected to the sidearm of the 'T' adapter through a rubber seal to serve as an air vent. The apparatus was clamped to a retort stand and during the drop volume measurements it was immersed in a thermostatted water bath in which the temperature was controlled to with $\pm$ 0.01°C. The water bath had a glass window to facilitate the viewing of the formation of the drops. The water level was adjusted so that it was above the level of the bottom of the plunger of the syringe. A schematic diagram of the drop volume apparatus is shown in Figure (6-1).

6.4 General Technique for Drop Volume Measurements

Before a series of drop volume measurements was carried out the syringe was cleaned with chromic acid, washed with distilled water and acetone, and dried with compressed air. The dropping tip was cleaned with distilled water. The dropping tip was attached to the syringe which was then filled with the solution to be studied. The apparatus was assembled with a small quantity of water in the round bottom flask so that the

Figure (6-1) Schematic Diagram of Drop Volume Apparatus

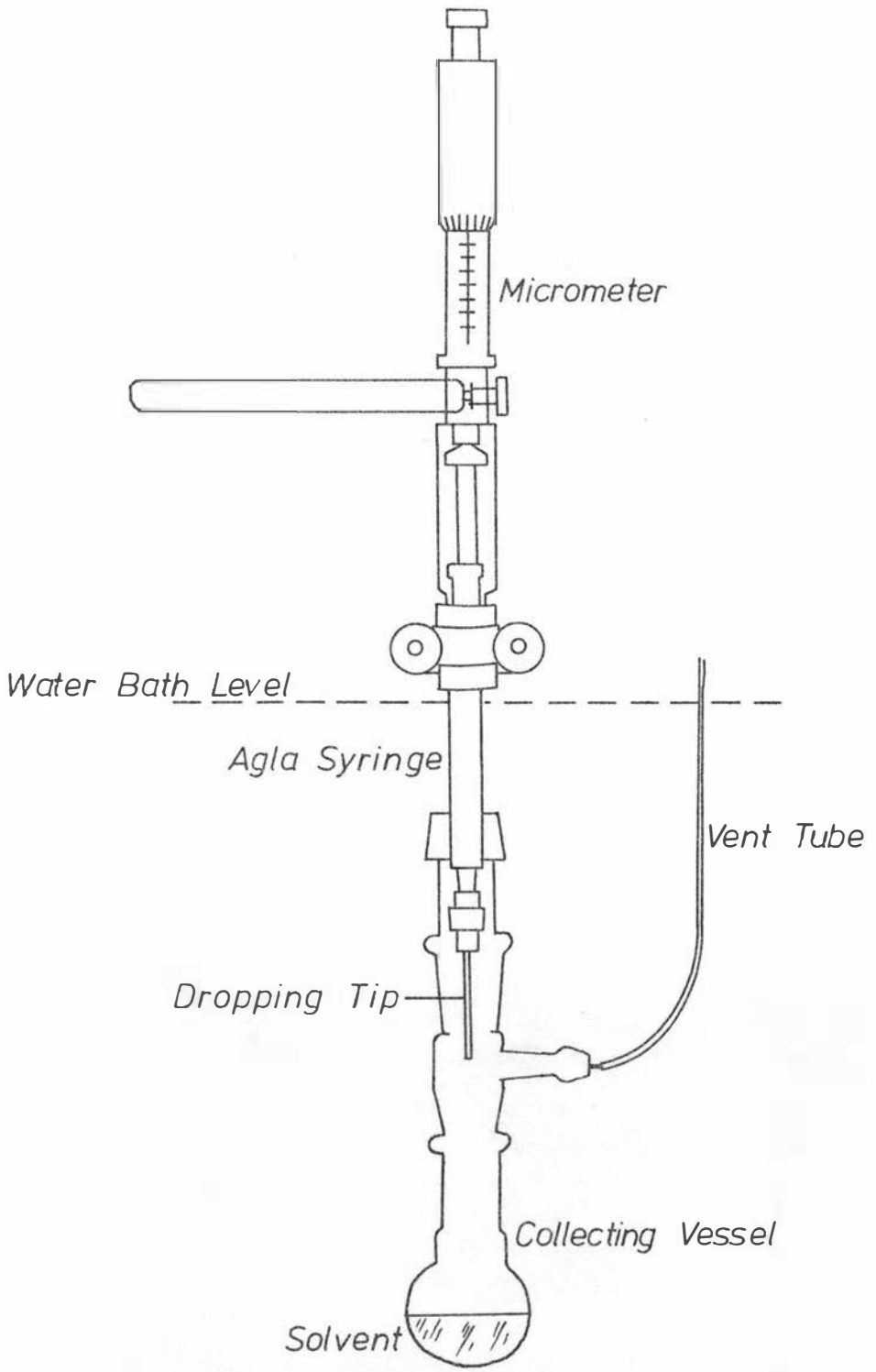

atmosphere surrounding the dropping tip became saturated with water vapour while the apparatus came to temperature equilibrium in the water bath. A period of at least 20 minutes was allowed for this equilibration. A preliminary drop volume measurement was then made to obtain an estimate of the expected drop size. The subsequent drop volume measurements were carried out according to the procedure described by Wilkinson (1972). This involved an initial rapid formation of each drop to about 95% of its maximum size over a period of 30 seconds. The drop thus formed was allowed to hang for a further period of at least 60 seconds before the final 5% of the drop was slowly formed over about 30 seconds until the drop detached from the tip. The drop volume used in the determination of the surface tension was taken as the average over at least 10 successive drops. The syringe was then rinsed out with some of the solution of the next concentration to be studied and then refilled for the next set of measurements.

6.5 Measurements on Distilled Water

The accuracy of the drop volume apparatus was checked by determining the surface tension at 25°C of water which had been twice distilled from alkaline potassium permanganate. The drop volumes were found to be reproducible to within 0.2%. The correction factor required to convert the drop volume values into surface tension values was outside the range of the tables of Harkins and Brown (1919). It was decided therefore to use the tables of Wilkinson (1972) in conjunction with equation (6-7) for the surface tension calculation. The value of the surface tension of distilled water experimentally determined in this study at 25°C was found to be 71.3 mN m^{-1} which was about 0.9% below the literature value of 71.97 mN m^{-1}. This degree of accuracy is sufficient for the purposes of the determination of cmc values of surfactant solutions as only the change in surface tension with concentration is required in this case rather than the absolute values.

6.6 Measurements on Brij 35 Solutions

Solutions of Brij 35 in distilled water were prepared as described in Section (3.5.1) with concentrations ranging from 1.0 to 0.01mg cm^{-3}. Drop volume measurements were carried out at 25° and 35°C and it was found that the drop volumes at any one concentration were reproducible to within about 0.5 to 1.0%. For the very dilute aqueous solutions used in this study the value of $\Delta\rho$ in equation (6-7) is close to unity and as a high degree of accuracy was not required the drop volumes were converted into surface tension by the following expression,

$$\gamma = \frac{r^2 g}{2(r/a)^2} \qquad (6\text{-}8)$$

The values of the surface tension for the Brij 35 solutions at 25° and 35°C calculated using equation (6-8) are recorded in Table (7-8). The determination of the cmc at each temperature from these surface tension values is set out in Chapter 8.

6.7 Measurements on β-Casein A^1 Solutions

β-Casein A^1 solutions were prepared as described in Section (3.6.1) to give a concentration range from 2.0 to 0.01mg cm^{-3}. Attempts were made to carry out drop volume measurements at 21, 25 and 30°C, but the reproducibility was very poor and consistency of results could not be achieved at any of the temperatures used. The surface tension of the β-casein A^1 solutions was observed to be lower than that of pure water but a reproducible trend in the values as the concentration was varied could not be observed.

Gaddum (1931) observed that the surface tension of pure liquids and soap solutions apparently reached equilibrium values very rapidly when the drop volume technique was used, but he found that for biological surface active molecules the attainment of an equilibrium value for the surface tension was extremely slow. It was postulated that this observation was at least in part due to a slow rate of diffusion of the biological

surfactant from the bulk solution to the interface. It is therefore probable that the rate of diffusion of the relatively large β-casein A^1 monomer is too slow for the drop volume technique to be successfully used for surface tension determinations using these solutions. Another possible source of error which could have been significant at these low protein concentrations is that of adsorption onto the surface of the glass syringe. This would decrease the actual concentration of free protein in solution. Thus, the lack of reproducibility may have been partly a result of differing degrees of adsorption between each set of measurements.

It was concluded that on the basis of these observations the drop volume technique was not suitable for the determination of the surface tension of β-casein solutions, at least not at the low concentrations used in this study.

CHAPTER 7

EXPERIMENTAL RESULTS

7. EXPERIMENTAL RESULTS

The primary data obtained for the β-casein A[1] and Brij 35 systems using the methods outlined in the previous experimental sections are recorded in the following tables. The analysis of the data to obtain values for the various thermodynamic parameters involved in each self-association process is discussed in Chapter 8.

Table (7-1) Heat Changes Observed for Dilution of Brij 35 Solutions

T = 298.2 K	T = 308.2 K
$-q_{obs}$/mJ	$-q_{obs}$/mJ
17.18	11.53
16.85	11.90
16.73	11.60
17.25	11.73
17.22	11.92
17.15	11.74
$-\bar{q}_{obs}$/mJ	$-\bar{q}_{obs}$/mJ
17.06 ± 0.09	11.74 ± 0.07

Table (7-2) Heat Changes Observed for Dilution of β-Casein A[1] Solutions

T = 294.2 K	T = 298.2 K	T = 303.2 K	T = 313.2 K
$-q_{obs}$/mJ	$-q_{obs}$/mJ	$-q_{obs}$/mJ	$-q_{obs}$/mJ
1.75	2.49	2.03	0.96
1.77	2.73	2.30	1.25
2.04	2.58	2.47	0.95
1.92		2.17	1.20
1.85		2.18	
1.88		2.49	
1.79		2.38	
$-\bar{q}_{obs}$/mJ	$-\bar{q}_{obs}$/mJ	$-\bar{q}_{obs}$/mJ	$-\bar{q}_{obs}$/mJ
1.86 ± 0.05	2.60 ± 0.08	2.29 ± 0.07	1.09 ± 0.08

Table (7-3) Low Speed Sedimentation Equilibrium Data for 0.74 mg cm^{-3} Brij 35 Solution

T = 298.2 K Rotor speed[a] = 20, 180 rpm		T = 308.2 K Rotor speed = 20, 230 rpm	
$\ln C_A$ [b]	r^2/cm^2	$\ln C_A$	r^2/cm^2
-1.063	46.001	-1.151	46.230
-1.019	46.248	-1.089	46.446
-0.970	46.495	-1.025	46.663
-0.910	46.743	-0.956	46.881
-0.857	46.992	-0.893	47.099
-0.809	47.241	-0.827	47.317
-0.725	47.491	-0.759	47.536
-0.655	47.742	-0.689	47.756
-0.574	47.993	-0.618	47.976
-0.495	48.245	-0.543	48.196
-0.410	48.498	-0.469	48.417
-0.314	48.751	-0.397	48.638
-0.226	49.005	-0.322	48.861
-0.128	49.260	-0.236	49.083
-0.025	49.515	-0.148	49.306
0.072	49.771	-0.053	49.530
0.164	50.028	0.042	49.754
0.274	50.285	0.141	49.978
0.392	50.543	0.235	50.203
0.428	50.620	0.336	50.429
		0.435	50.655
		0.472	50.736

[a] The rotor speed quoted is the average rotor speed taken over the duration of the sedimentation equilibrium run.

[b] C_A is the total Brij 35 concentration in mg cm^{-3}.

Table (7-4) Low Speed Sedimentation Equilibrium Data for 1.59 mg cm^{-3} Brij 35 Solution

T = 298.2 K Rotor speed = 20, 240 rpm		T = 308.2 K Rotor speed = 20, 140 rpm	
$\ln C_A$	r^2/cm^2	$\ln C_A$	r^2/cm^2
-0.614	45.590	-0.532	46.054
-0.445	46.140	-0.367	46.522
-0.299	46.560	-0.226	46.902
-0.172	46.895	-0.102	47.219
-0.060	47.210	0.007	47.493
0.042	47.458	0.107	47.732
0.134	47.682	0.197	47.958
0.218	47.885	0.280	48.161
0.296	48.063	0.356	48.352
0.367	48.240	0.427	48.518
0.435	48.396	0.493	48.679
0.498	48.547	0.555	48.829
0.557	48.680	0.614	48.971
0.613	48.800	0.669	49.110
0.666	48.920	0.722	49.233
0.716	49.035	0.771	49.351
0.764	49.140	0.819	49.458
0.810	49.240	0.864	49.572
0.854	49.335	0.907	49.669
0.895	49.425	0.949	49.765
0.936	49.515	0.989	49.861
0.974	49.603	1.027	49.952
1.011	49.690	1.064	50.039
1.047	49.771		
1.082	49.841	1.099	50.125
1.116	49.914		
1.148	49.985	1.134	50.201
1.179	50.056		
1.210	50.124	1.167	50.283
1.239	50.194		
1.268	50.254	1.199	50.357
1.296	50.313		
1.323	50.375	1.233	50.435
1.343	50.417		

Table (7-5) Low Speed Sedimentation Equilibrium Data for 4.12 mg cm^{-3} Brij 35 Solution

T = 298.2 K Rotor speed = 20, 280 rpm		T = 308.2 K Rotor speed = 20, 290 rpm	
$\ln C_A$	r^2/cm^2	$\ln C_A$	r^2/cm^2
0.220	46.189	0.266	46.116
0.499	46.785	0.543	46.719
0.717	47.238	0.764	47.203
0.896	47.610	0.942	47.613
1.048	47.942	1.094	47.963
1.180	48.247	1.225	48.261
1.296	48.500	1.342	48.525
1.400	48.732	1.446	48.766
1.495	48.941	1.540	48.975
1.581	49.140	1.626	49.168
1.661	49.304	1.706	49.354
1.734	49.467	1.779	49.519
1.803	49.617	1.848	49.681
1.867	49.764	1.912	49.837
1.927	49.900	1.972	49.981
1.984	50.034	2.029	50.119
2.038	50.150	2.083	50.247
2.089	50.265	2.134	50.376
2.134	50.377	2.182	50.488
2.214	50.571	2.220	50.583

Table (7-6) High Speed Equilibrium Data for 0.72mg cm^{-3} β-Casein A[1] Solution at 288.2 K

Rotor speed = 32, 410 rpm

ln (Y(r) - Y_o)*	r^2/cm^2
2.398	49.519
2.639	49.648
2.890	49.776
3.068	49.904
3.258	50.032
3.466	50.160
3.689	50.289
3.850	50.419
4.060	50.548
4.256	50.677
4.465	50.806
4.659	50.934

* Y(r) - Y_o is the fringe displacement in 10^{-3}cm as directly measured by the Topcon PP - 30E profile projector. Y_o is the reading at the zero concentration level and Y(r) is the reading for the fringe position at radial position r.

Table (7-7) Densities of Brij 35 Solutions at 298 and 308 K

T/K	C_A/mg cm^{-3}	ρ/g cm^{-3}
298.2	4.92	0.99762
	9.84	0.99819
	15.54	0.99888
	19.55	0.99933
308.2	4.90	0.99459
	9.81	0.99516
	15.49	0.99582
	19.49	0.99622

Table (7-8) Surface Tension of Brij 35 Solutions at 298 and 308 K

	T = 298.2 K	T = 308.2 K
C_A/mg cm^{-3}	γ/mN m^{-1}	γ/mN m^{-1}
1.00	41.2	40.0
0.80	41.2	39.8
0.60	41.4	39.8
0.50	41.2	40.0
0.40	41.2	40.0
0.30	41.3	39.8
0.25	41.2	40.0
0.20	41.8	40.0
0.15	43.0	40.6
0.10	45.2	42.5
0.08	46.1	43.6
0.06	47.7	45.4
0.05	49.1	46.3
0.03	51.5	49.1
0.01	57.5	54.8

CHAPTER 8

ANALYSIS OF RESULTS

8. ANALYSIS OF RESULTS

8.1 Brij 35 Solutions

8.1.1 Analysis of Surface Tension Measurements

8.1.1.1 Critical Micelle Concentrations

It was noted in Section (6.1) that the critical micelle concentration (cmc) can be determined from the point of intersection of the two straight lines drawn through the linear portions of a plot of surface tension against the log of solute concentration. The surface tension values for the Brij 35 solutions recorded in Table (7-8) were plotted against ln C_A at 25° and 35°C as illustrated in Figure (8-1). Within experimental error it can be seen that the value of γ decreases linearly with ln C_A as the concentration is increased until an abrupt change in slope occurs, after which γ essentially remains constant with increasing concentration. The cmc values determined from the points of intersection of the straight lines drawn in Figure (8-1) are given in Table (8-1). The precision to which the surface tension values were determined gave rise to an uncertainty of about $\pm$ 5% in the cmc values. Becher (1961) reported a value of 0.11mg cm^{-3} for the cmc of Brij 35 as determined by light scattering measurements at 25°C. This is significantly lower than the value of 0.21mg cm^{-3} determined in this study and cannot be accounted for by experimental error. The lack of agreement may be a reflection of differing degrees of purity or heterogeneity between the commercial Brij 35 preparations used in the separate studies.

8.1.1.2 Effective Surface Area of the Monomer

Below the cmc the magnitude of the slope of the γ versus ln C_A plot can be used to determine the surface excess of Brij 35 from equation (6-2), that is

$$\Gamma_{A1} = - \frac{1}{RT}\left(\frac{\partial \gamma}{\partial \ln C_{A1}}\right)_{T,\,p} \qquad (8\text{-}1)$$

Figure (8-1) Plot of Surface Tension vs Log of Solute Concentration for Brij 35 Solutions

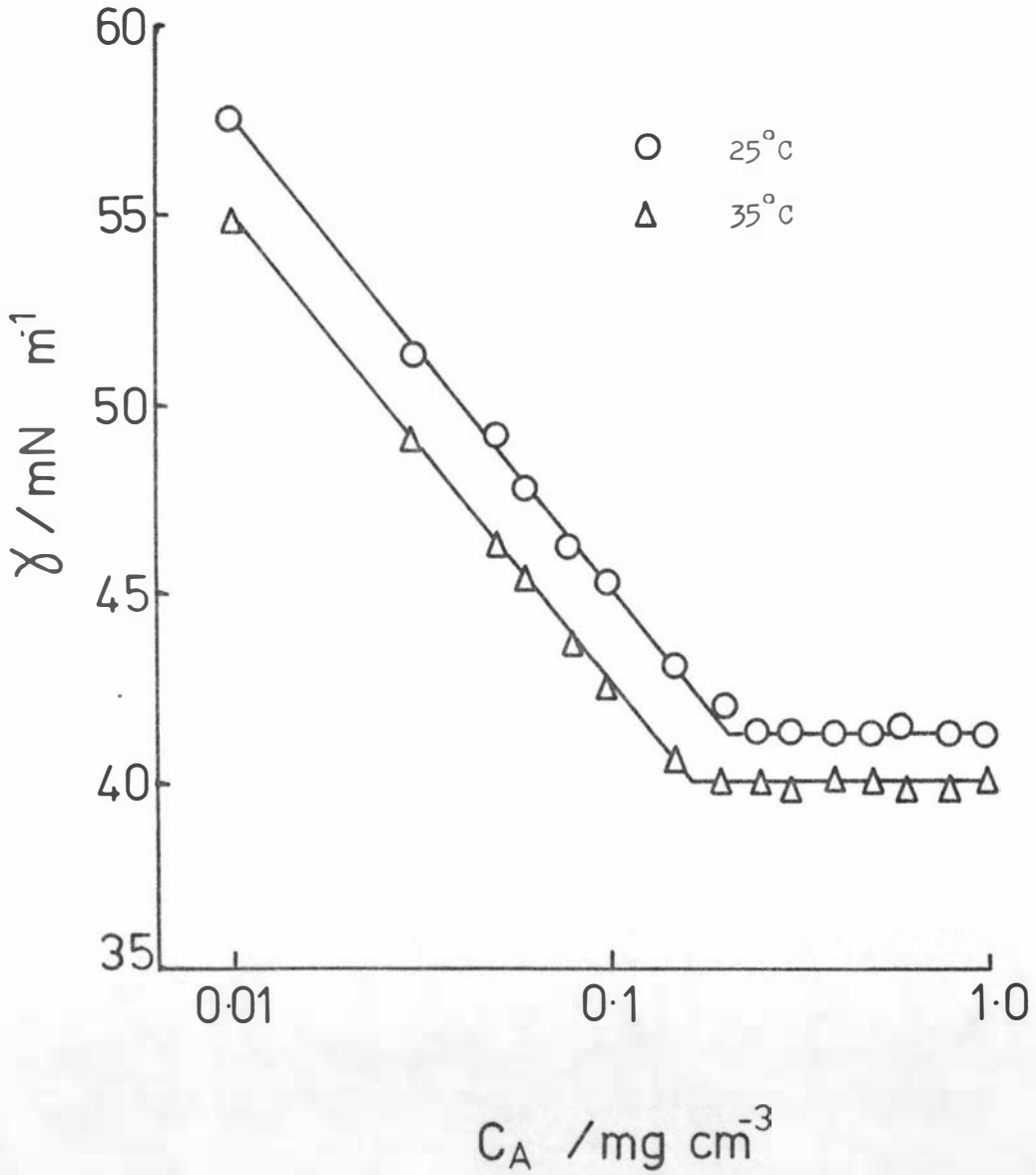

The effective surface area of a Brij 35 monomer at the solution-air interface can be calculated from the value of Γ_{A1} by using equation (6-3) where

$$A_{A1} = \frac{1}{\Gamma_{A1} N_o} \qquad (8\text{-}2)$$

The calculated values of Γ_{A1} and A_{A1} for Brij 35 at 25° and 35°C are given in Table (8-1). The value of 0.77nm^2 determined in this study at 25°C is in reasonable agreement with the value of 0.74nm^2 reported by Becher (1961).

8.1.2 Analysis of Density Measurements

8.1.2.1 Partial Specific Volumes

The values recorded in Table (7-7) for the density of the Brij 35 solutions at 25° and 35°C have been plotted in Figure (8-2) as a function of the solute concentration expressed in mg cm^{-3}. The literature value for the density of water at each temperature have been included in the plots. The value of ρ for the Brij 35 solutions appears to bear a linear relationship with concentration, within experimental error, over the concentration range studied. Therefore, from Equation (5-4) the slope of the plots can be used to determine the value of $\bar{v}_{app}$ at each temperature, that is

$$\rho = \rho_s + \frac{(1 - \bar{v}_{app}\rho_s) C_A}{10^3} \qquad (8\text{-}3)$$

As noted in Section (5.1), the value of $\bar{v}_{app}$ equals that of $\bar{v}$ when $\bar{v}_{app}$ is independent of concentration. This has been shown to be the case for the Brij 35 solutions used in this study by the linearity of the ρ versus C_A plots. The values of $\bar{v}$ calculated by the above procedure for the Brij 35 solutions at 25° and 35°C are given in Table (8-2). The 0.003% precision to which the ρ values were determined resulted in an error of about $\pm$ 0.3% in the $\bar{v}$ values.

Figure (8-2) Plot of Density vs Solute Concentration for Brij 35 Solutions

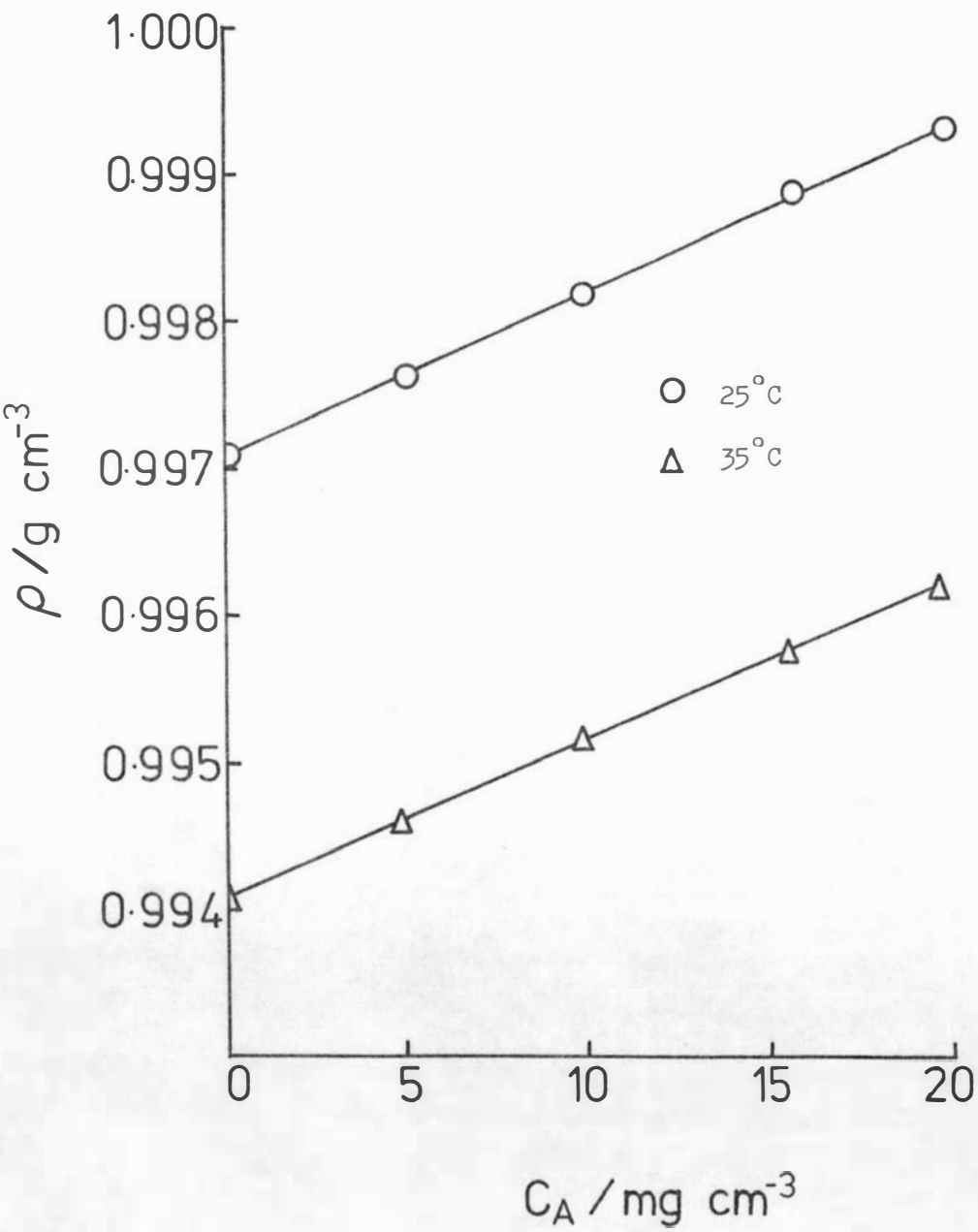

Table (8-1) Critical Micelle Concentrations, Surface Excess and Monomer Surface Areas for Brij 35 Solutions

T/K	cmc/mg cm^{-3}	Γ_{A1}/mol cm^{-2}	A_{A1}/nm^2
298.2	0.21	2.17×10^{-10}	0.77
308.2	0.16	2.09×10^{-10}	0.79

Table (8-2) Partial Specific Volumes and Bouyancy Terms for Brij 35 Solutions

T/K	$\bar{v}/cm^3\ g^{-1}$	$(1 - \bar{v}\rho)$
298.2	0.887	0.115
308.2	0.893	0.112

8.1.2.2 Bouyancy Terms

The values for the $(1 - \bar{v}\rho)$ term were found to be close to 0.1 at both temperatures studied, hence the $\pm$ 0.3% uncertainty in $\bar{v}$ gave rise to an uncertainty of about $\pm$ 3% in the value of $(1 - \bar{v}\rho)$. Therefore, over the concentration range employed in the sedimentation equilibrium experiments on the Brij 35 solutions, the value of $(1 - \bar{v}\rho)$ is independent of concentration within experimental error. The value of the $(1 - \bar{v}\rho)$ term at 25° and 35°C is given in Table (8-2).

8.1.3 Analysis of Low Speed Sedimentation Equilibrium Experiments

8.1.3.1 Apparent Weight Average Molar Mass

The apparent weight average molar mass ($M_{w,app}$) can be calculated from low speed sedimentation equilibrium experiments by using equation (4-11), that is

$$M_{w,app} = \frac{2RT}{(1 - \bar{v}\rho)^2} \cdot \frac{d \ln C_A}{dr^2} \qquad (8-4)$$

The variation of $M_{w,app}$ with concentration can be determined from the slope of a plot of $\ln C_A$ against r^2. The plots using the data recorded in Table (7-4) for the 1.59mg cm^{-3} Brij 35 solutions at 25° and 35°C are illustrated in Figures (8-3) and (8-4). It can be seen that there is a significant upward curvature in the plots indicating that the value of $M_{w,app}$ is increasing with concentration. The following procedure was used in this study to obtain the value of $M_{w,app}$ at various Brij 35 concentrations. The least squares best-fit straight line was determined through five adjacent points in the $\ln C_A$ versus r^2 plot. The slope of this line was taken to be an approximation of the slope of the best-fit curve through these points at the mean value of $\ln C_A$ for the five points. This procedure is similar to the one described by Yphantis (1964), the difference being that the points used in this study were not quite equally spaced. However, the nature of the $\ln C_A$ versus r^2 plots for the Brij 35 solutions was such that the above approximation did not introduce serious error.

Figure (8-3) Plot of Log of Solute Concentration vs r^2 for 1.59mg cm^{-3} Brij 35 Solution at 25°C

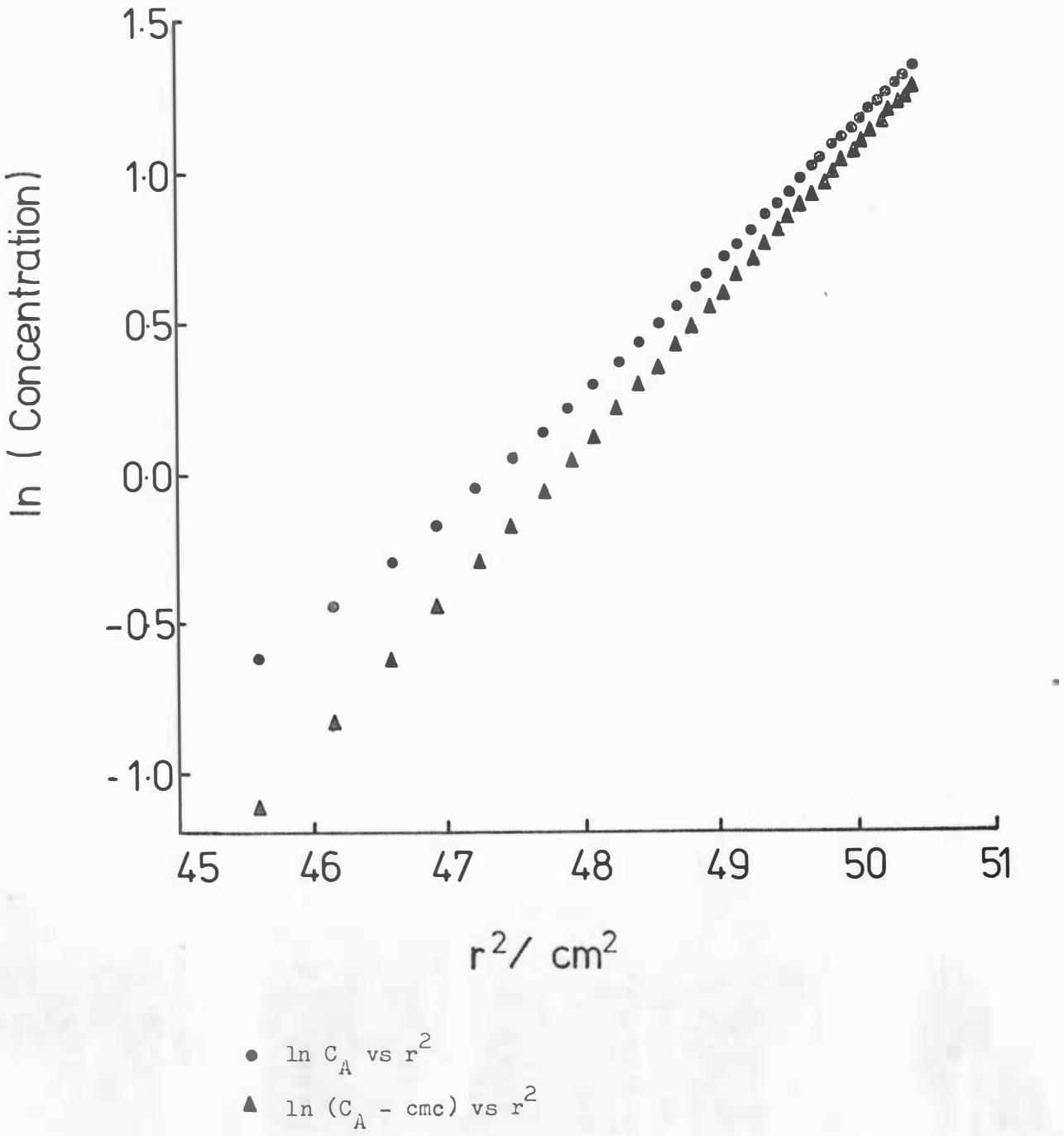

Figure (8-4) Plot of Log of Solute Concentration vs r^2 for 1.59mg cm^{-3} Brij 35 Solution at 35°C

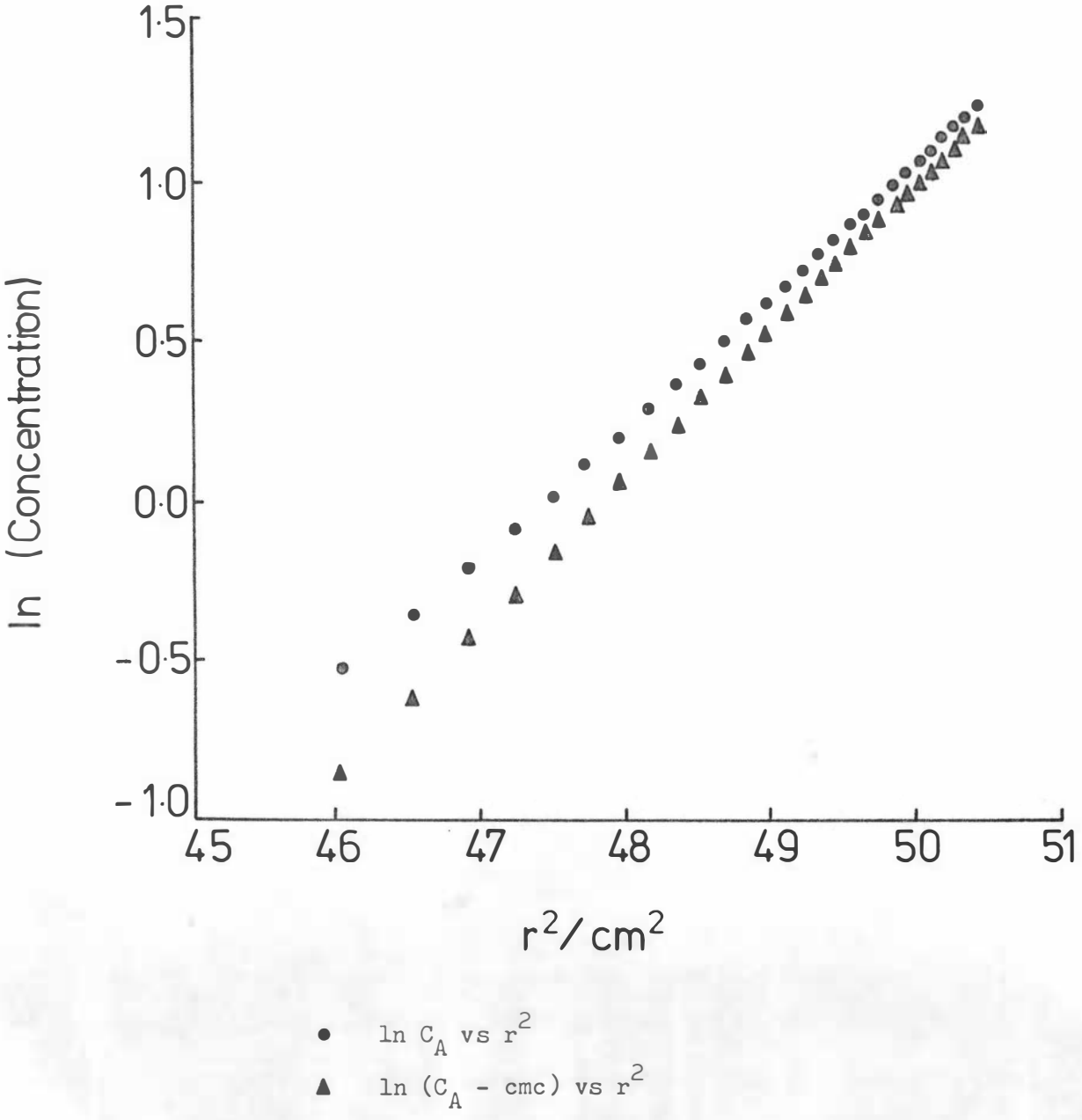

The $M_{w,app}$ value at each of the mean ln C_A values was calculated from Equation (8-4) using the $(1 - \bar{v}\rho)$ values recorded in Table (8-2). The results of $M_{w,app}$ calculations for the Brij 35 solutions at 25° and 35°C using the data in Tables (7-3) to (7-5) are plotted against C_A in Figures (8-5) and (8-6) respectively. At both temperatures there is reasonable overlap of the data from the runs carried out using the different initial concentrations. It can be seen that as C_A is increased the value of $M_{w,app}$ rapidly increases until a maximum is reached which is followed by a slow decrease. The decrease in $M_{w,app}$ at the higher concentrations indicates that nonideality is significant in the Brij 35 system at these concentrations. The next section will describe how both the extent of the nonideality and the molar mass of the N-mer were determined from the sedimentation equilibrium data.

8.1.3.2 N-mer Molar Mass and the Second Virial Coefficient

The total concentration of solute for a monomer-N-mer system in which the N-mers are polydisperse is given by

$$C_A = C_{A1} + C_m \tag{8-5}$$

where C_m is the total concentration of all the N-mers and can be expressed as

$$C_m = \sum_N C_{AN} \tag{8-6}$$

From equation (8-5) the total N-mer concentration is also given by

$$C_m = C_A - C_{A1} \tag{8-7}$$

It was noted in Sections (1.4.2) and (1.4.3) that if N is large,

$$C_{A1} \simeq \text{cmc} \tag{8-8}$$

For polydisperse micelles, from Equation (8-4) the apparent weight average molar mass of the N-mers ($\bar{M}_{m,app}$) is given by

$$\bar{M}_{m,app} = \frac{2RT}{(1 - \bar{v}\rho)\omega^2} \cdot \frac{d \ln C_m}{dr^2} \tag{8-9}$$

Figure (8-5) Plot of Apparent Weight Average Molar Mass vs Solute Concentration for Brij 35 Solutions at 25°C

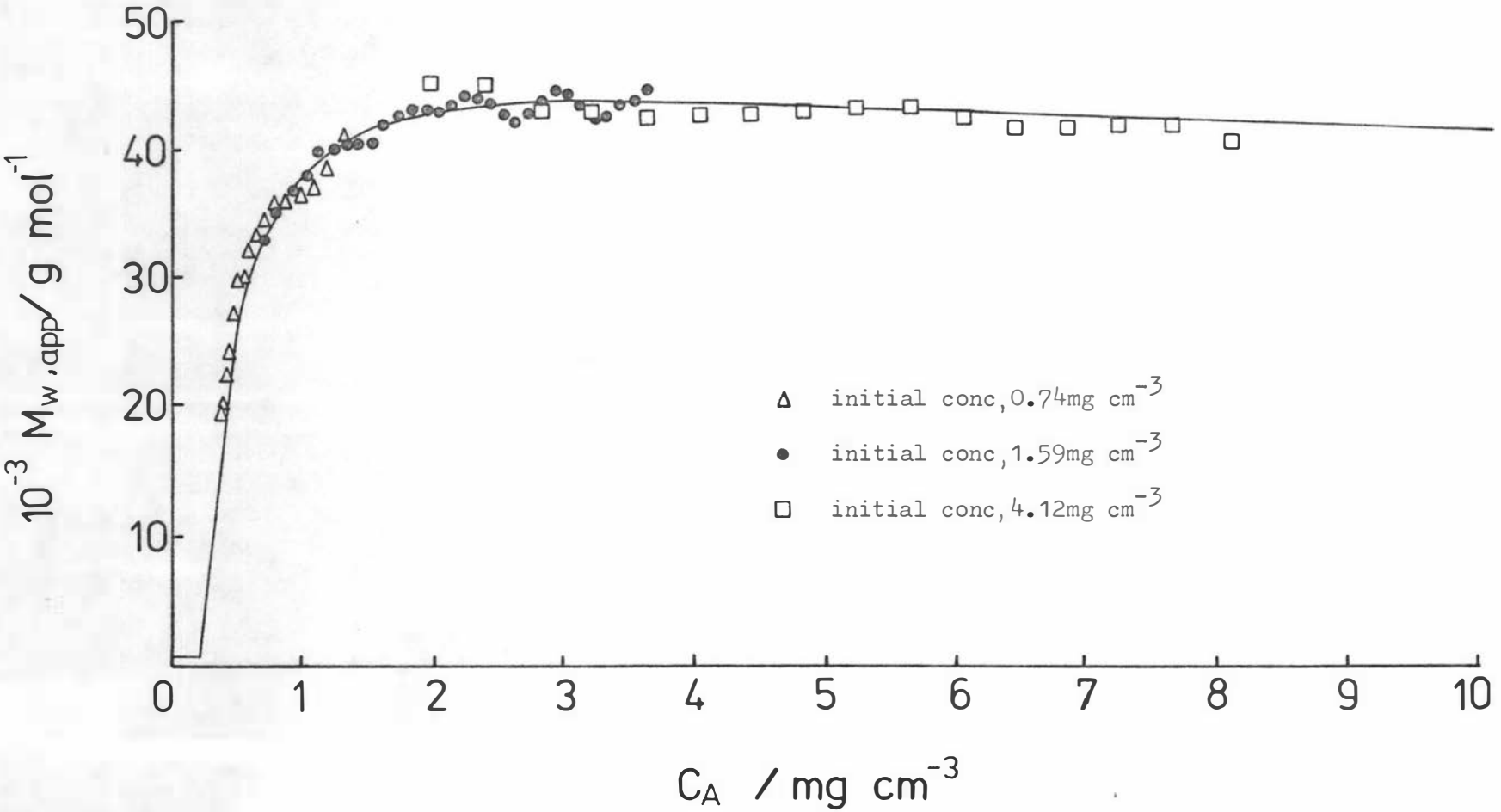

Figure (8-6) Plot of Apparent Weight Average Molar Mass vs Solute Concentration for Brij 35 Solutions at 35°C

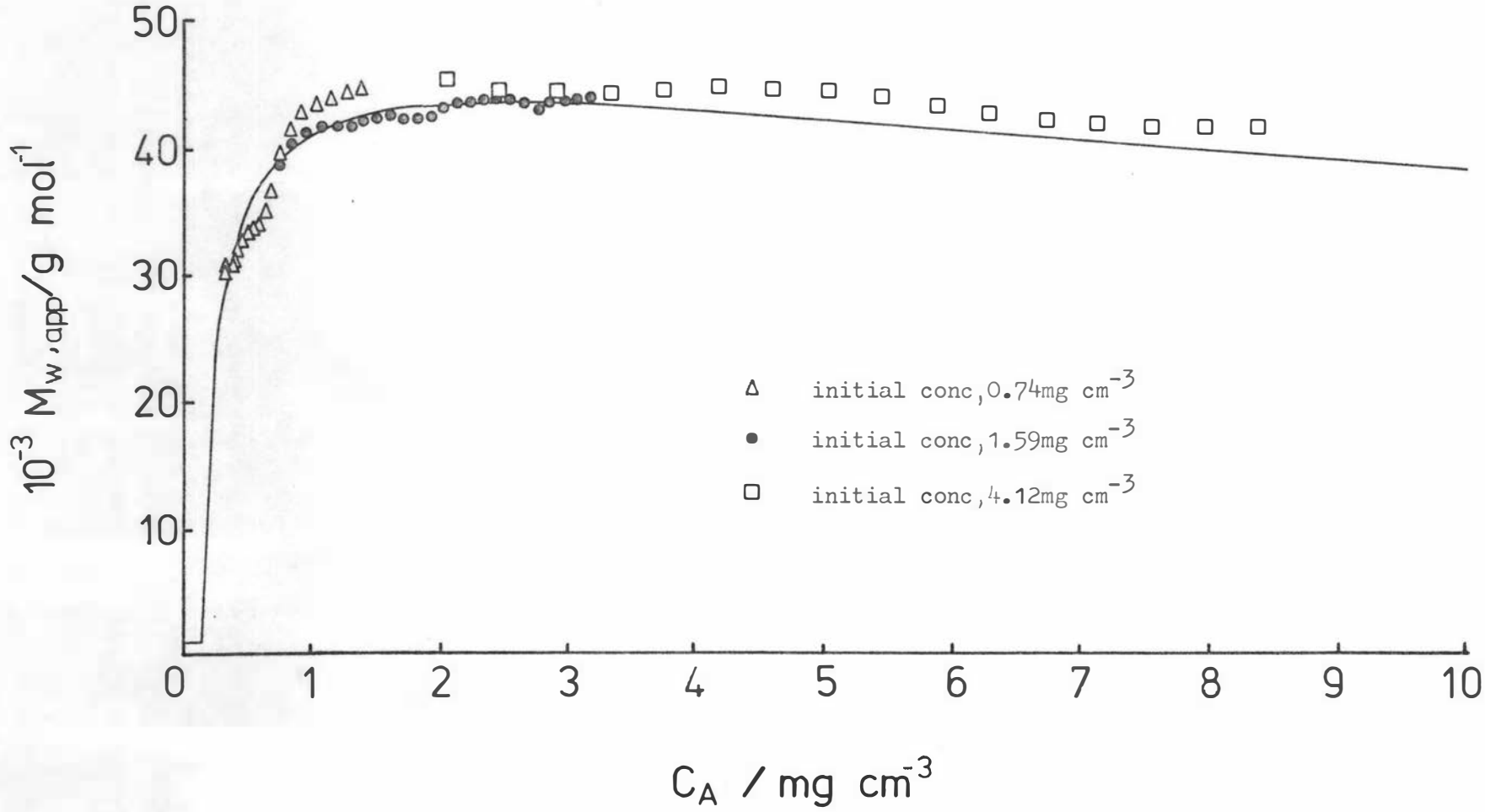

Combining Equations (8-7), (8-8) and (8-9) $\bar{M}_{m,app}$ can be expressed as

$$\bar{M}_{m,app} = \frac{2RT}{(1 - \bar{v}\rho)\omega^2} \cdot \frac{d \ln(C_A - cmc)}{dr^2} \qquad (8\text{-}10)$$

Thus, the slope of a plot of $\ln(C_A - cmc)$ against r^2 will give the value of $\bar{M}_{m,app}$ from Equation (8-10). This approach has been used by Ikeda and Kakuichi (1967) and Anacker et al. (1964) in the analysis of detergent systems. The sedimentation equilibrium data obtained in the present study from the 1.59mg cm^{-3} Brij 35 solutions at 25° and 35°C were used to calculate the value of $\bar{M}_{m,app}$ at each temperature. The initial concentration of 1.59mg cm^{-3} was chosen for this purpose as it is close to the value of 2.0mg cm^{-3} recommended for low speed equilibrium runs. For this reason it was expected that the data derived from the runs carried out using the 1.59mg cm^{-3} initial concentration would be more accurate than the data from the other concentrations. The plots of $\ln(C_A - cmc)$ versus r^2 for the 1.59mg cm^{-3} solutions at 25° and 35°C are illustrated in Figures (8-3) and (8-4) respectively. The cmc values recorded in Table (8-1) were used in the plots at the corresponding temperatures.

The $\ln(C_A - cmc)$ plots were analysed by the least squares method described in Section (8.1.3.1) to obtain point average values of $\bar{M}_{m,app}$ which were used to determine the variation of $\bar{M}_{m,app}$ with C_m. Equation (4-12) can be rearranged to give

$$\frac{1}{\bar{M}_{m,app}} = \frac{1}{\bar{M}_m} + BC_m \qquad (8\text{-}11)$$

where $\bar{M}_m$ is the weight average molar mass of the N-mers, defined by

$$\bar{M}_m = \frac{\sum_N C_{AN} M_{AN}}{C_m} \qquad (8\text{-}12)$$

From equation (8-11) the slope of a plot of $1/\bar{M}_{m,app}$ against C_m will give the value of B and the intercept will give $1/\bar{M}_m$, and hence the value of $\bar{M}_m$. The $\bar{M}_{m,app}$ values derived from the $\ln(C_A - cmc)$ versus r^2

plots in Figures (8-3) and (8-4) were used to plot $1/\bar{M}_{m,app}$ against$(C_A - cmc)$ as illustrated in Figures (8-7) and (8-8). The values obtained for $\bar{M}_m$ and B at 25° and 35°C from a linear least squares analysis of the plots are recorded in Table (8-3).

8.1.3.3 Monomer and N-mer Concentrations

Rearrangement of Equation (4-12) gives

$$\frac{1}{M_{w,app}} = \frac{1}{M_w} + BC_A \qquad (8\text{-}13)$$

where the weight average molar mass (M_w) for a monomer-N-mer system is defined from Equation (4-13) as

$$M_w = \frac{C_{A1}M_{A1} + \sum_N C_{AN}M_{AN}}{C_A} \qquad (8\text{-}14)$$

From Equation (8-12) it can be seen that

$$\sum_N C_{AN}M_{AN} = C_m \bar{M}_m \qquad (8\text{-}15)$$

hence Equation (8-14) can be written as

$$M_w = \frac{C_{A1}M_{A1} + C_m \bar{M}_m}{C_A} \qquad (8\text{-}16)$$

Equation (8-16) can be rearranged to give the following expressions for the monomer and total micelle concentrations,

$$C_{A1} = \frac{(\bar{M}_m - M_w)\, C_A}{(\bar{M}_m - M_{A1})} \qquad (8\text{-}17)$$

$$C_m = \frac{(M_w - M_{A1})\, C_A}{(\bar{M}_m - M_{A1})} \qquad (8\text{-}18)$$

The $M_{w,app}$ values for the 1.59mg cm^{-3} solutions plotted in Figures (8-5) and (8-6) and the B values recorded in Table (8-3) were used to obtain the value of M_w at each C_A by using Equation (8-13). Equations (8-17) and (8-18) were used to calculate the value of C_{A1} and C_m at each C_A value and the results of these calculations are plotted against C_A in Figures (8-9) and (8-10) for the runs at 25° and 35°C respectively.

Figure (8-7) Plot of Reciprocal of Apparent Weight Average Micelle Molar Mass vs Micelle Concentration for 1.59mg cm^{-3} Brij 35 Solution at 25°C

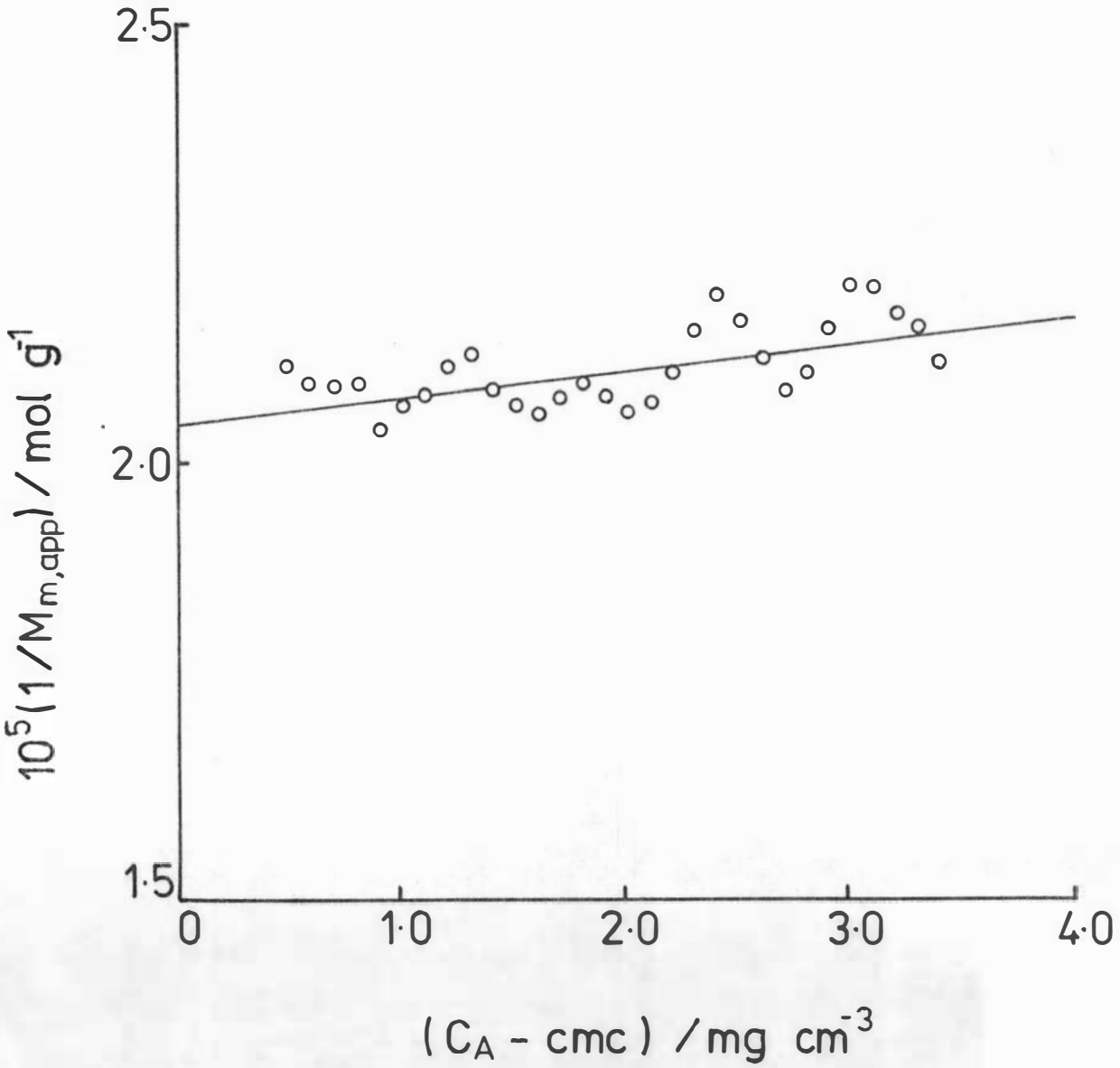

Figure (8-8) Plot of Reciprocal of Apparent Weight Average Micelle Molar Mass vs Micelle Concentration for 1.59mg cm^{-3} Brij 35 Solution at 35°C

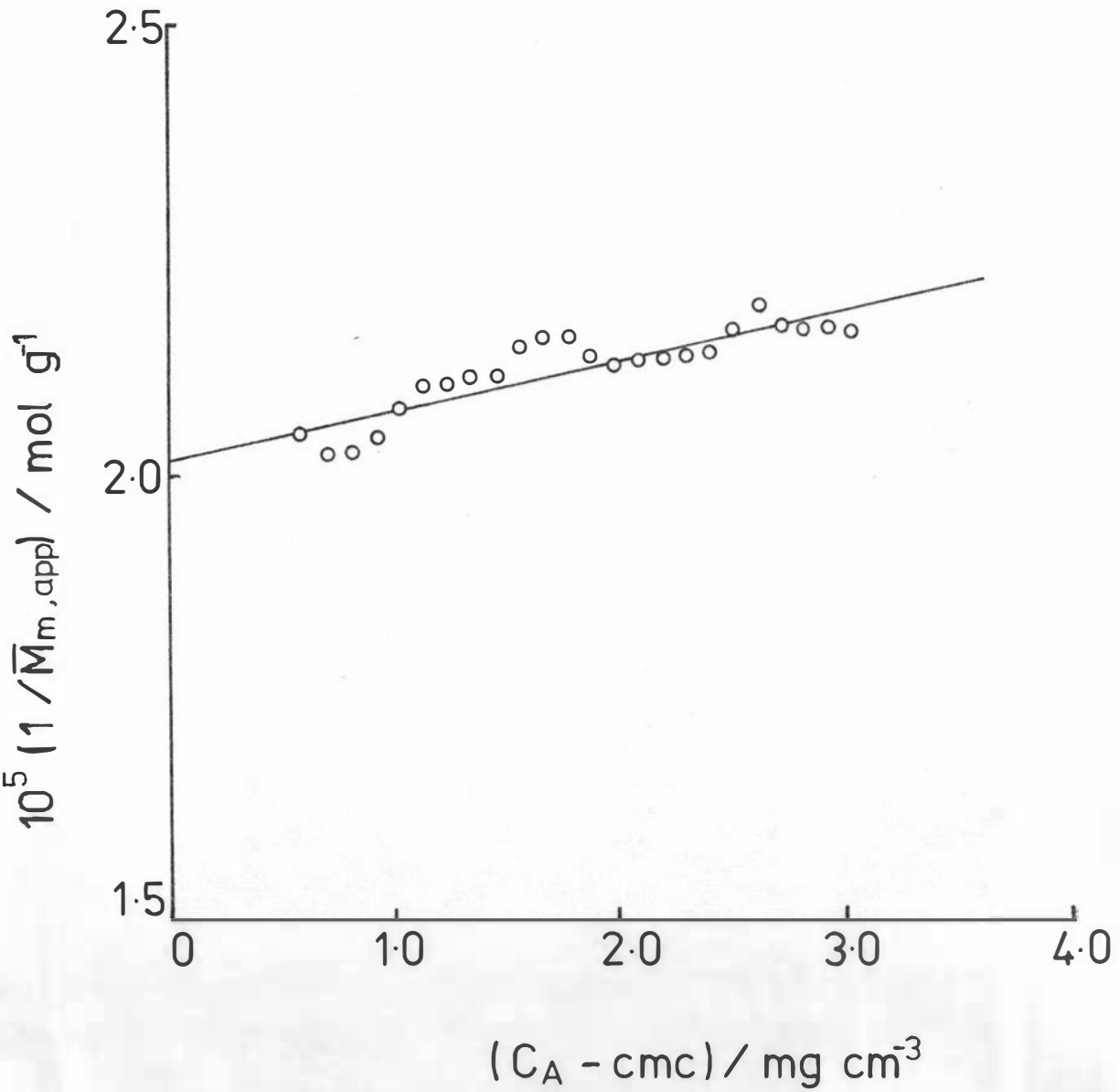

Figure (8-9) Plot of Monomer and Micelle Concentration vs Total Concentration for 1.59mg cm^{-3} Brij 35 Solution at 25°C

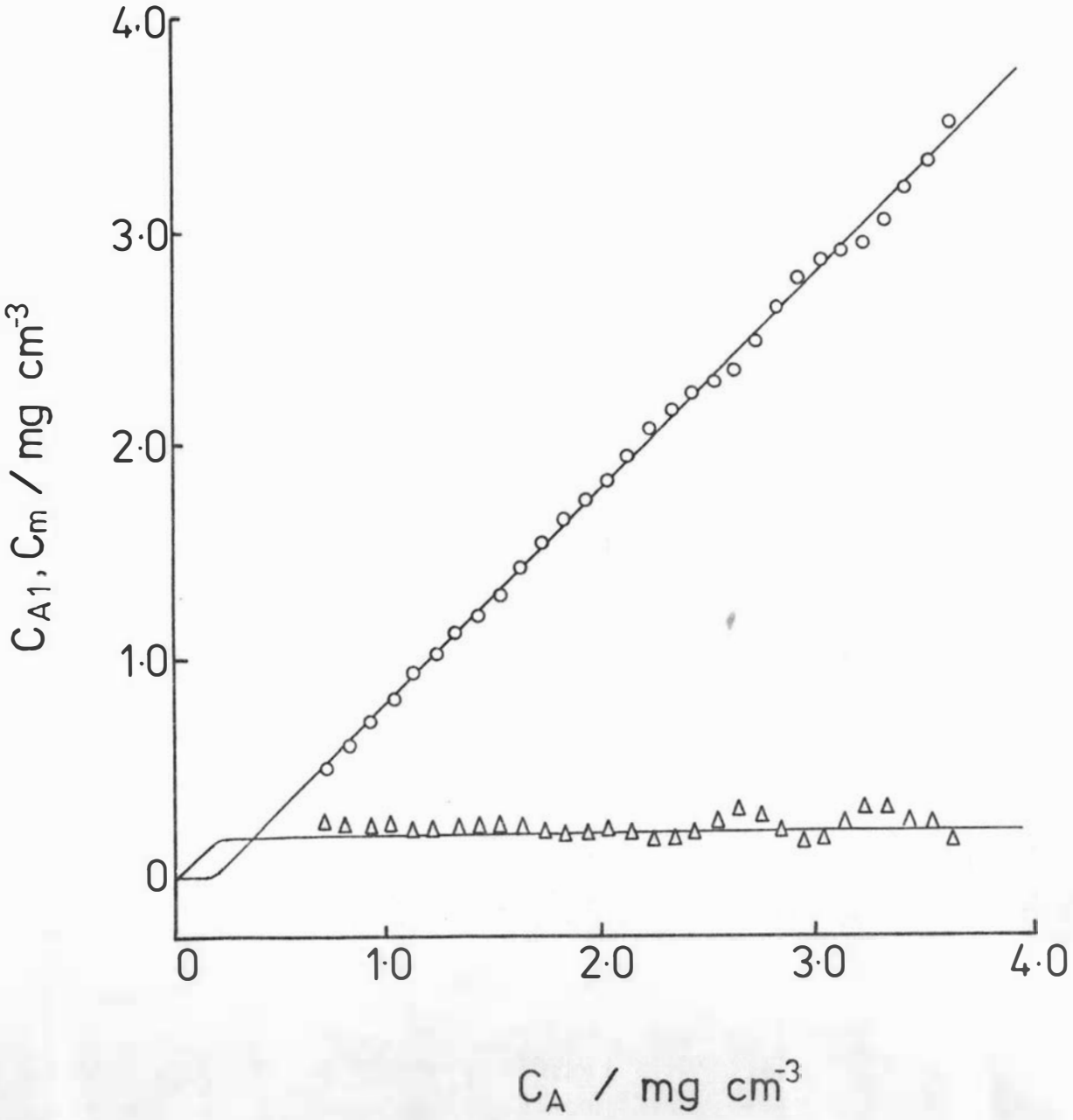

Figure (8-10) Plot of Monomer and Micelle Concentration vs Total Concentration for 1.59mg cm^{-3} Brij 35 Solution at 35°C

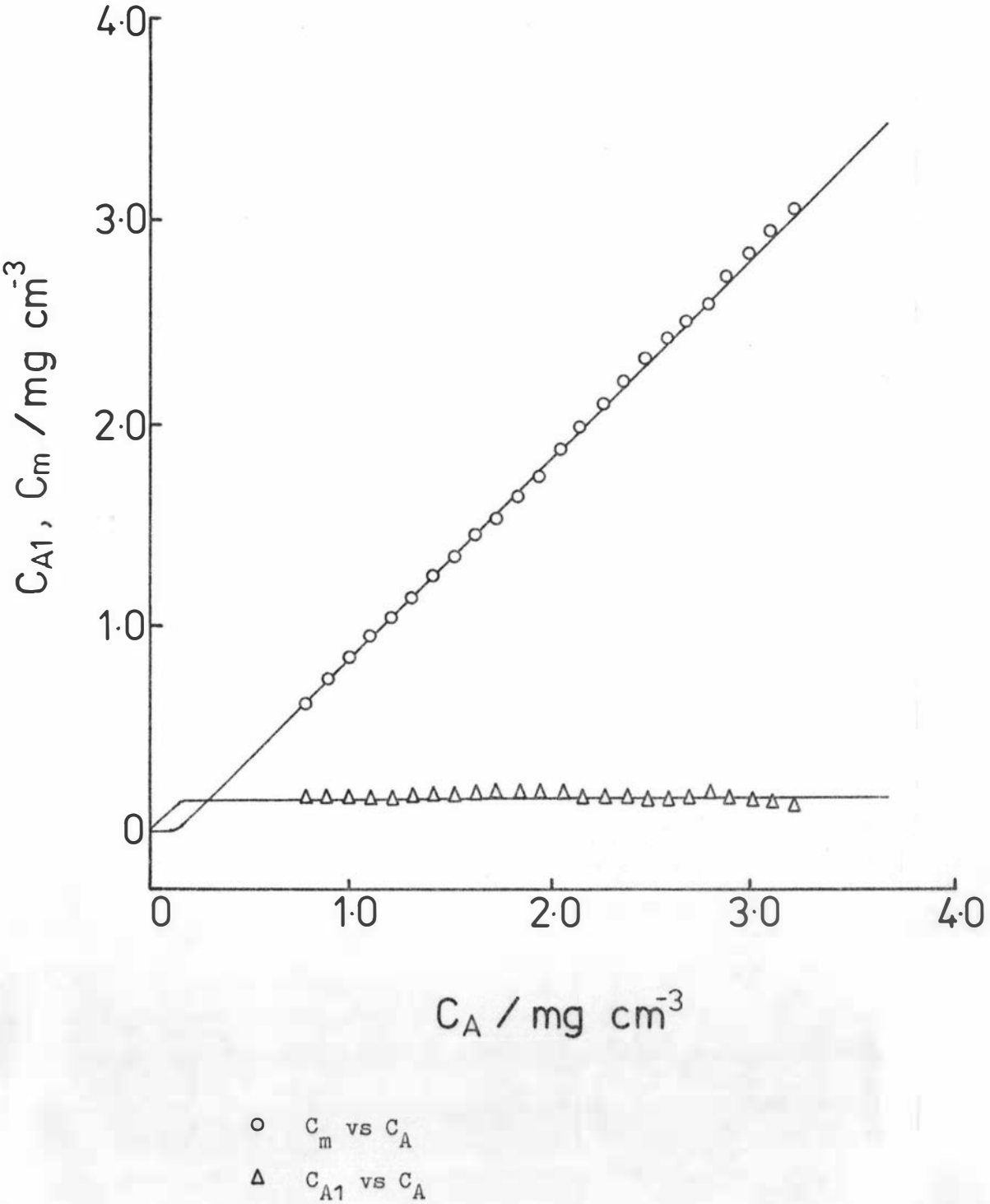

8.1.3.4 Degree of Association and the Equilibrium Constant

The number average degree of association was defined by Equation (1-40) as

$$\bar{N} = \frac{\sum_N n_{AN} N}{\sum_N n_{AN}} \tag{8-19}$$

The weight average degree of association ($\bar{N}_w$) is given by

$$\bar{N}_w = \frac{\sum_N n_{AN} N^2}{\sum_N n_{AN} N} \tag{8-20}$$

The weight average molar mass of the micelles can be expressed as

$$\bar{M}_m = \frac{\sum_N n_{AN} M_{AN}^2}{\sum_N n_{AN} M_{AN}} \tag{8-21}$$

Combining Equation (8-21) with the following relation

$$M_{AN} = N M_{A1} \tag{8-22}$$

the following expression can be written for $\bar{M}_m$,

$$\bar{M}_m = \frac{M_{A1} \sum_N n_{AN} N^2}{\sum_N n_{AN} N} \tag{8-23}$$

Hence, from Equations (8-20) and (8-23),

$$\bar{N}_w = \frac{\bar{M}_m}{M_{A1}} \tag{8-24}$$

Micelle formation in detergent systems is generally characterized by large N values and narrow micelle size distributions. In this situation

$$\bar{N} \simeq \bar{N}_w \tag{8-25}$$

hence the molar mass ratio expressed in Equation (8-24) can be used to calculate $\bar{N}$. The $\bar{N}$ values determined in this way for the Brij 35 solutions at 25° and 35°C are recorded in Table (8-3).

The average" equilibrium constant ($K_{\bar{N}}$) was defined by Equation (1-47) as

$$K_{\bar{N}} = \frac{x_m}{(x_{A1})^{\bar{N}}} \tag{8-26}$$

where x_{A1} and x_m are the mole fractions of the monomers and micelles respectively. If the concentrations are expressed in units of mg cm^{-3}, by analogy with Equation (1-17) the following expression can be written

$$\left(\bar{N}k\ \bar{N} - 1\right)K_{\bar{N}} \equiv K_{\bar{N}}' = \frac{C_m}{(C_{A1})^{\bar{N}}} \qquad (8\text{-}27)$$

It is convenient to express Equation (8-27) in logarithmic form, that is

$$\ln K_{\bar{N}}' = \ln C_m - \bar{N} \ln C_{A1} \qquad (8\text{-}28)$$

The values of C_{A1} and C_m, plotted in Figures (8-9) and (8-10) were used to determine $\ln K_{\bar{N}}'$ from Equation (8-28). The value of $\ln K_{\bar{N}}'$, recorded in Table (8-3) for each temperature, was taken as the mean of the $\ln K_{\bar{N}}'$ values calculated over the range of C_{A1} and C_m values.

The smooth curves in Figures (8-9) and (8-10) were drawn, as described in Section (1.4.2), by combining Equations (8-5) and (8-27) and using the experimentally determined values of $\bar{N}$ and $K_{\bar{N}}'$. Similarly, the experimental values of $\bar{N}$, $K_{\bar{N}}'$ and B were substituted into Equations (8-5), (8-13), (8-16) and (8-27) to draw the smooth $M_{w,app}$ versus C_A curves in Figures (8-5) and (8-6).

8.1.3.5 Error Analysis

An underlying error in the molar mass determinations from the sedimentation equilibrium data arises from the uncertainty in the $(1 - \bar{v}\rho)$ and ω^2 terms. The largest error is inherent in the $(1 - \bar{v}\rho)$ term and is about 3% in magnitude. The error in ω^2 can be assumed to be negligible in comparison. The uncertainty in each $M_{w,app}$ value is therefore expected to be at least about $\pm$ 3%. The values of $\bar{M}_{m,app}$ determined from the $\ln (C_A - cmc)$ versus r^2 plots involve the additional uncertainty associated with the cmc value (i.e. $\pm$ 5%). The effect of this error in the cmc was to introduce an error of about $\pm$ 20% in the slopes of the $1/\bar{M}_{m,app}$ versus C_m plots and an error of about $\pm$ 1% in the intercepts. Each value of $\bar{M}_m$

determined from the intercept is expected to involve an uncertainty of about ± 4.5%, made up of the 3% error in $(1 - \bar{v}\rho)$, the 1% error introduced by the error in cmc and the 0.5% standard error in the intercept calculated from the linear least squares analysis. This error in $\bar{M}_m$ will produce a similar error in the value of $\bar{N}$. The uncertainty in the slopes of the $1/\bar{M}_{m,app}$ versus C_m plots, as indicated by the standard error, was about ± 15%. The total error in the B values was therefore about ±40% resulting from the uncertainty in the slopes and the effects of the errors in the cmc and $(1 - \bar{v}\rho)$ values.

The uncertainty in the mean value of ln K_N' at each temperature was determined by calculating the effect of varying the cmc, $(1 - \bar{v}\rho)$ and $\bar{N}$ values over the range of the uncertainties in each of these terms, and them combining these effects with the standard error in ln K_N'. It was found that the total error in ln K_N' calculated in this way was about ± 15%.

The determination of errors in the above way gives the maximum possible error in each value and therefore exaggerates the degree of uncertainty involved. If a set of repeat experiments was carried out, the standard error in each of the mean values of the various parameters would be expected to be considerably less than the degree of uncertainty indicated above.

The $M_{w,app}$ versus C_A curves drawn in Figures (8-5) and (8-6), which were derived from the sedimentation equilibrium data for the 1.59mg cm^{-3} initial concentration, both lie within the range of the experimental error in the $M_{w,app}$ values for the 0.74 and 4.12mg cm^{-3} runs. This indicates that the sets of results obtained from the three initial concentrations are reasonably compatible with each other at each temperature, thus providing support for the validity of the data derived from the runs using the 1.59mg cm^{-3} solutions. However, the agreement at 35°C is not as good as at 25°C as the curve at 35°C tends to lie below the points determined from the 4.12mg cm^{-3} run. This could be an indication that at

35°C the value calculated for B is too high.

8.1.4 Free Energy of Micelle Formation

For a monomer-N-mer system containing polydisperse micelles the standard free energy of micelle formation ($\Delta G^{\circ}_{\bar{N}}$) is related to ln $K_{\bar{N}}$ by Equation (1-46), that is

$$\Delta G^{\circ}_{\bar{N}} = -\left(\frac{RT}{\bar{N}}\right) \ln K_{\bar{N}} \qquad (8\text{-}29)$$

The values of ln $K'_{\bar{N}}$ and $\bar{N}$ recorded in Table (8-3) were used with Equations (8-27) and (8-29) to calculate the value of $\Delta G^{\circ}_{\bar{N}}$ for the self-association of Brij 35 at 25° and 35°C. The results are recorded in Table (8-5). The error associated with each $\Delta G^{\circ}_{\bar{N}}$ value was calculated from the uncertainty in the corresponding ln $K'_{\bar{N}}$ value as determined in Section (8.1.3.5).

8.1.5 Enthalpy of Micelle Formation

The standard enthalpy of micelle formation is given by Equation (3-4) as

$$\Delta H^{\circ}_{\bar{N}} = -\left(\frac{q_{diss}}{n_{A1}}\right) \qquad (8\text{-}30)$$

where Δn_{A1} is defined by Equation (3-3) as

$$\Delta n_{A1} = n^{f}_{A1} - n^{i}_{A1} \qquad (8\text{-}31)$$

For the calorimetry experiments described in Chapter 3 it will be assumed that the heat of dilution (q_{dil}) was negligible for the dilute Brij 35 solutions used. Therefore, from Equation (3-2)

$$q_{obs} = q_{diss} \qquad (8\text{-}32)$$

The value of Δn_{A1} was determined for the calorimetry experiments by using the expression

$$\Delta n_{A1} = \frac{V_f C^{f}_{A1} - V_i C^{i}_{A1}}{1000 M_{A1}} \qquad (8\text{-}33)$$

where C^{i}_{A1} and C^{f}_{A1} are the monomer concentrations (in mg cm^{-3}) before and after dilution, V_i and V_f are the solution volumes (in cm^{-3}) before and

after dilution and M_{A1} is the molar mass of the monomer. The initial and final total Brij 35 concentration for each experiment was 5.0 and 1.0mg cm^{-3} respectively, hence C^{i}_{A1} is the monomer concentration when C_A equals 5.0mg cm^{-3} and C^{f}_{A1} is the monomer concentration when C_A equals 1.0mg cm^{-3}. The value of C_{A1} at each of these total concentrations was calculated as described in Section (8.1.3.3), using the ln $K'_{\bar{N}}$ and $\bar{N}$ values recorded in Table (8-3). The results of these calculations are recorded in Table (8-4). The error recorded with each C_{A1} value is the same as the error associated with the cmc values as these latter values were used to provide an initial estimate of C_{A1}. The value of Δn_{A1} at each temperature as calculated from Equation (8-33) is given in Table (8-4).

The value of $\Delta H^{\circ}_{\bar{N}}$ at 25° and 35°C recorded in Table (8-5) was calculated from Equations (8-30) and (8-32) using the q_{obs} values recorded in Table (7-1) and the Δn_{A1} values in Table (8-4). The error in each $\Delta H^{\circ}_{\bar{N}}$ value was determined from the combined uncertainties in the q_{obs} and Δn_{A1} values.

8.1.6 Heat Capacity Change

The standard heat capacity change at constant pressure was defined by Equation (1-55) as

$$\Delta C^{\circ}_{p} = \left(\frac{\partial \Delta H^{\circ}_{\bar{N}}}{\partial T} \right)_{p} \qquad (8\text{-}34)$$

If it is assumed that there is a linear relationship between $\Delta H^{\circ}_{\bar{N}}$ and T over the given temperature range, ΔC°_{p} can be expressed as

$$\Delta C^{\circ}_{p} = \frac{(\Delta H^{\circ}_{\bar{N}})_2 - (\Delta H^{\circ}_{\bar{N}})_1}{T_2 - T_1} \qquad (8\text{-}35)$$

where $(\Delta H^{\circ}_{\bar{N}})_1$ and $(\Delta H^{\circ}_{\bar{N}})_2$ are the standard enthalpy values at temperatures T_1 and T_2 respectively. The ΔC°_{p} values recorded in Table (8-5) were calculated from Equation (8-35) using the $\Delta H^{\circ}_{\bar{N}}$ values in Table (8-5). The errors were estimated from the combined uncertainties in the $\Delta H^{\circ}_{\bar{N}}$ values.

Table (8-3) Micelle Size, Virial Coefficients and Equilibrium Constants for Brij 35 Self-Association

T/K	$\bar{M}_m$/g mol^{-1}	$\bar{N}$	10^7 B/mmol cm^3 mg^{-2}	ln $K_{\bar{N}}'$
298.2	49,000	41	3.2	64
308.2	50,000	42	5.6	75

Table (8-4) Monomer Concentrations and Δn_{A1} Values for Brij 35 Self-Association

T/K	C_A/mg cm^{-1}	C_{A1}/mg cm^{-3}	Δn_{A1}/μmol
298.2	5.0	0.22 ± 0.01	0.69 ± 0.05
	1.0	0.21 ± 0.01	
308.2	5.0	0.17 ± 0.01	0.53 ± 0.04
	1.0	0.16 ± 0.01	

Table (8-5) Thermodynamic Parameters for Brij 35 Self-Association

T/K	$\Delta G_{\bar{N}}^{\circ}$/kJ mol^{-1}	$\Delta H_{\bar{N}}^{\circ}$/kJ mol^{-1}	ΔC_p/kJ mol^{-1}K^{-1}	$T\Delta S_{\bar{N}}^{\circ}$/kJ mol^{-1}	$\Delta S_{\bar{N}}^{\circ}$/kJ mol^{-1}K^{-1}
298.2	-30.5 ± 4.6	24.6 ± 1.9	-0.2 ± 0.4	55.1 ± 6.5	0.185 ± 0.022
308.2	-32.2 ± 4.8	22.2 ± 1.8		54.4 ± 6.6	0.177 ± 0.022

8.1.7 Entropy of Micelle Formation

The standard entropy of micelle formation was defined by Equation (1-56) as

$$\Delta S^{\circ}_{\bar{N}} = \frac{\Delta H^{\circ}_{\bar{N}} - \Delta G^{\circ}_{\bar{N}}}{T} \qquad (8\text{-}36)$$

The values of $\Delta S^{\circ}_{\bar{N}}$ recorded in Table (8-5) were calculated from Equation (8-36) using the $\Delta H^{\circ}_{\bar{N}}$ and $\Delta G^{\circ}_{\bar{N}}$ values also recorded in Table (8-5), with the error in $\Delta S^{\circ}_{\bar{N}}$ being determined from the combined errors in $\Delta H^{\circ}_{\bar{N}}$ and $\Delta G^{\circ}_{\bar{N}}$.

8.2 β-Casein A^1 Solutions

8.2.1 Analysis of High Speed Sedimentation Equilibrium Run

The fringe displacement $(Y(r) - Y_o)$ in a high speed sedimentation equilibrium run is proportional to the solute concentration at the radial position r in the cell. Therefore Equation (4-8) can be written as

$$M_{app} = \frac{2RT}{(1 - \bar{v}\rho)\omega^2} \cdot \frac{d \ln(Y(r) - Y_o)}{dr^2} \qquad (8\text{-}38)$$

From Equation (8-38) the slope of a plot of $\ln(Y(r) - Y_o)$ will be proportional to the apparent molar mass of the solute. The plot using the high speed sedimentation equilibrium data recorded in Table (7-6) is illustrated in Figure (8-11). With the possible exception of the first two points it can be seen that the plot is linear, indicating the β-casein A^1 sample was homogeneous and exhibited ideal behaviour in this region of the cell. Yphantis (1964) recommended that, owing to experimental uncertainty, points which represent a fringe displacement greater than 0.01cm should not be included in this type of plot. The first two $\ln(Y(r) - Y_o)$ values in Table (7-6) represent fringe displacements close to 0.01cm and were therefore not included in the determination of the slope of the plot. An unweighted linear least squares analysis was used to determine the slope of the plot and the value of the slope was used in Equation (8-38) to determine the molar mass of the β-casein A^1 sample. The $(1 - \bar{v}\rho)$ term was given the

Figure (8-11) Plot of Log of Fringe Displacement vs r^2 for β-casein A^1 Solution at 15°C

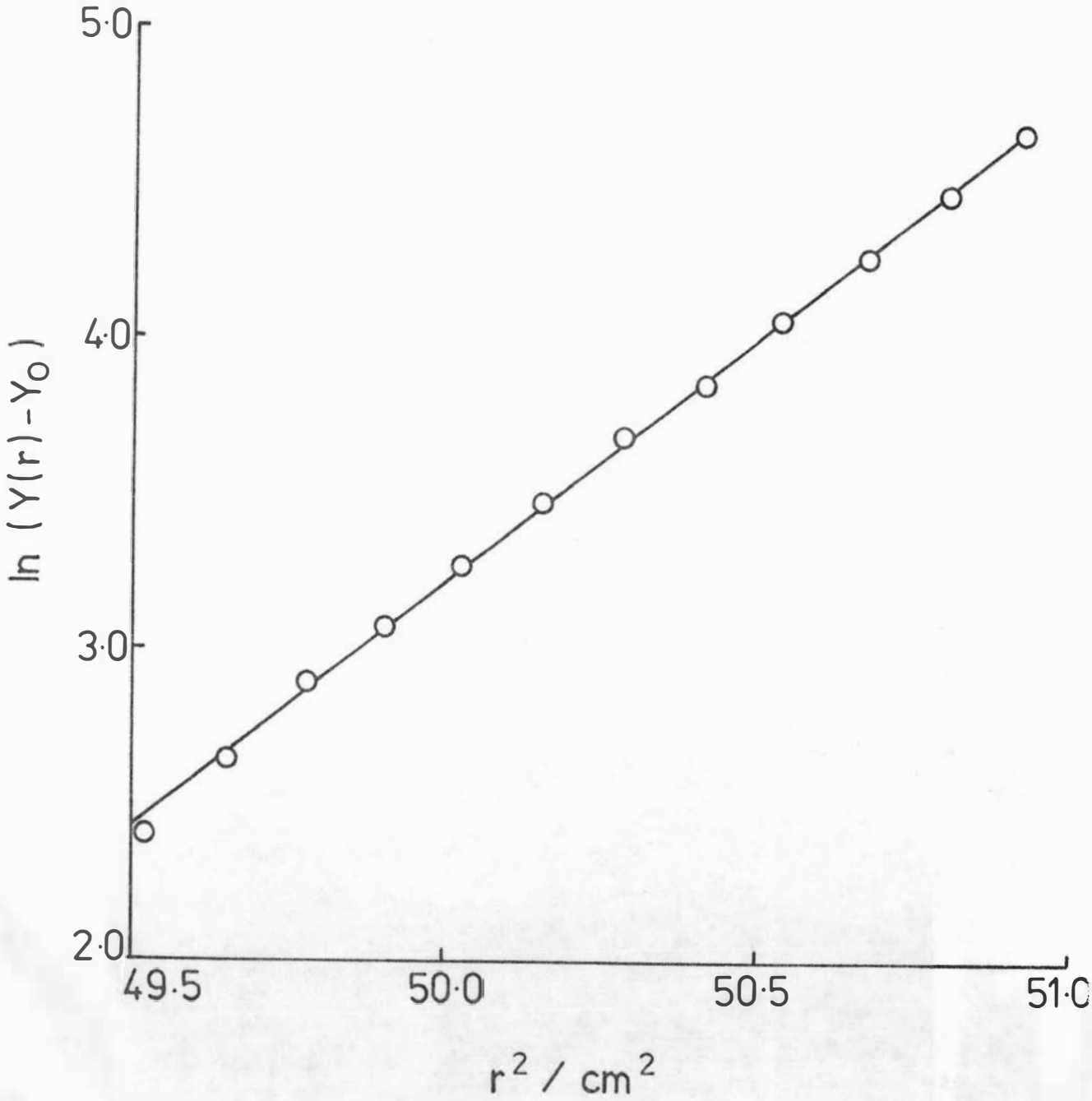

value of 0.268 (Payens and van Markwijk, 1963) which resulted in a monomer molar mass value of 23,800g mol^{-1}, which is within 1% of the value of 24,020g mol^{-1} calculated from the amino acid content of β-casein A^1.

8.2.2 Thermodynamic Parameters for β-casein A^1 Self-Association

The heat changes associated with the self-association of β-casein A^1 in solution were measured by calorimetry as described in Section (3.6). However, the attempts in this study to determine the degree of association and the equilibrium concentrations of the monomer and N-mer forms of β-casein A^1 were not successful. It was therefore decided to use the fluorescence emission data of Pearce (1975) in conjunction with the calorimetry data to determine the standard free energy, enthalpy, heat capacity and entropy for the self-association of β-casein A^1 by treating the process as being one of micelle formation.

Pearce (1975) analysed the self-association of β-casein A^1 in terms of a two-state transition from state I (assumed to be free monomer) to state II (assumed to be the associated species). The two states were assumed to be in equilibrium with each other. The concentration of free monomer can be calculated from the results of Pearce by using the expression

$$C_{A1} = \left(\frac{C_A}{1 + K} \right) \tag{8-39}$$

where

$$K = \frac{C_m}{C_{A1}} = \exp\left(\frac{\Delta S^\circ - \Delta H^\circ / T}{R} \right) \tag{8-40}$$

It should be noted that ΔS° and ΔH° in Equation (8-40) refer to parameters associated with the two-state analysis of the fluorescence data and are not directly related to the ΔH°_N and ΔS°_N parameters defined in this thesis. The values of ΔS° and ΔH° are published in the paper of Pearce, although it should be noted that the superscripts are omitted in that paper. The concentrations of the monomer form of β-casein A^1 as determined from Equations (8-40) and (8-30), using the data of Pearce determined under

the same experimental conditions used for the calorimetry experiments (i.e. pH 6.8, I = 0.11), are set out in Table (8-6). The errors in the C_{A1} values were derived from the errors in the ΔS° and ΔH° parameters.

8.2.2.1 Enthalpy of Micelle Formation

The value of $\Delta H_{\bar{N}}^{\circ}$ for β-casein A^1 self-association at 21, 25, 30 and 40°C was calculated from equations (8-30) and (8-32) using the values of q_{obs} recorded in Table (7-2) and the values of Δn_{A1} in Table (8-6). The use of Equation (8-32) implies the assumption has been made that the heat of dilution of β-casein A^1 is negligible at the low protein concentration used in the calorimetry experiments. The Δn_{A1} values were determined from Equation (8-33) using values of 2.0 and 5.0mg cm^{-3} for V_i and V_f respectively. The initial total β-casein concentration for each calorimetry dilution experiment was 1.80mg cm^{-3} and the final concentration was 0.72mg cm^{-3}. Therefore, the values of C_{A1}^{i} and C_{A1}^{f} were taken from Table (8-6) as being the values of C_{A1} at C_A values of 1.80 and 0.72mg cm^{-3} respectively. M_{A1} in Equation (8-33) was given the value of 24,020g mol^{-1}. The error in each Δn_{A1} value, and the errors in the other parameters for the β-casein self-association process, were calculated as described in Section (8.1) for the corresponding parameters involved in the self-association of Brij 35. The values calculated for $\Delta H_{\bar{N}}^{\circ}$ are recorded in Table (8-7).

8.2.2.2 Heat Capacity Change

The $\Delta H_{\bar{N}}^{\circ}$ values in Table (8-7) were used to determine ΔC_p° values for the β-casein self-association from Equation (8-35). Each ΔC_p° value recorded in Table (8-7) was calculated from the difference of two successive $\Delta H_{\bar{N}}^{\circ}$ values.

8.2.2.3 Free Energy of Micelle Formation

The average degree of association of the β-casein A^1 micelles could not be determined from the fluorescence data of Pearce (1975). However, it was decided that a reasonable estimate of the value of $\bar{N}$ would

Table (8-6) Monomer Concentrations and Equilibrium Constants for β-Casein A^1 Self-Association *

T/K	C_A/mg cm^{-1}	C_{A1}/mg cm^{-3}	Δn_{A1}/nmol	ln K'_N
294.2	1.80	1.34 ± 0.06	28 ± 6	0 ± 11
	0.72	0.67 ± 0.02		
298.2	1.80	0.98 ± 0.06	43 ± 7	7 ± 8
	0.72	0.60 ± 0.02		
303.2	1.80	0.52 ± 0.04	50 ± 6	21 ± 3
	0.72	0.45 ± 0.02		
313.2	1.80	0.09 ± 0.01	18 ± 4	68 ± 9
	0.72	0.12 ± 0.02		

* Calculated from the fluorescence data of Pearce (1975).

Table (8-7) Thermodynamic Parameters for β-Casein A^1 Self-Association

T/K	ΔG°_N/kJ mol^{-1}	ΔH°_N/kJ mol^{-1}	ΔC°_p/kJ mol^{-1}K^{-1}	$T\Delta S^\circ_N$/kJ mol^{-1}	ΔS°_N/kJ mol^{-1}
294.2	-33.0 ± 0.9	66 ± 16	-2 ± 7	99 ± 17	0.34 ± 0.06
298.2	-34.1 ± 0.7	60 ± 12	-3 ± 4	94 ± 13	0.32 ± 0.04
303.2	-35.9 ± 0.2	46 ± 7	2 ± 3	82 ± 7	0.27 ± 0.02
313.2	-41.1 ± 0.8	61 ± 18		102 ± 19	0.33 ± 0.06

be about 30, based on the data published in the literature from several different authors (see Table (1-1) on p. 9). The C_{A1} values in Table (8-6) and the value of 30 for $\bar{N}$ were used to calculate ln $K'_{\bar{N}}$ at each C_A value from Equations (8-28) and (8-5). The mean value of ln $K'_{\bar{N}}$ at each temperature is recorded in Table (8-6). The value of $\Delta G^{\circ}_{\bar{N}}$ at each temperature was calculated using these mean ln $K'_{\bar{N}}$ values. Although a 30% change in the value of $\bar{N}$ produced a similar change in ln $K'_{\bar{N}}$ it was found that it only resulted in a 2% change in the value of $\Delta G^{\circ}_{\bar{N}}$. Therefore, as long as $\bar{N}$ is large it does not have to be known very accurately for the purposes of the determination of $\Delta G^{\circ}_{\bar{N}}$. The values of $\Delta G^{\circ}_{\bar{N}}$ calculated as described above are recorded in Table (8-7).

8.2.2.4 Entropy of Micelle Formation

The $\Delta H^{\circ}_{\bar{N}}$ and $\Delta G^{\circ}_{\bar{N}}$ values recorded in Table (8-7) were used to calculate $\Delta S^{\circ}_{\bar{N}}$ for the self-association of β-casein A[1] at each temperature from Equation (8-36). The results of these calculations are recorded in Table (8-7).

CHAPTER 9

DISCUSSION

9. DISCUSSION

In the following sections an attempt will be made to explain qualitatively the values and trends of the thermodynamic parameters observed for the self-association of Brij 35 and β-casein A^1 in aqueous solution. No attempt will be made to provide a quantitative discussion of the observations. The Brij 35 system will be discussed first and then a comparison will be made with the β-casein A^1 system.

9.1 Brij 35 Self-Association

The molar mass of 49,000 g mol^{-1} determined in this study for the Brij 35 micelle is in good agreement with the value of 48,800 determined by Becher (1961) using light scattering techniques. It can be seen from Table (8-3) on p. 123 that the size of the Brij 35 micelle does not appear to alter significantly with temperature. This is in contrast with the apparent increase observed for short chain polyoxyethylene detergents (Balmbra et al., 1964). However, owing to the degree of uncertainty in the $\bar{N}$ values recorded in Table (8-3), a significant change in micelle size with temperature is not actually precluded. The values of the second virial coefficients in Table (8-3) are of the same order as those observed for similar long-chain polyoxyethylene detergents by El Eini et al. (1976) and Biaselle and Millar (1975).

From Table (8-5) on p. 123 it can be seen that there is a negative free energy change, a positive enthalpy change and a positive entropy change on micelle formation for Brij 35 under standard state conditions at both 25° and 35°C. The signs and magnitudes of these parameters are similar to those observed by Barry and El Eini (1976) for micelle formation in a homologous series of cetyl (C_{16}) long-chain polyoxyethylene surfactants. The free energy change is related to the change in enthalpy and entropy by the expression

$$\Delta G_{\bar{N}}^{\circ} = \Delta H_{\bar{N}}^{\circ} - T\Delta S_{\bar{N}}^{\circ} \qquad (9\text{-}1)$$

The endothermic enthalpy change does not favour micelle formation,

however the magnitude of $T\Delta S_N^\circ$ is just over twice that of ΔH_N°, giving an overall negative value for ΔG_N°. The driving force for Brij 35 micelle formation is therefore entropic in nature.

As noted in Section (1.5), the Brij 35 monomer consists of a hydrophilic head group (the polyoxyethylene chain) and a hydrophobic tail group (the 12-carbon alkyl chain). The above observations can be qualitatively explained by considering the separate contributions of the polar head group and the nonpolar tail group to the thermodynamics of micelle formation. That is, the free energy of micelle formation can be separated into hydrophilic and hydrophobic contributions.

9.1.1 Effect of the Alkyl Chain

It has been proposed that the tail group of a free amphiphilic monomer in aqueous solution is surrounded by a highly structured "cage" of water molecules (Kauzmann, 1959; Goddard *et al.*, 1957; Frank and Evans, 1945). The hydrogen bonds between the water molecules surrounding the tail group are thought to be stronger than those in the bulk water. When the free monomers self-associate to form micelles the tail groups lie within the core of the micelle and are presumed to have little, if any, contact with water. Therefore, the structured solvent cage is broken down and these water molecules are absorbed into the bulk water. The entropy of a water molecule in the solvent cage is lower than in the bulk water and therefore an increase in entropy results when a water molecule is absorbed back into the bulk water. Owing to the stronger hydrogen bonding in the solvent cage compared to the bulk water, an increase in enthalpy results when the structured cage is broken down. Therefore, the positive enthalpy and entropy changes observed for the formation of Brij 35 micelles can be explained in terms of the changes in solvent structure when a monomer goes from the free state into the micelle.

An increase in entropy may also arise from an increase in the flexibility of the hydrocarbon chains in the micelle core compared with

their flexibility in the aqueous solvent (Stainsby and Alexander, 1950; Aranow and Witten, 1960). A decrease in enthalpy could result from the loss of translational kinetic energy of the monomer and from the heat released when the tail groups condense in the interior of the micelle (Anacker, 1970). However, for the Brij 35 system such an enthalpy decrease cannot be important as a net increase in enthalpy was observed.

There appears to be a decrease in the value of ΔH_N° with increasing temperature for Brij 35 resulting in a negative ΔC_p° (see Table (8-5)). However, a definite conclusion cannot be made with respect to the sign of ΔC_p° owing to the magnitude of the associated experimental uncertainty. A decrease in the enthalpy of micelle formation with temperature is a common phenomenon and has been attributed to the effect of temperature on water structure (Tanford, 1973). It is suggested that as the temperature is increased the hydrogen bonds in the solvent cage surrounding the alkyl chain are weakened more rapidly than the hydrogen bonds in the bulk water. At the same time the degree of structuring of the water molecules is decreased. The result is a decrease in both the enthalpy and entropy change associated with the transfer of a monomer to the micelle state. A decrease in ΔS_N° was observed for Brij 35 as the temperature was increased from 25° to 35°C but as the change was well within the experimental uncertainty of the two values, no definite conclusion can be drawn.

9.1.2 Effect of the Head Group

In Section (1-3) it was noted that the size of a micelle is limited by the repulsion between the head groups. The effect of this repulsion is to provide a positive contribution to the free energy of micelle formation. The repulsion between nonionic head groups has been attributed to a preference for hydration rather than self-association (Tanford, 1973) and also to steric effects (Tanford, 1974). Moroi *et al.* (1975) determined that for nonionic detergents, there is a large increase

in enthalpy when the head groups come together in the micelle in addition to the enthalpy change associated with the tail groups. This results in a large positive net enthalpy of micelle formation, as was observed in the present study for the Brij 35 system.

9.2 β-Casein Self-Association

β-casein would be expected to resemble an ionic rather than a nonionic detergent owing to the large net negative charge present under the experimental conditions used in this study. In contrast to nonionic surfactants, micelle formation involving ionic amphiphiles often changes from being endothermic at low temperatures to being exothermic at higher temperatures (Moroi et al., 1975; Barry and Russell, 1972; Anacker, 1970). The decrease in entropy of micelle formation with increasing temperature, coupled with the increasingly negative enthalpy change, can result in a change in the nature of micelle formation of ionic surfactants from a predominately entropic process at low temperatures to a mainly enthalpic process at higher temperatures. The magnitude of the enthalpy change for ionic systems is usually small at lower temperatures resulting in a relatively high $T\Delta S_N^\circ$ to ΔH_N° ratio.

The thermodynamic parameters for the self-association of β-casein A^1 recorded in Table (8-7) on p. 128 were determined using the same thermodynamic expressions as used in the treatment of the Brij 35 results. This means the assumption has been made that the counterion concentration in the β-casein solutions was constant and therefore was not included in the calculations. Such an assumption is reasonable as the salt concentration at the ionic strength of 0.11 is much higher than the concentration of the protein, hence the binding of counterions to the protein would have a negligible effect on the concentration of free ions. It can be seen from a comparison of Tables (8-5) and (8-7) on pages 123 and 128 that the signs, relative magnitudes and trends in the thermodynamic parameters for β-casein self-association are similar to those observed for Brij 35. The enthalpy changes for the β-casein system are all large and positive

and the ratio of the T ΔS_N° to ΔH_N° values at each temperature is similar to that observed for Brij 35 micelle formation. The temperature trends are also similar in both sets of results. The values of ΔH_N° for β-casein self-association appear to decrease as the temperature is increased from 21°C to 30°C resulting in negative ΔC_p° values. However, it should be noted that this trend lies within the experimental uncertainty of each of the values. There appears to be a change in the trend between 30° and 40°C, but the accuracy of the monomer concentrations determined from the fluorescence data at 40°C could be questioned. This is because the monomer concentration at 40°C was found to be very low, hence a small systematic error in this value will result in a very large percentage error in the concentration and in the thermodynamic parameters derived from it. The relatively sudden change in the value of ΔG_N° in going from 30° to 40°C could be an indication of an inaccurate monomer concentration at 40°C since the ΔG_N° value was determined from fluorescence data alone. The ΔS_N° values appear to decrease with increasing temperature (except at 40°C) but again the results are inconclusive owing to the large experimental uncertainty.

On the basis of the comparison of the thermodynamic parameters for β-casein self-association with those for Brij 35 self-association, the β-casein system apparently exhibits similar behaviour to that of a nonionic detergent under the experimental conditions used in the present study. Mukerjee (1967) has shown that the positive contribution of ionic head groups to the free energy of micelle formation is reduced as the ionic strength of the solution is increased. The respective contributions of the head and tail groups to the overall free energy change eventually approach that of a nonionic amphiphile when the ionic strength is sufficiently high. It therefore appears that the ionic strength of 0.11 used in the study of the β-casein self-association process was sufficient to effectively neutralize the electrostatic charge on the

protein. The self-association of β-casein has been shown to be enhanced by increasing ionic strength (Pearce, 1975; Payens et al., 1969; Halwer, 1954), indicating that the electrostatic repulsion between the ionic groups is reduced. The hydrophobic n-alkyl chain of a simple amphiphile in the free monomer state in aqueous solution is thought to exist in extended form rather than being folded back on itself (Mukerjee, 1967). Therefore, all the carbon atoms of the chain will be exposed to contact with the water molecules. In the case of the free β-casein monomer the hydrophobic portion is thought to exist in a folded configuration (Waugh et al., 1970). Therefore, all of the hydrophobic residues in the free monomer may not be exposed to the solvent. Also, a fairly loose structure has been proposed for the β-casein micelle (Payens and van Markwijk, 1963), hence the solvent may have considerable access to the groups in the core of the micelle. It would therefore be difficult to determine the extent of the transfer of the hydrophobic residues of the β-casein molecule from an aqueous to a nonaqueous environment during micelle formation. This uncertainty in the extent of transfer of the hydrophobic residues has been discussed for proteins in general by Némethy and Scheraga (1962). On this basis the self-association of β-casein cannot be considered to be completely analogous to micelle formation in simple detergent systems.

From the results, however, it appears that the transfer of hydrophobic groups from an aqueous to a nonaqueous environment is the dominating factor in β-casein self-association, as the driving force behind the process is a large positive entropy change. Further evidence to support the importance of the hydrophobic effect in this system is provided by the observation of an apparent increase in the partial specific volume during the self-association of β-casein (Payens and Heremans, 1969). This is a characteristic of processes involving the hydrophobic effect (Némethy and Scheraga, 1962). McKenzie and Wake

(1959) observed that β-casein self-association was prevented in the presence of urea, which is known to be an effective agent for inhibiting the hydrophobic effect (Anacker, 1970).

9.3 Conclusion

It has been shown in this thesis that the self-association of β-casein A^1 is similar in several respects to the process of micelle formation exhibited by a synthetic detergent. However, it should be noted that although the heats of association were measured directly by calorimetry, the equilibrium concentrations of the β-casein species in solution were determined indirectly from the fluorescence experiments of Pearce (1975). Pearce has noted there were several fundamental assumptions made during the analysis of the fluorescence results. It is therefore desirable that a more direct method should be used to obtain equilibrium data for β-casein self-association as a check on the validity of the fluorescence data. This was attempted in the present study by using various ultracentrifugation techniques but success was not achieved for the reasons outlined in the appropriate sections of this thesis. Light scattering techniques and a modification of the Archibald technique of ultracentrifugation were considered as possible alternative methods for studying β-casein self-association, but time did not permit these studies to be carried out for this thesis.

REFERENCES

Adams, E.T., Jr. (1965) Biochemistry, 4, 1646

Adams, E.T., Jr. (1967) Fractions, No. 3, 1

Adams, E.T., Jr. and Filmer, D.L. (1966) Biochemistry, 5, 2971

Adams, E.T., Jr. and Fujita, H. (1963) in "Ultracentrifugal Analysis in Theory and Experiment" (J.W. Williams, ed.), p. 119, Academic Press, New York

Adams, E.T., Jr. and Williams, J.W. (1964) J.Am.Chem.Soc., 86, 3454

Anacker, E.W. (1970) in "Cationic Surfactants" (E. Jungerman, ed.), p. 203, Marcel Dekker, New York

Anacker, E.W., Rush, R.M. and Johnson, J.S. (1964) J.Phys.Chem., 68, 81

Aranow, R.H. and Witten, L. (1960) J.Phys.Chem., 64, 1643

Aschaffenburg, R. (1961) Nature (Lond.), 192, 431

Aschaffenburg, R., Sen, A. and Thompson, M.P. (1968) Comp.Biochem.Physiol., 25, 177

Balmbra, R.R., Clunie, J.S., Corkill, J.M. and Goodman, J.F. (1964) Trans.Faraday Soc., 60, 979

Barry, B.W. and El Eini, D.I.D. (1976) J.Colloid Interface Sci., 54, 339

Barry, B.W. and Russell, G.F.J. (1972) J. Colloid Interface Sci., 40, 174

Becher, P. (1961) J.Colloid Sci., 16, 49

Benjamin, L. (1963) Canad.J.Chem., 41, 2210

Berry, G.P. and Creamer, L.K. (1975) Biochemistry, 14, 3542

Biaselle, C.J. and Millar, D.B. (1975) Biophys.Chem., 3, 355

Cann, J.R. (1970) "Interacting Macromolecules", Academic Press, New York

Casassa, E.F. and Eisenberg, H. (1964) Advan.Protein Chem., 19, 287

Chen, J.H. and Ledford, R.A. (1971) J.Dairy Sci., 54, 763

Chervanka, C.H. (1969) "A Manual of Methods for the Analytical Ultracentrifuge", Beckman Instruments Inc., Palo Alto, California

Coates, J.H. (1970) in "Physical Principles and Techniques of Protein Chemistry" (S.J. Leach, ed.), Part B, p. 1, Academic Press, New York

Creamer, L.K. (1971) Biochim.Biophys.Acta., 271, 252

Cuatrecasas, P. (1970) J.Biol.Chem., 245, 3059

Davis, B.J. (1964) Ann.N.Y.Acad.Sci., 121, 404

Debye, P. (1949) Ann.N.Y.Acad.Sci., 51, 575

Dyson, R.D. (1970) Anal.Biochem., 33, 193

El Eini, D.I.D., Barry, B.W. and Rhodes, C.T. (1976) J.Colloid Interface Sci., 54, 348

Elias, H.-G. (1976) in "Order in Polymer Solutions" (K. Solc, ed.), p. 209, Gordon and Breach Science Publishers, London

Evans, M.T.A., Irons, L. and Jones, M. (1971) Biochim.Biophys.Acta, 229, 411

Feinstein, G. (1970) Biochim.Biophys.Acta, 214, 224

Fisher, L.R. and Oakenfull, D.G. (1977) Chem.Soc.Rev., 6, 25

Frank, H.S. and Evans, M.J. (1945) J.Chem.Phys., 13, 507

Franks, F. and Reid, D.S. (1974) in "Water: A Comprehensive Treatise" (F. Franks, ed.) Vol. 2, p. 337, Plenum Press, New York

Fujita, H. (1962) "The Mathematical Theory of Sedimentation Analysis", Academic Press, New York

Gaddum, J.H. (1931) Proc.Roy.Soc. (London), B109, 114

Garnier, J. (1966) J.Mol.Biol., 19, 586

Gilbert, G.A. (1955) Discussions Faraday Soc., 20, 68

Gilbert, G.A. (1959) Proc.Roy.Soc. (London), A250, 377

Goddard, E.D., Hoeve, C.A.J. and Benson, G.C. (1957) J.Phys.Chem., 61, 593

Goldberg, R.J. (1953) J.Phys.Chem., 57, 194

Grosclaude, F., Mahé, M.-F., Mercier, J.-C. and Ribadeau-Dumas, B. (1972) Eur.J.Biochem., 26, 328

Gucker, F.T., Jr., Pickard, H.B. and Planck, R.W. (1939) J.Am.Chem.Soc., 61, 459

Gurney, R.W. (1953) "Ionic Processes in Solution", McGraw-Hill, New York

Hall, D.G. and Pethica, B.A. (1967) in "Nonionic Surfactants" (M.J. Schick, ed.) p. 516, Marcel Dekker, New York

Halwer, M. (1954) Arch.Biochem.Biophys., 51, 79

Harkins, W.D. and Brown, F.E. (1919) J.Am.Chem.Soc., 41, 499

Herskovits, T.T. (1966) Biochemistry, 5, 1018

Hexner, P.E., Radford, L.E. and Beams, J.W. (1961) Proc.Natl.Acad.Sci. U.S., 47, 1848

Hoagland, P.D. (1966) J.Dairy Sci., 49, 783

Holt, C. (1974) XIX International Dairy Congress, 1E, 272

Holtzer, A. and Holtzer, M.F. (1974) J.Phys.Chem., 78, 1442

Ikeda, S. and Kakiuchi, K. (1967) J.Colloid Interface Sci., 23, 134

Johnston, J.P. and Ogston, A.G. (1946) Trans.Faraday Soc., 42, 789

Jones, E.R. and Bury, C.R. (1927) Phil.Mag., 4, 841

Josephs, R. and Harrington, W.F. (1966) Biochemistry, 5, 3474

Josephs, R. and Harrington, W.F. (1967) Proc.Natl.Acad.Sci.U.S., 58, 1587

Josephs, R. and Harrington, W.F. (1968) Biochemistry, 7, 2834

Kaufman, S. (1976) J.Colloid Interface Sci., 57, 399

Kauzmann, W. (1959) Advan.Protein Chem., 14, 1

Kresheck, G.C. (1965) Acta Chem. Scand., 19, 375

Kresheck, G.C., van Winkle, Q. and Gould, I.A. (1964) J.Dairy Sci., 47 117

Lamm, O. (1929) Z.physik.Chem., A143, 177

Leslie, R.B., Irons, L. and Chapman, D. (1969) Biochim.Biophys.Acta, 188, 237

Lewis, J.A. and Lyttleton, J.W. (1973) Anal.Biochem., 56, 52

Matijévic, E. and Pethica, B.A. (1958) Trans.Faraday Soc., 54, 587

McKenzie, H.A. (1971) in "Milk Proteins" (H.A. McKenzie, ed.), Vol. II, p. 87, Academic Press, New York

McKenzie, H.A. and Wake, R.G. (1959) Aust.J.Chem., 12, 734

McMeekin, T.L., Groves, M.L. and Hipp, N.J. (1949) J.Am.Chem.Soc., 71, 3298

Moroi, Y., Nishikido, N., Uehara, H. and Matuura, R. (1975) J.Colloid Interface Sci., 50, 254

Mukerjee, P. (1967) Advan.Colloid Interface Sci., 1, 241

Murray, R.C. and Hartley, G.S. (1935) Trans.Faraday Soc., 31, 183

Némethy, G. and Scheraga, H.A. (1962) J.Phys.Chem., 66, 1773

Nichol, L.W., Bethune, J.L., Kegeles, G. and Hess, E.L. (1964) in "The Proteins" (H. Neurath, ed.), 2nd ed., Vol. II, p. 305, Academic Press, New York

Noelken, M. and Reibstein, M. (1968) Arch.Biochem.Biophys., 123, 397

Parreira, H.C. (1965) J.Colloid Sci., 20, 44

Payens, T.A.J. and Heremans, K. (1969) Biopolymers, 8, 335

Payens, T.A.J. and van Markwijk, B.W. (1963) Biochim.Biophys.Acta, 71, 517

Payens, T.A.J., Brinkhuis, J.A. and van Markwijk, B.W. (1969) Biochim. Biophys.Acta, 175, 434

Pearce, K.N. (1975) Eur.J.Biochem., 58, 23

Peterson, R.F. and Kopfler, F.C. (1966) Biochem.Biophys.Res.Commun., 22, 388

Phillips, J.N. (1955) Trans.Faraday Soc., 51, 561

Pierson, F.W. and Whitaker, S. (1976) J.Colloid Interface Sci., 54, 219

Prigogine, I. and Defay, R. (1954) "Chemical Thermodynamics" Longmans, London

Richards, E.G., Teller, D.C. and Schachman, H.K. (1968) Biochemistry, 7, 1054

Rose, D., Brunner, J.R., Kalan, E.B., Larson, B.L. and Melynchyn, P., Swaisgood, H.E. and Waugh, D.F. (1970) J.Dairy Sci., 53,1

Schachman, H.K. (1959) "Ultracentrifugation in Biochemistry", Academic Press, New York

Schachman, H.K. (1963) in "Ultracentrifugal Analysis in Theory and Experiment" (J.W. Williams, ed.), p. 171, Academic Press, New York

Schmidt, D.G. and Buchheim, W. (1976) Neth.Milk Dairy J., 30, 17

Schmidt, D.G. and Payens, T.A.J. (1972) J.Colloid Interface Sci., 39, 655

Shahani, K.M., Harper, W.J., Jensen, R.G., Parry, R.M. and Little, C.A. (1973) J.Dairy Sci., 56, 531

Shinoda, K. and Hutchinson, E. (1962) J.Phys.Chem., 66, 577

Skinner, H.A. (1969) in "Biochemical Microcalorimetry" (H.D. Brown, ed.), p. 1, Academic Press, New York

Stainsby, G. and Alexander, A.E. (1950) Trans.Faraday Soc., 46, 587

Sullivan, R., Fitzpatrick, M., Stanton, E., Annino, R., Kissel, G. and Palermiti, F. (1955) Arch.Biochem.Biophys., 55, 455

Svedberg, T. (1925) Kolloid-Z., 36, 53

Svedberg, T. and Nicols, J.B. (1923) J.Am.Chem.Soc., 45, 2910

Svedberg, T. and Pedersen, K.O. (1940) "The Ultracentrifuge", Clarendon Press, Oxford

Swaisgood, H.E. (1973) CRC Critical Reviews in Food Technology, 3, 375

Tanford, C. (1973) "The Hydrophobic Effect", John Wiley and Sons, New York

Tanford, C. (1974) J.Phys.Chem., 78, 2469

Thompson, M.P. (1966) J.Dairy Sci., 49, 792

Thompson, M.P. (1971) in "Milk Proteins" (H.A. McKenzie, ed.), Vol. II, p. 117, Academic Press, New York

Thompson, M.P. and Pepper, L. (1964) J.Dairy Sci., 47, 633

Tiselius, A. (1926) Z.physik.Chem., 124, 449

Tiselius, A. (1932) Kolloid-Z., 59, 306

Trautman, R. and Schumaker, V. (1954) J.Chem.Phys., 22, 551

van Holde, K.E. (1967) Fractions, No. 1, 1

van Holde, K.E. and Rossetti, G.P. (1967) Biochemistry, 6, 2189

von Hippel, P.H. and Waugh, D.F. (1955) J.Am.Chem.Soc., 77, 4311

Wadsö, I. (1968) Acta Chem.Scand., 22, 927

Wadsö, I. (1970) Quart.Rev.Biophys., 3, 383

Warner, R.C. and Polis, E. (1945) J.Am.Chem.Soc., 67, 529

Waugh, D.F., Creamer, L.K., Slattery, C.W. and Dresdner, G.W. (1970) Biochemistry, 9, 786

Wilkinson, M.C. (1972) J.Colloid Interface Sci., 40, 14

Yamauchi, K. and Kaminogawa, S. (1972) Agr.Biol.Chem., 36, 249

Yphantis, D.A. (1964) Biochemistry, 3, 297